Joachim Neumann

Recording Techniques, Theory and Audiological Applications of Otoacoustic Emissions

Bibliotheks- und Informationssystem der Universität Oldenburg
1997

Acknowledgments

This work was supported by Deutsche Forschungsgemeinschaft (Ko942/1-1). The collaboration of all members of the "AG Medizinische Physik" as well as the helpful comments from several anonymous reviewers are gratefully acknowledged.

Verlag/Druck/
Vertrieb:

Bibliotheks- und Informationssystem
der Carl von Ossietzky Universität Oldenburg
(BIS) - Verlag -
Postfach 25 41, 26015 Oldenburg
Tel.: 0441/798 2261, Telefax: 0441/798 4040
e-mail: sip@bis1.uni-oldenburg.de

ISBN 3-8142-0576-6

Preface

The subject of Joachim Neumann's dissertation project was to improve the measurement techniques, the theoretical models and the applications of otoacoustic emissions, i.e., weak acoustic emissions from the inner ear that can be recorded in the occluded ear canal with a sensitive microphone and appropriate noise reduction techniques. This is a very important topic, because otoacoustic emissions caused by „active" mechanisms in the cochlea have initiated a revolution in the development of our theory of hearing ever since their discorvery by David Kemp in 1978. In addition, certain kinds of otoacoustic emissions have found a broad application in clinics as 'objective hearing tests' which can be used, e.g., for auditory screening in neonates. The work by Joachim Neumann now provides a remarkable step towards a better understanding of our hearing system as well as refined measurement methods and more sophisticated applications of these otoacoustic emissions.

The outline of this thesis is oriented at the structure of our hearing system: It starts with examinations of comparatively peripheral functions of the auditory system and concentrates on more central functions in later chapters. Simultaneously, each of the chapters forms a complete, well-structured scientific paper which helps the reader to find his (or her) way through the book.

The first chapter gives the technical basis for the later work by introducing the so-called chirplets, i.e., short transient signals with increasing instantaneous frequencies that exhibit a (to a certain degree) selectable spectral content while still being limited in the time domain. These signals are used in the further work to obtain an improved signal-to-noise ratio and not to overload the transducers employed even at high sound pressure levels. In the second and third chapter, the functioning and the frequency selectivity of the inner ear are examined by measuring the interaction between otoacoustic emissions and additionally presented sinusoids or complex tones. A surprising result of these studies concerns the 'suppression effect' observed

in the literature for otoacoustic emissions during the presence of an additional stimulus: It is experimentally demonstrated that this effect is due to the synchronization of the otoacoustic emission (that yields some decrease of the recorded, not synchronised response) rather than a decrease of the power of the otoacoustic emission itself. In addition, nonlinear distortion products and nonlinear effects occur if a (specially designed) tone complex is used as masker instead of a simple continuous sinusoid. Obviously, these effects need further experimental and theoretical evaluation that can be based on the solid foundations set here.

The fourth chapter gives the introduction of a promising and very interesting new method for detecting the acoustic reflex at low stimulus levels which has been discovered by Joachim Neumann and has meanwhile been filed for being patented. With the acoustic reflex method, the function of the inner ear can be tested as well as the first stations of the auditory pathway and the efferent part of the reflex circuit (which produces a contraction of the musculus stapedius). The special feature of this new method is the comparatively low technical expense which can be reached by using standard equipment for recording otoacoustic emissions. On the other hand, the high sensitivity of the method is a key feature which allows to record the acoustical reflex far below those stimulus levels which had to be employed with the conventional methods so far. Because of these prerequisites and because of the applicability of this method with hearing-impaired listeners demonstrated here, this method is extremely interesting for clinical applications and might eventually reach broad practical significance.

In the final chapter (chapter 5), the functioning of the whole auditory system is examined by looking at the relation between the physiologically (objectively) measured otoacoustic emissions and the psychoacoustically (subjectively) measured 'critical band', i.e., the 'effective' bandwidth of spectral analysis employed by the human ear. The special feature of this approach is that exactly the same stimuli are employed both for the objective and subjective measurements and that the critical bandwidths measured with several subjects show the same values both for the objective and the subjective method. However, this intriguing coincidence does not occur generally for all subjects, since subjects without spontaneous otoacoustic emissions exhibit much larger objective critical bandwidths than those values obtained with the subjective method. Thus, the initial hope that simple objective methods might be able to replace the sophisticated and valid psychoacoustical measurement of the critical bandwidth could not be supported by the experimental data. However, this study shows the first

approach for quantifying psychoacoustical phenomena with objective, physically determined signals that can be recorded with the techniques optimized and described here.

Overall, the dissertation submitted by Joachim Neumann is a very impressive collection of excellent papers on otoacoustic emissions that witness the originality, the experimental capabilities, and the theoretical background of the author. It is therefore not surprising, that most of these chapters have meanwhile been accepted by internationally renowned scientific journals and that the results have elicited wide interest by the scientific community. I therefore hope that the reader will profit from the work written down in this book. By reading it, the reader might perhaps get some impression of how much fun it was both for Stefan Uppenkamp and myself and the remainder of our interdisciplinary working group ‘Medizinische Physik’ to work with Joachim. Please read yourself!

Oldenburg, January 1997 Birger Kollmeier

1 Introduction

Otoacoustic emissions are weak acoustic signals, which are detectable in the ear canal of most normal hearing subjects. Over the last 15 years the recording of otoacoustic emissions (OAE) has progressed from an experimental procedure used in a few isolated laboratories to a routine clinical tool used at many places all over the world. The major tasks with measuring the otoacoustic emissions are a) the reduction of background noise and b) the design of an appropriate stimulation paradigm to separate the low-level OAE from undesired stimulus components. A missing solution for these problems is presumably the reason why OAE were not detected before 1978, although microphones with sufficient sensitivity have been available since more than three decades. The pioneering research by KEMP (1978) solved these problems and stimulated hundreds of studies on otoacoustic emissions. Though the underlying physical mechanism of OAE is not completely understood until now and the connection of OAE results to other audiometric findings is not yet clear in detail, OAE can provide a powerful tool for audiometric diagnostics. As an introduction into the topic, a short overview over the properties of otoacoustic emissions (and their implication for the design of OAE experiments) will be given here.

1. Otoacoustic emissions are a consequence of the active preprocessing of sound in the inner ear. The source of the acoustic energy is of physiological nature. The generator is most probably connected to the motility of outer hair cells (BROWNELL et al., 1985; ZENNER, 1986). Thus, OAE are unlikely to be detectable in ears with cochlear hearing loss. Although the concept of a "cochlear amplifier" (DAVIS, 1983) seems obvious to most authors, there is still some disagreement on the nature of the activity along the cochlear partition (cf. ALLEN and FAHEY, 1992; KANIS and DE BOER, 1993).
2. Due to the nonlinear nature of cochlear preprocessing of sound, the presentation of different frequencies can lead to the generation of several additional combination frequencies. To a good approximation,

these additional tones behave as being generated by a static nonlinearity. In addition, the physical properties of the basilar membrane mechanics change with stimulus level. This "compressive" nonlinearity leads to compressive amplitude growth functions in any OAE experiment.

3. Otoacoustic emissions are delayed with respect to the onset of acoustical stimulation. Similar to the traveling wave, OAE exhibit strong dispersion. The latency of otoacoustic emissions increases from approximately 3 ms at frequencies of about 6 kHz to more than 10 ms at frequencies near 1 kHz.
4. Otoacoustic emissions are influenced by the presentation of additional tones. Two effects are observable: synchronization (shift of the emission phase or frequency), and suppression (reduction of emission level).
5. Otoacoustic emissions are highly reproducible. The temporal and spectral properties of OAE are unique for each subject ("fingerprint of the inner ear").

Generally, the amplitude of naturally audible sounds and acoustic stimuli is much larger than the amplitude of an emission. All OAE recording techniques described in the literature therefore involve a method for the separation of undesired components in the microphone signal and the emission. Each technique utilizes a different subset of the properties given above. The results of the obtained techniques are known as different "types of otoacoustic emissions", although it is conceivable that different recording techniques for OAE merely show different perspectives of the same effect. The interrelation of these "types of OAE" is still an ongoing field of research. The most popular recording techniques and the corresponding utilized properties of the OAE are:

Transiently evoked otoacoustic emissions (TEOAE). These emissions were first reported by KEMP in 1978. TEOAE are recorded as response to a short acoustic click, tone pip or chirplet (property 1). The OAE are separated from the stimulus in time (due to the latency of the OAEs, property 3). The repetition of the stimulus allows an averaging of the responses to efficiently improve the signal-to-noise-ratio (property 5). BRAY and KEMP (1987) further improved the temporal separation of the emission from stimulus artifacts by means of a nonlinear averaging mode (property 2). The

recording of TEOAE is popular as standard clinical test of the functionality of the inner ear. Although many studies have found that TEOAE do not correlate very well with the clinical audiogram (BONFILS et al., 1988, COLLET et al., 1991, UPPENKAMP et al., 1992), TEOAE are successfully used in screening tests (WHITE et al., 1993).

Spontaneous otoacoustic emissions (SOAE). These emissions are unique since they can be observed without external stimulation. This reflects the "active" nature of the cochlea (property 1). The experimental setup is based on the averaging of power spectra. An emission can be detected as peak in the background noise spectrum. The clinical significance of SOAE is unclear, although some authors report that SOAE primarily occur at boundaries between regions of better hearing and regions of hearing loss (WILSON and SUTTON, 1981; RUGGERO et al., 1983). SOAE can be observed in recording systems for TEOAE, since the phase of the SOAE can synchronize to the periodic repetition of a transient stimulus (property 4).

Distortion product otoacoustic emissions (DPOAE). These emissions are observed as a series of combination tones in response to stimulation of the ear with two sinusoids with frequencies f_1 and f_2 ($f_1 < f_2$). The most dominant is the cubic difference tone at $2f_1$-f_2. They originate from nonlinear interaction of the stimuli in the inner ear (Property 2). The experimental setup utilizes averaging in the time or in the frequency domain (property 5). Recent research has shown the significance of level growth functions as a diagnostic tool (KUMMER et al., 1995, property 4). Along with TEOAE, DPOAE are widely used as an audiological instrument.

Simultaneously evoked otoacoustic emissions (SEOAE). These emissions are present at the same time and frequency as the stimulus. A special recording procedure is required to extract the OAE. One possibility is to take advantage of the nonlinear growth function of SEOAE (property 2). For this purpose, SEOAE are recorded at low stimulus level in a first measurement and the stimulus is eliminated by subtracting the re-scaled result from a second measurement at high stimulus level. However, if the amplitude of the linear portion varies slightly in one of the measurements, the difference signal would be interpreted, wrongly, as SEOAE.

Within this thesis, otoacoustic emissions are used as a noninvasive tool to study the interaction of acoustical stimuli within the cochlea and the interrelation of cochlear preprocessing and sound perception. In a first step,

chirplets are introduced as stimuli in order to improve the recording technique of transitory evoked otoacoustic emissions (NEUMANN et al., 1994). In normal hearing and hearing-impaired subjects, these stimuli allow a selected stimulation of basilar membrane regions and improve the signal-to-noise ratio of broadband measurements. The benefit of these stimuli in hearing research and for clinical applications is described in chapter one. The level of transitory evoked otoacoustic emissions is reduced if a tone is presented in addition to the evoking stimulus. This interaction is investigated in detail in chapter two. The underlying nonlinearities involve synchronization effects and may contribute to a better understanding of the generation of OAE (NEUMANN et al., 1997a). A measurement paradigm for the simultaneous observation of SEOAE and DPOAE that was first described by KEMP and SOUTER (1988) is based upon the same principles - the nonlinear interaction of multiple stimuli within the cochlea. The underlying mechanism is discussed in chapter three. Some of the experimental results presented in this chapter show an effect which at a first glance appeared to be an artifact. A closer investigation revealed that the results were impaired by a contraction of the stapedius muscle at high stimulus level. Acoustic signals of sufficient intensity can enervate the stapedius muscle through the acoustic reflex arc (including cranial nerve VII and VIII) and thereupon change the acoustic compliance of the middle ear. These observations inspired investigations on temporal effects of the acoustic reflex and opened up a new possibility to detect the acoustic reflex with the experimental setup used for the recording of otoacoustic emissions (NEUMANN et al., 1996). The fourth chapter compares the sensitivity of this new approach with a setup used in routine audiometry. In chapter five, the relation between OAE and properties of the auditory system that are relevant for the perception of sound is studied. The influence of a broadband suppressor on narrowband evoked emissions is correlated with masked thresholds in the presence of a notched-noise masker (NEUMANN et al., 1997b, UPPENKAMP and NEUMANN, 1996). The exciting aspect of these experiments is that the same stimuli and the same evaluation techniques were applied in the OAE experiments and in the psychoacoustical detection task. A single driven van der Pol-oscillator is utilized to model the experimental results. Each chapter of this thesis is published in or prepared for submission to an international journal and should be understandable at its own.

2 Chirplet Evoked Otoacoustic Emissions

Summary

The principles of short frequency sweeps (chirplets) and their application to evoke transiently evoked otoacoustic emissions (TEOAE) are developed in comparison to using standard click stimuli. In contrast to click stimuli, chirplet signals have the advantage of stimulating a freely selectable frequency range. In addition, chirplet signals contain more energy than a click stimulus with the same maximum amplitude. The effects of different stimuli on TEOAE were investigated in normal hearing and hearing-impaired subjects. Using wideband chirplet signals yields a better signal-to-noise ratio compared to click stimulation. In addition, the stimulation of selected regions of the basilar membrane with frequency-limited chirplets evokes TEOAE with frequency components that lie within the stimulated frequency range. The characteristic fine structure of this spectrum was found to be independent of the stimulus applied. The utilization of chirplet stimuli appears to be useful for evoking TEOAE in, e.g., clinical applications.

2.1 Introduction

Transiently evoked otoacoustic emissions (TEOAE) are low-level acoustic responses of the inner ear to short acoustic stimuli in the occluded external ear canal. These emissions can be observed in nearly all normal hearing ears (KEMP, 1978; reviewed in PROBST, 1991). Although TEOAE are being used in clinical examinations as an objective hearing test, there is no model that can explain all aspects of their generation. An important fact that has to be accounted for in any model is that the human hearing system shows a high sensitivity at low sound levels in addition to high frequency and temporal resolution. Since these properties are already observed in the macromechanical movement of the cochlea (RUGGERO and RICH, 1991), an active undamping mechanism has to be assumed. This active mechanism is thought to be related to the generation of otoacoustic emissions (KEMP, 1979; ZWICKER, 1986). This point of view is supported by the fact that TEOAE are very rarely found in ears with severe hearing loss, and never in deaf ears. In addition, the maxima in the TEOAE spectrum correlate to the hearing threshold microstructure that is visible when the audiogram is measured with a high frequency resolution (WILSON, 1980; SCHLOTH, 1983; HORST et al., 1983; ZWICKER and SCHLOTH, 1984; LONG and TUBIS, 1988). On the other hand, the spectrum of a typical TEOAE is dominated by irregularly distributed frequency components, whereas the absolute threshold typically exhibits smaller variability. Therefore, the spectrum of an emission cannot directly serve as an estimate for the clinical audiogram.

Clearly, such an estimate would be valuable for clinical purposes, for example to fit hearing aids in young children. Several studies that have focused on the relationship between TEOAE and hearing level agree that otoacoustic emissions can primarily be used as an indication of normal hearing (PROBST et al., 1986; BRAY and KEMP, 1987; BONFILS et al., 1988; KEMP et al., 1990b; UPPENKAMP et al., 1992). These studies use global measures such as the level of the emission, correlation or spectral bandwidth. Even if a local measure is used, i.e., the TEOAE spectrum, poor correlations were found (COLLET et al., 1991). This is probably due to the structure of the TEOAE spectrum which in turn is related to the spectrum of the stimulus.

The typical stimulus used to evoke TEOAE is a short rectangular pulse ("click"). This signal has a short duration and results in a broadband stimulation. On the other hand, a click stimulus contains little energy. The maximum stimulus amplitude is limited by the properties of the electro-acoustic transducers, and thus cannot be exceeded without distortion. In order to obtain a good signal-to-noise ratio in the response, more acoustic energy is desirable. The only way to overcome this energy limitation of the click stimulus is to take advantage of the time between stimulus onset and the first detectable emissions from the inner ear which amounts to about 3 milliseconds. In light of these restrictions to the stimulus (i.e., a limited maximum amplitude and a limited duration), a signal should be selected which transmits maximal energy into the inner ear without distortion. This property of the signal corresponds to a low "peak factor", which is defined as the range of the waveform amplitude divided by its RMS.

Apart from the lower peak factor, another desired attribute of a stimulus is the free choice of the stimulated frequency range. In order to generate a finite signal that contains spectral energy only within a certain frequency range, it is not possible to simply use an inverse Fourier transform of the desired spectrum. Such a transform would lead to a time signal of infinite length. Design methods for digital finite impulse response (FIR) filters solve this problem, but conventional design methods are not concerned with the generation of a signal with a low peak-factor. To satisfy these requirements, a new approach has therefore been devised which employs chirplet signals, i.e., sinusoidal signals with an instantaneous frequency that changes monotonically. In contrast to narrowband stimulation with tone pulses, this approach attempts to screen the functionality of selected basilar membrane regions in a single measurement by selecting the frequency range of the stimulus applied.

SCHROEDER (1970) described a method to construct low peak-factor signals that exactly reproduces a given power spectrum. The appropriate selection of the phase of equal amplitude harmonics ("Schroeder phase") leads to a chirplike signal. Since this signal is periodic, it is not suitable as a stimulus for TEOAE.

Chirplet signals with linearly increasing instantaneous frequency ("FM-chirplets") have been used in various applications, e.g., in sonar and radar (KLAUDER et al., 1960). BURGESS (1991) used FM-chirplets for acoustical system identification. His design achieves a minimum peak factor while

most of the signal power can be concentrated in a desired frequency band. However, this design method is not optimal for short chirplet signals (as required for TEOAE), since the spectral smearing in short signals is not accounted for in an efficient way. In this study, we therefore attempt to optimize chirplet stimuli to yield an optimum approximation of a "target" spectrum while maintaining a short temporal extent.

2.2 Chirplet generation

The basic idea to generate a chirplet signal for a given power spectrum is that the spectral energy at a certain frequency increases if the instantaneous frequency of the chirplet takes values close to this frequency during a longer period of time. Thus, by suitably selecting the time course of the instantaneous frequency of a signal, it is possible to manipulate its spectrum. Therefore, we specify the chirplet signal in terms of its instantaneous frequency $F(t)$ and its envelope $A(t)$:

$$\begin{aligned} &\text{time signal: } s(t) = A(t) \cdot \sin\phi(t) \\ &\text{phase : } \phi(t) = 2\pi \int_0^t F(\tau)\,d\tau \\ &\text{instantaneous frequency : } F(t) = \frac{1}{2\pi}\frac{d\phi(t)}{dt} \end{aligned} \qquad (2.1)$$

The distribution of the instantaneous frequencies can be selected to be identical to the prescribed power spectrum $L(f)$. Within the limitations discussed below, the spectrum of the generated signal would match the desired spectrum. In addition, the correspondence between the desired power spectrum and the observed power spectrum of the signal is better if the instantaneous frequency changes slowly with time. This implies that the instantaneous frequency function $F(t)$ should be monotonic.

To obtain a distribution of the instantaneous frequency identical to the desired spectrum $L(f)$, the rate of change of the instantaneous frequency $F(t)$ must be inversely proportional to the spectral energy $L(f)$ at this frequency. For example, a high energy of a particular frequency component in the desired spectrum of the signal should lead to a slow change of the instantaneous frequency at this particular frequency:

$$\frac{dF(\tau)}{dF} = \frac{1}{L(F(\tau))} \tag{2.2}$$

To obtain the instantaneous frequency function F(t)we initially consider the derivative of the inverted function t(F).

$$\frac{d\tau(F)}{dF} = \frac{d\tau}{dF(\tau)} = L(F(\tau)) \tag{2.3}$$

Integration yields

$$\tau(F) = \int_0^F L(f)df \tag{2.4}$$

provided that

$$\int_0^\infty L(f)df \overset{!}{=} T \tag{2.5}$$

is achieved through normalization of $L(f)$. As a first attempt, we therefore calculate the time signal $s(t)$ by the inverted function $t^{-1}(F)$:

$$s(t) = A(t) \cdot \sin\left(2\pi \int_0^t \tau^{-1}(F)\,dt\right) \tag{2.6}$$

The envelope $A(t)$ is not specified yet. To demonstrate the significant effect of the envelope $A(t)$ on the resulting signal spectrum, a rectangular and a Hanning window is used to generate the chirplet signals shown in Figs. 2.1a and 2.1b. The signals in these figures were calculated for a duration of 3 milliseconds with a flat target spectrum between 500 Hz and 6000 Hz, with no power falling outside this range. Therefore, the instantaneous fr e-quency function increases linearly from 500 Hz to 6000 Hz. The abrupt transitions of the signal in Fig. 2.1a (rectangular window) leads to an undesirable widening of the spectrum.

This widening effect can be reduced by using a Hanning window of length T as the envelope function $A(t)$. The resulting signal is shown in Fig. 2.1b.

Although the power spectrum is now limited to the desired range, the signal still does not match the target spectrum since the power is not uniformly distributed over the desired frequency range. This new difficulty is caused by the weighting introduced by the Hanning window. The reduction in signal amplitude at the beginning and at the end of the chirplet also reduces the contributions of these regions to the power spectrum.

To compensate the power loss in the low and high frequency regions the distribution of the instantaneous frequency is modified: Until now, the time variable used in the instantaneous frequency function $F(t)$ was a linear function of time. The substitution of this time variable with a function $\tilde{t}(t)$ enables a change in the instantaneous frequency distribution. This function $\tilde{t}(t)$ compensates the effect of the weighting Hanning window by increasing with the integral of the window function. Since a loss in signal power should be compensated, the new function $\tilde{t}(t)$ is given by the normalized integral of $A^2(t)$:

$$\tilde{t}(t) = \frac{\int_0^t A^2(\tau)\mathrm{d}\tau}{\int_0^T A^2(\tau)\mathrm{d}\tau} \cdot T \qquad (2.7)$$

This gives

$$s(t) = A(t) \cdot \sin\left(2\pi \int_0^{\tilde{t}(t)} \tau^{-1}(F)\mathrm{d}t \right) \qquad (2.8)$$

as the final chirplet formula.

Fig. 2.1c shows a chirplet signal after applying the described correction to the instantaneous frequency. It can be seen that the resulting chirplet signal matches the target spectrum much better than before.

In order to uniformly distribute the stimulus energy over the entire basilar membrane, a non-uniform target spectrum can be used in the design of the stimulus. The chirplet signal in Fig. 2.1d was therefore designed for a target spectrum that is uniform on the bark scale using the formula according to ZWICKER and TERHARDT (1980). This stimulus is in the following referred to as the "bark" chirplet.

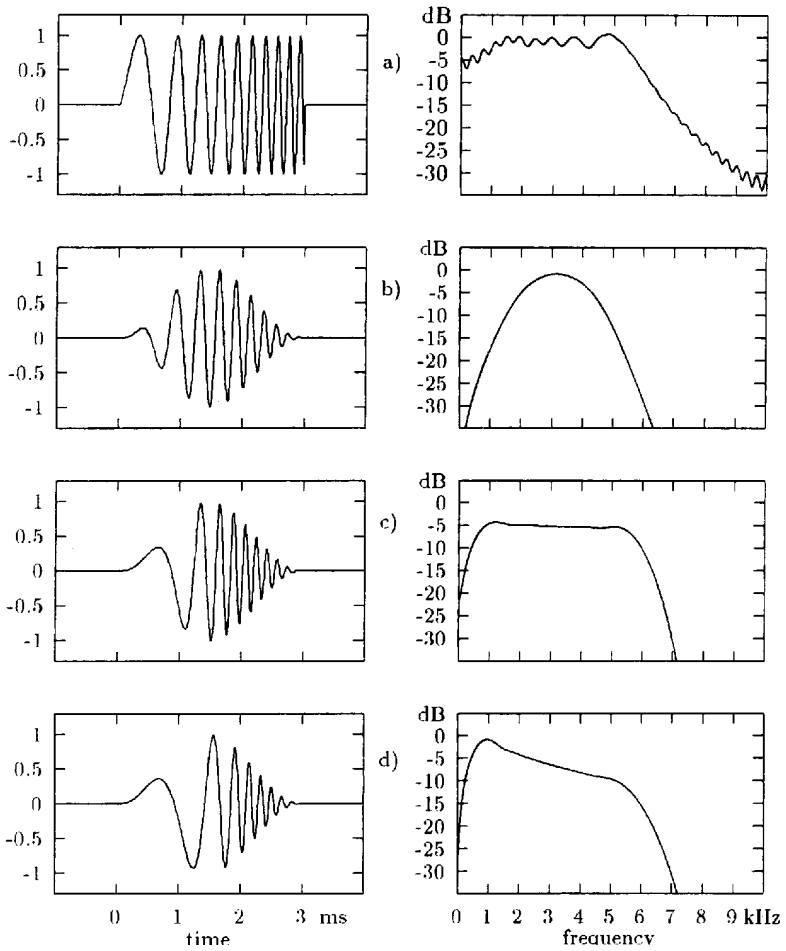

Figure 2.1: Time signal and spectrum of chirplet signals with increasing instantaneous frequency from 500 Hz to 6000 Hz: a) rectangular window, linear increase of instantaneous frequency, b) Hanning window, linear increase of instantaneous frequency. c) Hanning window, compensation of the window effect by a nonlinear increase of the instantaneous frequency. d) same as c) with a target spectrum uniformly distributed on a bark scale.

2.3 Method

The acoustical stimulation of the ear was carried out with an Etymotic Research ER-2 insert ear phone. It has a flat frequency response up to 10 kHz. The amplitude of four successive stimuli was multiplied with the factors 1,1,1,-3, respectively. This nonlinear averaging suppresses the linear response and thus provides a better separation between stimulus and TEOAE (BRAY and KEMP, 1987). The acoustic response of the inner ear was recorded in the sealed ear canal with a miniature electret microphone (Knowles EA 1843). The microphone sensitivity, including a pre-amplifier with a gain of 46 dB, was 2.47 V/Pa at 1000 Hz. The output of the pre-amplifier was connected to a measurement amplifier (Brüel & Kjaer 2610, gain 20 dB). The signal was then passed through a band-pass filter (KEMO VBF/40) with cutoff frequencies of 400 Hz and 7000 Hz. The signal was digitized using a 16-bit A/D converter on a DSP-32C signal-processing board (Ariel corporation) and recorded in two separate memory buffers.

The digital signal processor was used to calculate the root-mean-square (RMS) of four successive segments of the signal in real time. The noise reduction was carried out by a weighted averaging technique which utilizes the inverse of the respective RMS value. Segments with high RMS values were rejected. In addition, the cross-Fourier-transform of the two buffers was calculated concurrently. The real part of this cross-spectrum was summed for all frequencies to serve as an estimate of the power in the oto acoustic emission. The power of the noise was estimated by the RMS of the difference of the two buffers. The time signals and TEOAE spectra were displayed on the host PC throughout the recording session.

Twenty-five subjects, aged from 24 to 71 years, participated voluntarily in this study. Six subjects had a normal pure-tone hearing threshold on both sides. The other subjects had a cochlear hearing loss of different etiology on at least one side. The mean hearing loss, defined as the mean threshold for the audiogram frequencies 500 Hz, 1 kHz, 2 kHz, 4 kHz and 8 kHz, ranged from 15 dB HL to 80 dB HL. Twenty ears showed a high-frequency hearing loss, six ears showed low-frequency hearing loss, four had a notch, five ears had a flat hearing loss and the remaining three ears were deaf. There was no instance of middle ear damage. Brainstem response audiometry was used to rule out retrocochlear hearing loss.

Otoacoustic emission recording took place in an IAC403A sound-insulated chamber. The stimulation was carried out with a 90-microseconds rectangular pulse ("click") and three different chirplet signals. Due to microphone sensitivity limitations, the frequency range of these chirplet signals was restricted from 500 Hz to 6000 Hz. A wide band "bark" chirplet (500 Hz to 6000 Hz), a low frequency chirplet stimulus (500 Hz to 1000 Hz) and a high frequency stimulus (3000 Hz to 6000 Hz) were employed. The spectrum of the latter two stimuli was uniformly distributed in the selected frequency range. The output level of the acoustic transducer was set to 40 dB HL for the click stimulus. The stimulation with the chirplet signals was carried out with the same setting of the maximum amplitude. This results in an stimulus level of 48 dB HL due to the longer duration of the chirplet signals.

2.4 Results

To demonstrate the effect of the wideband "bark" chirplet signal in comparison to a standard click stimulus, we recorded TEOAE from a subject with a high-frequency hearing loss. The audiogram of the subject is shown in Fig. 2.2. The left panel of Fig. 2.3a shows the TEOAE using click stimulation. A typical evoked otoacoustic emission is visible in the two buffers. The click stimulus applied is displayed on a compressed scale in the upper left of the figure. The stimulus artifact in the onset of the recorded acoustic signal was suppressed by means of a suitable time window. The cross-spectrum of the two buffers

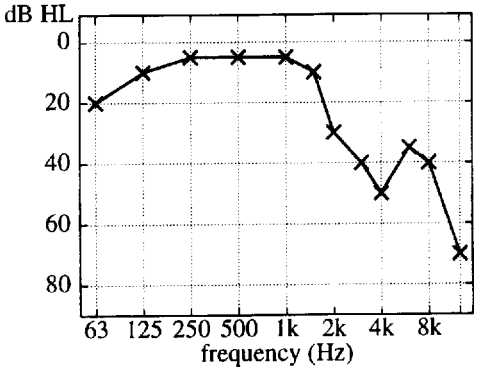

Figure 2.2: Pure tone audiogram of a subject with predominately a high-frequency hearing loss

is displayed in the right panel of Fig. 2.3a. The peaked fine structure of the spectrum in Fig. 2.3a is typical for a TEOAE. The level of the TEOAE and the noise are shown above each measurement (left panel).

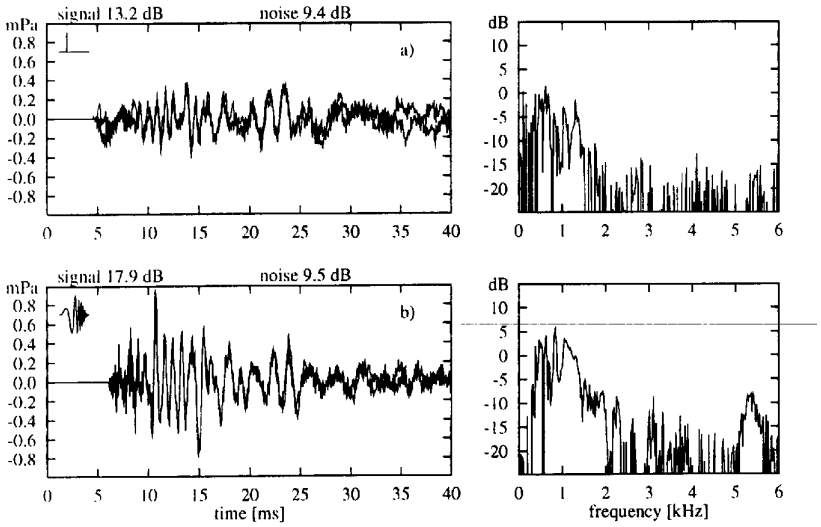

Figure 2.3: TEOAE from the same subject as in Figure 2.2 using: a) click stimulation, b) the "bark" chirplet stimulus from Figure 2.1d

Figure 2.3b shows a chirplet-evoked emission from the same ear. In an attempt to stimulate each region of the basilar membrane to an equal extent, the spectral power density of the chirplet was selected to be uniform on a Bark frequency scale (cf., Fig. 2.1d). The main effect of the chirplet stimulation is a higher level of the otoacoustic emission (18 dB vs. 13 dB) and an improved signal-to-noise ratio. This effect is mainly due to the higher amount of energy applied to the ear with the chirplet stimulus though using the same maximum amplitude as the click stimulus. Similar observations hold for nearly all other subjects tested. Only subjects with a very small or absent TEOAE (i.e., severely hearing impaired subjects and one moderately impaired subject) did not show an increase in emission level or signal-to-noise ratio. The difference in level and signal-to-noise ratio for click vs.

chirplet stimulation for all 50 ears tested in this study is shown in Figure 2.4. The results of the subjects are ordered from left to right with increasing hearing loss. As already noted above, subjects with a severe hearing impairment (>60 dB) and deaf subjects show no improvement, since in neither case an emission was detectable. The median value for the increase in level is 3.1 dB.

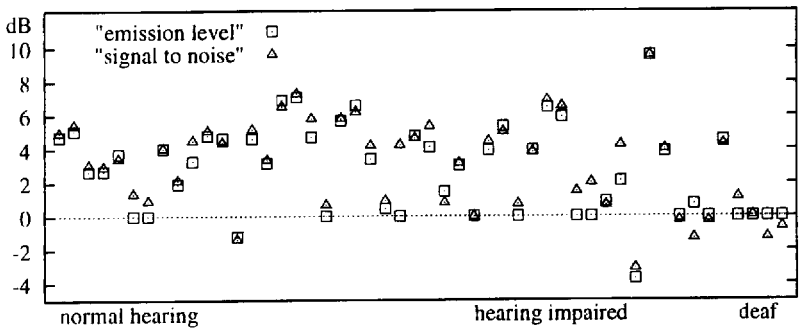

Figure 2.4: Level difference and improvement of the signal-to-noise ratio, chirplet vs. click stimulation. Subjects are ordered according to their average hearing loss

When comparing Figs. 2.3a and 2.3b, a strong resemblance of the emissions in the time and frequency domain can be observed. In both figures, the components with high frequencies are recorded first, followed by components with lower frequencies. This behavior reflects the macromechanical response of the basilar membrane: Since high-frequency components are mapped more basal in the cochlear than low-frequency components, they exhibit a smaller total travel time on the basilar membrane from the stapes to their place of maximum displacement (and vice versa). By using a chirplet stimulus with monotonically increasing instantaneous frequency, this frequency-dependent group delay is at least partially compensated for. If a complete compensation would be achieved, the maximum displacement of the basilar membrane would be synchronized across frequencies and the TEOAE might be confined to a small time period.

To investigate the importance and relative contribution of this effect on the recorded emission, we also used a chirplet signal with a monotonically

decreasing instantaneous frequency as a stimulus. Fig. 2.5 gives the obtained TEOAE with both kinds of chirplet stimuli for a normal listener who is distinct from the subject in Fig. 2.3. Apparently, the responses differ only slightly. For the chirplet signal with decreasing frequency (upper panel in Fig. 2.5), the passive decay of the low-frequency components at the end of the stimulus overlaps temporally with the emission evoked by the high-frequency components at the onset of the stimulus.

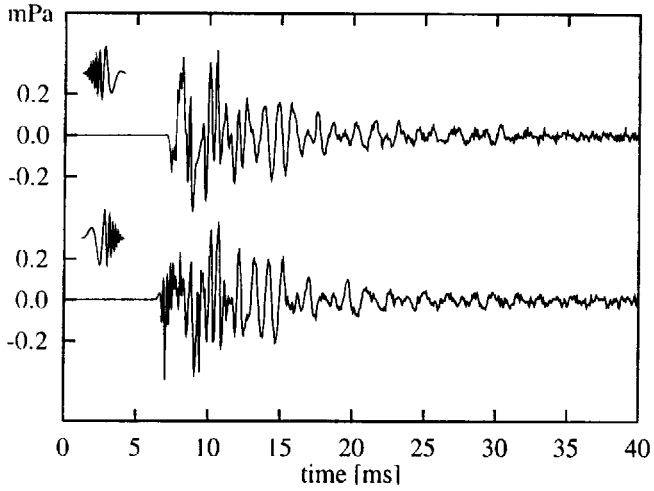

Figure 2.5: TEOAE from a normal hearing subject. Upper trace: chirplet stimulus with decreasing instantaneous frequency from 500 Hz to 6000 Hz. Lower trace: chirplet stimulus with increasing instantaneous frequency from 6000 Hz to 500 Hz

Thus, the separation between stimulus and evoked response is more difficult in this case than for the chirplet signal with increasing frequency and a longer time period has to be blanked out at the onset of the response. The same observations were made for two more normal hearing subjects where both kinds of chirplet stimuli were applied. The small differences in the response for increasing and decreasing instantaneous frequency may be partly due to the small duration of the chirplet stimuli in comparison with a

maximum difference in travel time on the basilar membrane of about 10 ms. In addition, the impulse response of the transmission system from the electrical signal to the acoustical input to the basilar membrane has a duration in the same order of magnitude as the chirplet stimuli applied. Therefore, much of the differences observed between the electrical stimuli will be smeared out in the signal driving the basilar membrane.

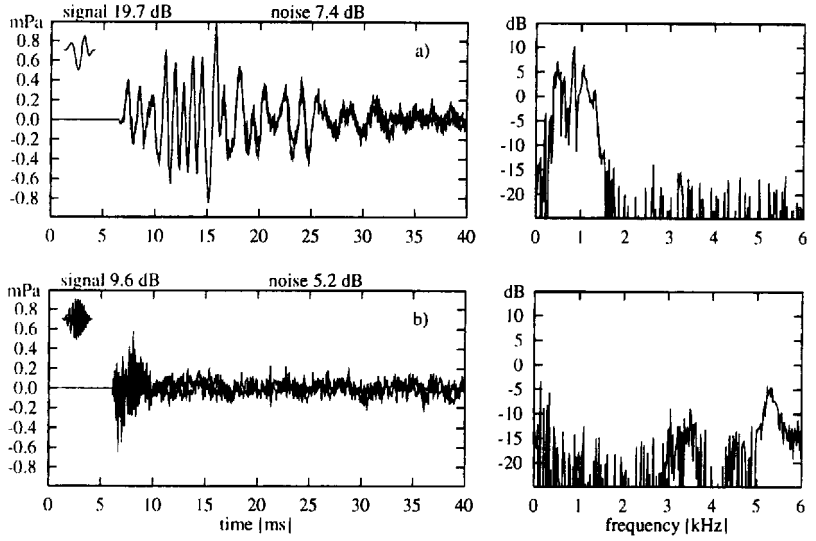

Figure 2.6: Narrowband evoked OAE from the same subject as in Figs. 2.2 and 2.3 using a) lowfrequency chirplet from 500 Hz to 1000 Hz and b) highfrequency chirplet from 3000 Hz to 6000 Hz

The effect of narrowband chirplet stimuli is demonstrated in Figs. 2.6a and 1.6b for the same subject as in Fig. 2.3. Fig. 2.6a shows an emission using a chirplet signal with a uniform spectrum at low frequencies (500 Hz to 1000 Hz) and Fig. 2.6b for a chirplet signal with a uniform spectrum at high frequencies (3000 Hz to 6000 Hz). The otoacoustic emissions obtained with these chirplet stimuli differ substantially. It can be clearly seen that the dominant frequency components of the TEOAE lie within the stimulated frequency range. In this frequency range, the characteristic fine structure of

the spectrum is visible which strongly resembles the structure for the broad-band stimulation (Fig. 2.3). Thus, the narrowband stimulation appears to "cut out" a specific part of the spectrum of the broadband evoked OAE. This observation also holds for most other tested ears. In three ears out of the investigated 50 ears, however, spontaneous otoacoustic emissions were synchronized by narrowband stimuli even if the frequencies of the SOAE were not located in the stimulated frequency range.

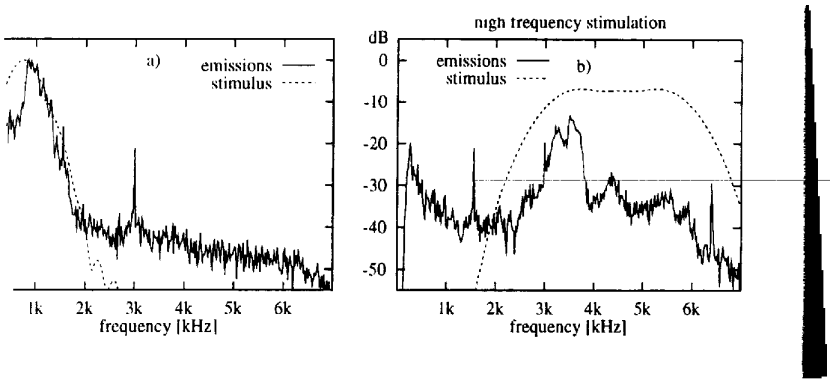

e 2.7: Spectra of the narrowband stimuli (on an arbitrary scale) and

Figure 2.7: Spectra of the narrowband stimuli (on an arbitrary scale) and average of the corresponding TEOAE power spectra: a) from 500 Hz to 1000 Hz. b) from 3000 Hz to 6000 Hz. The TEOAE power is concentrated in the frequency range of the stimuli. The peaks originate from synchronized spontaneous otoacoustic emissions

Figs. 2.7a and 2.7b show the spectra of the narrowband stimuli (on an arbitrary scale) and the corresponding TEOAE power spectra averaged across all 50 ears. The "cut out" effect causes the concentration of the TEOAE power in the frequency range of the stimuli, whereas the synchronized spontaneous otoacoustic emissions are visible as peaks. These peaks originate from individual measurements with subjects exhibiting a spontaneous OAE at the respective frequency.

2.5 Discussion

Our primary results may be summarized as follows:

1. The stimulation of TEOAE with different types of short, broadband stimuli (i.e., click and chirplet signals with increasing or decreasing instantaneous frequency) yields approximately the same responses both in the time and frequency domains.
2. The chirplet-evoked OAE exhibit a higher acoustic level and a better signal-to-noise ratio than the OAE evoked by clicks when the same maximum amplitude setting is employed.
3. The spectrum of a narrowband chirplet-evoked OAE duplicates the broadband evoked OAE spectrum within the predetermined frequency band.

The first finding may even be extended to narrowband stimuli: From a closer inspection of Figs. 2.3a and 2.3b where broadband stimuli were used and Fig. 2.6a, where a narrowband stimulus was used, it can be seen that the recorded signals are almost identical in the region between 10 ms and 25 ms (except for different amplitudes). The dominant frequency components for the recorded signal in this time period range between 500 Hz and 1500 Hz which corresponds well to the spectrum of the narrowband chirplet. Apparently, the frequency-dependent latency between the stimulus and the recorded response is the same for broadband and narrowband stimulation. As long as the stimulus extends only across a limited temporal interval (i.e., 3 ms in our case), the waveform of the recorded response is dominated by this frequency-dependent latency and only slight differences are observed for emissions evoked by quite different stimuli. In our data, this finding is supported by the small differences observed in the response to a click and a chirplet with increasing and decreasing instantaneous frequency. However, the impulse response of the acoustic transmission system which tends to smear out the stimuli and hence reduce the dissimilarities might also contribute to the similarity between the responses to different stimuli types. Within the limitations of such an approach, an inverse filter is desirable which compensates for this effect by inverting the transfer

function between the electric input signal and the acoustic signal applied to the inner ear.

Although the differences in the response to the chirplet signal with increasing and decreasing instantaneous frequency are small, the former one provides a better compensation for the frequency-dependent latency and thus allows a better separation between stimulus and response. This property is even more important for a linear averaging technique where the linear response to the stimulus is not suppressed. A better compensation for the frequency-dependent latency (which might be appealing for brainstem audiometry) and hence a larger difference for the two types of stimuli would require a larger signal duration. Unfortunately, the signal would then overlap more severely with the emission and thus renders this approach to be impractical for TEOAE measurements. Therefore, the 3-ms chirplet signal with increasing instantaneous frequency presented here seems to be the best compromise between duration of the signal and compensation for the basilar membrane traveling time.

With regard to the second general finding of this study, the increase in response level and in signal-to-noise ratio for both normal hearing and cochlearly-impaired subjects can be explained by the energy difference between the click and the chirplet stimulus. Although the chirplet stimulus has the same amplitude as the click stimulus, it encompasses more energy because it extends over a longer period of time. The level difference of the microphone signals recorded in a sealed 2 cm^3-cavity (artificial ear) is 8 dB, whereas an average increase of 3.1 dB was observed for the emission level in our subjects (cf. Fig. 2.4). These values confirm the relation between the level of the stimulus and the level of the evoked otoacoustic emission, which shows a slope of about 0.5 for frequencies at about 1000 Hz (GRANDORI, 1985; UPPENKAMP, 1992; UPPENKAMP and KOLLMEIER, 1994).

Thirdly, the application of narrowband chirplet stimuli reveals that the stimulus spectrum has a significant influence on the TEOAE. The emissions evoked by high- and low-frequency chirplet signals differ strongly both in their temporal and spectral properties. Specifically, the spectra of the TEOAE lie within the stimulated frequency range. Although some reports on narrowband evoked OAE did not show this effect clearly (NORTON and NEELY, 1987), possibly due to unfavorably signal-to-noise ratios, similar observations were reported by ZWICKER (1983) and PROBST

et al. (1986) with tone pulses. In comparison with tone pulses, the frequency range of chirplet stimuli can be freely selected at any stimulus duration. Within the range of the stimulated spectra, a reproducible fine structure can be observed that is characteristic for each investigated ear. In the stimulated frequency range, this fine structure is independent of the stimulus selection. This leads to the assumption that any TEOAE spectrum can be interpreted as the result of the multiplication of the subject's characteristic fine structure with the power spectrum of the stimulus.

Consequently, our results support the point of view of individually generated OAE's that sum up to the observed signal. This observation coincides with recent findings of NORTON (1992) and fits well with our interpretation of the model by STRUBE (1989). This model describes the generation of the TEOAE by a superposition of reflections at periodically distributed inhomogenities in the region of maximum basilar membrane displacement. On the other hand, AVAN et al. (1991) interpreted STRUBE'S model as an explanation for their finding that the amplitude of the TEOAE is proportional to the total length of the undamaged portions of the basilar membrane. This contrasts with our results reported so far as well as with our results in impaired listeners with high- and low-frequency hearing loss (NEUMANN et al., 1993): stimulating a frequency region with a large hearing loss on the average yielded a weaker TEOAE than stimulating frequency regions with a less hearing loss. In our view, Strube's model is consistent with these findings since only reflections at inhomogenities in undamaged and displaced basilar membrane portions contribute significantly to the total emission (STRUBE, personal communication). Thus, the amplitude and spectrum of the response depend both on the stimulus spectrum and the distribution of undamaged portions along the basilar membrane rather than the total length of undamaged portions. Further investigations on the influence of the level of narrowband stimuli and the influence of additional suppressor tones should clarify the degree to which portions of the basilar membrane other than the stimulated ones contribute to the observed OAE. Recent findings of BRASS and KEMP (1993) suggest the influence of more basal parts on OAE at low stimulus levels.

2.6 Conclusions

The use of chirplet stimuli appears to be useful for evoking TEOAE in, e.g., clinical applications. Due to the higher level of the chirplet versus the click the signal-to-noise ratio can be improved. Therefore the detection of an TEOAE and the observation of saturation with increasing stimulus level is facilitated, especially when using the "bark" chirplet signal. This holds especially in the case of very weak TEOAE. In addition, the stimulation with narrowband stimuli allows a specific evaluation of the functionality of selected basilar membrane regions in a single measurement.

3 Interaction of otoacoustic emissions with additional tones: Suppression or synchronization?*

Summary

The influence of an external tone on transitory evoked otoacoustic emissions (TEOAE) is investigated. Three different averaging techniques were used with the same acoustic stimulus paradigm. These techniques permitted the separation of those parts of the otoacoustic emission (OAE) that contribute to the transitory evoked otoacoustic emission and those parts of the otoacoustic emission that are synchronized to the continuous tone. The experiments show that the total energy of the OAE is not reduced in the presence of an additional tone. The "suppression" of transitory evoked otoacoustic emissions is an effect of synchronization and the subsequent elimination of the "suppressed" emission in the averaging procedure.

* published in: Neumann, J., Uppenkamp, S., and Kollmeier, B. (1997a). *"Interaction of otoacoustic emissions with additional tones: Suppression or synchronization?"* Hear. Res., 103, 19-27.

3.1 Introduction

In one of the first studies on otoacoustic emissions, KEMP (1979) presented an uncorrelated sinusoid during the recording of a narrowband transitory evoked otoacoustic emission (TEOAE) and observed a decrease of the OAE level in the presence of the suppressor tone. Similar experiments were made for other types of otoacoustic emissions, such as spontaneous otoacoustic emissions (SOAE) (WIT and RITSMA, 1979, 1980; WILSON, 1980a), distortion product otoacoustic emissions (DPOAE) (HARRIS et al., 1992) and simultaneously evoked otoacoustic emissions (SEOAE) (KEMP and CHUM, 1980a). These studies specify the required level of the suppressor tone to reduce the emission by a fixed level (e.g., 6 dB) and report a strong dependency on the spectral properties of the suppressor. The level reduction of a single OAE component is maximal if the frequency of the external tone is close to the OAE frequency. A variation of the suppressor in the frequency domain permits the recording of "suppression tuning curves". These exhibit a shape and Q_{10dB} similar to the tuning-curves known from measures of the response of the basilar membrane, or discharge rates of VIIIth nerve fibers (reviewed in PATUZZI and ROBERTSON, 1988).

In addition to a reduction of the evoked OAE level by an additional tone, it is also known that the phase of spontaneous otoacoustic emissions can be synchronized by an additional click or tone pulse stimulus of sufficient level (ZWICKER and SCHLOTH, 1984). This synchronization effect allows the observation of SOAE as peaks in the spectrum of a TEOAE although the recording utilizes averaging in the time domain[1]. WILSON and SUTTON (1981) reported three effects if a continuous tone is presented to an ear with SOAE. Firstly, the frequency of the emission is shifted by some Hz, typically towards the external tone. In this case, the SOAE still oscillates at a frequency different to that of the external tone. Secondly, the SOAE can be completely pulled in by the external tone, if the suppressor frequency further approaches the SOAE (cf. LONG et al., 1988). In this case, the emission is forced to oscillate at the same frequency as the stimulus. Thirdly, the

1 The SOAE is synchronized by a short stimulus signal in this case. An unaffected (and thus uncorrelated) SOAE would rapidly decrease in level during the averaging. For example, the contribution of an uncorrelated signal to the average of 256 signal segments would be reduced by a factor of 16 (i.e., 24 dB).

level of the SOAE is reduced. This holds for a measurement of the spectral power at the SOAE frequency as well as for the spectral power in a filter that follows the shifted emission.

The effects described above might be related to neurophysiological findings. The results of two-tone suppression experiments show that the neural discharge rate in response to a primary tone at the center frequency of a single unit is reduced if a second tone is added ("neurophysiological suppression"). The reduction of the total discharge rate is largest in two suppression regions at frequencies slightly above or below the areas of the unit´s excitatory response to a single tone. If the frequency of the suppressor tone further approaches the center frequency of the unit, the neural firing rate increases above the rate without the suppressor (ARTHUR et al., 1971). These findings indicate that the amplitude of the basilar membrane movement increases if the frequency of the suppressor approaches the frequency of the primary tone. Temporal patterns of neural firing in the case of a nonharmonic two-tone stimulation might be related to the synchronization effect of OAE in the presence of a suppressor tone. The discharge patterns show phase locking to one tone, or the other, or both tones simultaneously. In the case of a high suppressor level, the temporal pattern is indistinguishable from that which occurs when the suppressor is present alone (HIND et al., 1967). This effect is related to nonlinearities of the basilar membrane rather than neural interconnections (LEGOUIX et al., 1973; RHODE and ROBLES, 1974). The simultaneous observation of two different temporal patterns in the neural discharge pattern is evidence for a forced oscillation of the basilar membrane with the frequency of the suppressor (synchronization).

When studying suppression and synchronization effects in otoacoustic emissions one encounters the problem of the separation between the suppressor and the OAE. Such a separation is an important prerequisite since the level of the suppressor is typically well above the level of the emission. If the OAE detection and signal analysis is carried out in the frequency domain, as in the case of SOAE or DPOAE, a separation can be achieved by exploiting the spectral distance of the (narrowband) OAE and the suppressor tone. If the otoacoustic emission is obtained by averaging multiple responses in the time domain, as in the case of TEOAE, SEOAE and DPOAE, the suppressor can be separated by the averaging procedure. This approach does not require a minimal spectral distance and allows the use of wideband suppressors. If the suppressor is uncorrelated to the stimulus ("running phase"), the signal-to-noise ratio is improved by 3 dB

for each doubling of the number of averaged frames. In this case, the level of the suppressor and the number of averaged segments have to be chosen carefully.

In order to cancel the suppressor completely, the phase of the sinusoid has to be in a fixed relation to the averaging segments. If, for example, the suppressor exhibits a phase difference of π in successive segments and the time segments are averaged in pairs of two, the suppressor completely cancels in the resulting signal. SUTTON (1985) pointed out that one possible drawback arises with any separation technique[2]: *"It is conceivable that the suppressor might synchronize part of the response (probably the late ´secondary´ echos which might be less strongly phase-linked to the click stimulus). Any OAE thus synchronized would, like the suppressor, disappear on averaging, and be interpreted, wrongly, as having been suppressed"*. WILSON and SUTTON (1981) noted that phase-locking might only occur for a certain period: *"then, influences such as noise, change of sensitivity, etc., will allow the emission to escape the control and to oscillate at its natural frequency until the phases are again sufficiently close for locking to be re-established"*. Based on the findings reported so far, two alternative explanations for the suppression effect of OAE seem possible:

Explanation 1:	The otoacoustic emission is reduced in level, because the emission generation is truly suppressed. The mechanism that produces the OAE emits less acoustic energy.
Explanation 2:	The emitted OAE energy is partly synchronized to the suppressor. When eliminating all synchronized components, the corresponding energy portion is removed. The level of the remaining emission is reduced although the total emitted OAE energy is not reduced.

This study aims at testing both alternative hypotheses in three experiments. While the acoustical stimulation of the subjects remains unchanged, three different averaging techniques are employed to separate the recorded emission from those parts of the response that are entrained to the frequency and phase of the suppressor.

2 SUTTON (1985) used a phase difference of $\pi/5$ and averaged multiples of ten segments to eliminate the suppressor tone.

3.2 Method

3.2.1 Experimental Setup

Otoacoustic emission are recorded in an IAC403A sound-insulated chamber. The acoustic stimulation and the recording of the microphone signal are carried out with an insert ear probe (Etymotic Research ER-10C). The microphone sensitivity is 0.05 V per Pa at 1000 Hz. The microphone output is connected to a pre-amplifier with selectable gain (ER-10C DPOAE-preamp). The signal is then passed through a low-noise amplifier including butterworth high-pass filter at 300 Hz and low-pass filter at 10 kHz to reduce noise (Stanford Research 560). The signal is digitized using a 16-bit A/D converter on a signal-processing board (Ariel corporation DSP-32C) and recorded in two separate memory buffers. The time segments have a duration of 46 ms, yielding a stimulus rate of 21.6 Hz. The digital signal processor is used to calculate the root-mean-square of the segments in real time. Noise reduction is carried out by an averaging technique that uses the inverse of the RMS as a weighting function. Segments with high RMS values are rejected and segments with lower noise level receive a high weighting. Furthermore, the cross-Fourier-transform of the two memory buffers containing the averaged responses is calculated concurrently. The real part of this cross-spectrum is summed for all frequencies to serve as an estimate of the level of the otoacoustic emission. The noise level is estimated by the RMS of the difference of the two buffers. The time signals and TEOAE spectra are displayed on the host PC throughout the recording session.

3.2.2 Stimulation and suppression of the OAE

The signal configuration was similar to the experiments described in an earlier study (UPPENKAMP and KOLLMEIER, 1994). Narrowband tone pulses were employed as stimuli. These signals are theoretically described by STRUBE (1989) and yield a temporally localized response while keeping the stimulus bandwidth small. The time signal of such an "optimal" tone pulse is given by

$$s(t) = e^{-0.005(\omega t)^2} \cos(\omega t) \qquad (3.1)$$

The stimulus frequency was individually selected for each subject on the basis of the individual spectrum of a wideband-evoked TEOAE. Typically, most of the recorded energy is concentrated in a few spectral regions. Such a prominent component was selected for the subsequent narrowband stimulation.

The frequency of the suppressor tone was selected to be an odd harmonic of half of the stimulus repetition rate f_r in order to cancel completely in the averaged signal:

$$s(t) = \sin\left(2\ \ (2n+1)\frac{f_r}{2}t\right) \qquad \text{with } n \in \mathrm{N}. \tag{3.2}$$

Weighted averaging is performed based on the RMS value of the sum of two successive frames. Thus, the suppressor does not decrease the signal-to-noise ratio of the measurement and the artifact rejection properties of the averaging technique is maintained irrespective of the suppressor used.

3.2.3 Subjects

Four normal hearing male subjects, aged from 26 to 32 years participated voluntarily in this study. The subjects reported no previous hearing problems and showed normal results in clinical routine audiometry. One subject (TB) has a spontaneous emission at 1553 Hz. The other subjects had no measurable SOAE at the frequency region of interest.

3.3 Results and Discussion

Three different averaging techniques are used to extract both parts of the emission, synchronized to the transient stimulus and synchronized to the continuous tone. A schematic representation of these conditions is given in Figure 3.1.

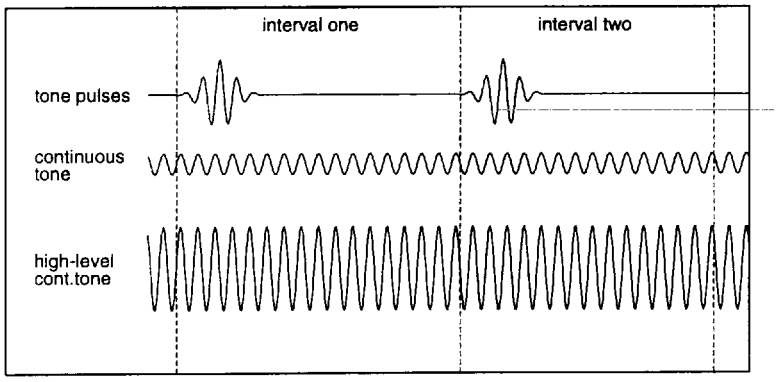

Figure 3.1: Schematic representation of the stimuli employed. A Gaussian-shaped tone-burst and a continuous tone are presented simultaneously. The tone-burst is played at same phase in two consecutive single intervals (i.e. Interval one, Interval two) while the continuous tone exhibits a phase difference of 180 degree. In experiment I, the sum of successive segments is calculated during averaging, leading to those parts of the response which are synchronized to the tone-burst. In experiment II, the difference of successive segments is calculated to extract the response synchronized to the continuous tone. In addition, a response to a continuos tone at a higher level is subtracted after appropriate scaling to separate the nonlinear part of the response due to simultaneous emissions from the primary tone. In experiment III, intervals one and two are averaged separately and corrected for the linear response.

Experiment I

In the first experiment, the influence of stimulus level and suppressor level on the suppression effect on narrowband-evoked TEOAE is studied. The top trace of Figure 3.2 shows the narrowband TEOAE from subject JV without suppressor.

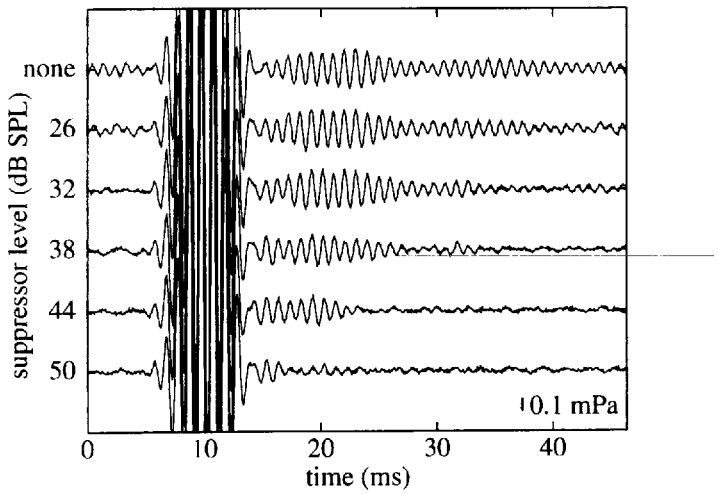

Figure 3.2: Experiment I (sum of successive segments). The traces show narrowband-evoked OAE from normal hearing subject JV (right ear). The frequencies of the continuous tone and carrier of the tone burst were 1000 Hz. Top trace: without suppressor, lower five traces: suppressed TEOAE. The level of the suppressor tone varies between 26 dB SPL and 50 dB SPL (18 dB HL to 42 dB HL). The level of the tone pulse is 40 dB SPL p.e. (24 dB HL) in all traces. The level and the temporal extent of the TEOAE decrease with increasing suppressor level. Note that the suppressor is eliminated in the averaging procedure and not visible in the recorded signals.

The level of the tone pulse stimulus is set to 40 dB SPL peak equivalent (24 dB HL) in all traces. The lower five traces are recorded in presence of a suppressor tone. The level of this suppressor varies from 26 dB SPL to 50 dB SPL (18 dB HL to 42 dB HL). The level of the respective suppressor is given at the left-hand side for each trace. As the suppressor level increases (from top to bottom), two effects can be observed: the level of the emission decreases and the temporal extent of the emission is reduced. Whereas the extent of the unsuppressed TEOAE stretches more than 30 ms

after the stimulus, the temporal extent is reduced to a few milliseconds for the highest suppressor level.

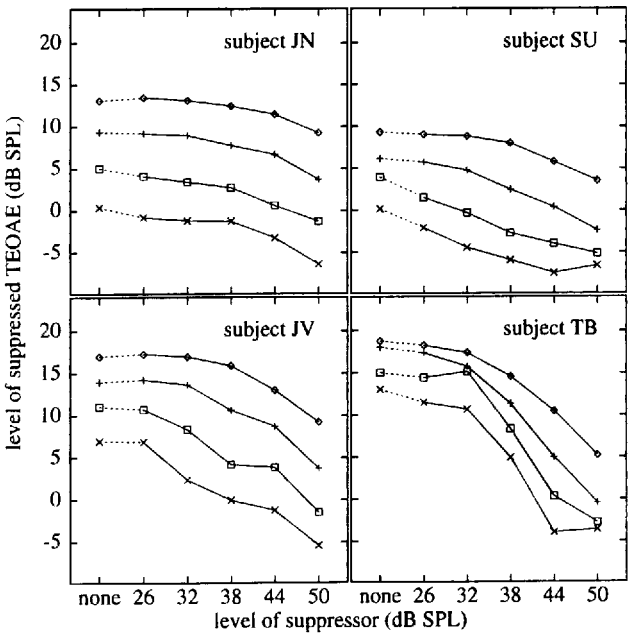

Figure 3.3: Level of the suppressed TEOAE from experiment I for all subjects. The connected points show the TEOAE level for the same tone pulse level as a function of the suppressor level. The level of the tone pulse increases from bottom to top in steps of 6 dB (from 28 dB SPL p.e. to 46 dB SPL p.e.). Tone-burst and continuous tone frequencies were 807 Hz (JN), 1000 Hz (SU, JV), 1500 Hz (TB).

The influence of the suppressor level on the level of the emission is summarized for all subjects in Figure 3.3. The connected points show the TEOAE level for the same tone pulse level as a function of the suppressor level. At high stimulus levels (top traces in all four panels), the suppression effect is small for moderate suppressor levels and exhibits a marked increase (i.e., lower TEOAE-level) with increasing suppressor level. The maximum slope of the curves in Figure 3.3 is in the order of 1 dB/dB. At low stimulus levels (bottom traces in Figure 3.3), the suppression effect is

observable even for moderate suppressor levels and the TEOAE can be completely suppressed, i.e., the emission level is reduced to the noise floor of approximately -8 dB SPL.

Discussion of Experiment I

The results of the first experiment are consistent with findings from the literature (e.g., KEMP, 1979). The observed TEOAE level reduction can be explained by both explanations given in the introduction: a reduction of the emitted energy (explanation 1) or a partly synchronization of the emitted OAE energy to the suppressor tone (explanation 2). A measurement of this synchronized energy would help to distinguish between the two explanations. Thus, the following second experiment was designed to track the "missing energy".

Experiment II

The acoustical stimulation of the ear is identical for experiments I and II. As opposed to the first experiment, a different averaging technique is utilized: Instead of summing up subsequent recording segments, the difference of successive segments was calculated. Thus, any signal components that are identical in successive segments are eliminated (such as the tone pulse) and those components of the emission that exhibit an alternating polarity remain in the measurement (such as the suppressor). The resulting averaged signal is dominated by the continuous suppressor tone. In order to cancel this dominant signal, a level-corrected response to a high-level tone (50 dB SPL) is subtracted from each measurement. This procedure resembles the recording method of SEOAE (KEMP and CHUM, 1980b).

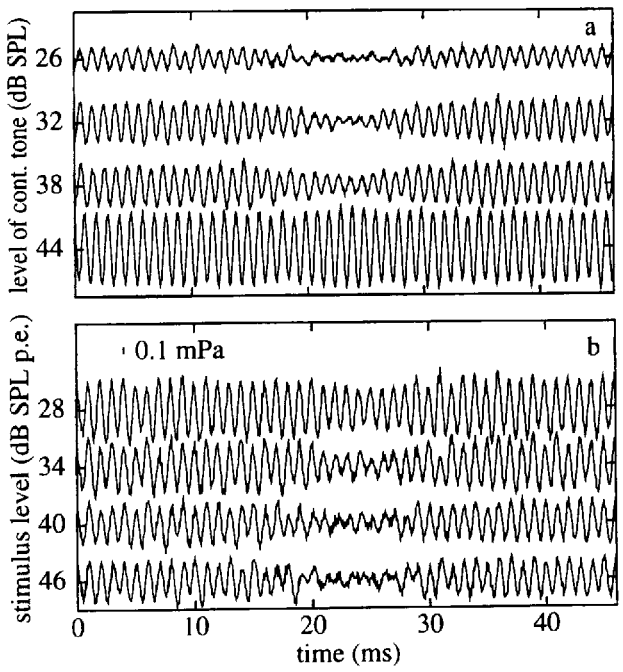

Figure 3.4: upper panel: Experiment II (difference of successive segments). The traces result from the subtraction of the response to a high-level tone from the response to a tone of the level given on the ordinate. The resulting signal is a SEOAE. Same acoustical stimulation and subject as in Fig. 3.2. lower panel: The level of the tone pulse varies between 28 dB SPL p.e. whereas the level of the continuous tone is fixed (26 dB SPL).

Figure 3.4a shows the resulting signals for different levels of the continuous tone and a fixed tone pulse level of 24 dB HL. The acoustical stimulation of the ear is the same as for the results shown in Figure 3.2. The tone pulse (24 dB HL) causes a dip in the SEOAE. The influence of the tone pulse is decreasing with increasing level of the continuous tone.

The influence of the level of the tone pulse is demonstrated in Fi gure 3.4b. The level of the continuous tone is 26 dB SPL and the level of the tone pulse is varied. The magnitude of the dip varies with the tone pulse level: a small dip occurs in the case of low tone pulse levels (which is evoking a

small TEOAE) whereas a large dip occurs in the case of a high tone pulse levels (which is evoking a large TEOAE).

The results for Figure 3.4 can be summarized as follows:

- In Figure 3.4a, the recorded "SEOAE" increases with increasing level of the continuous tone (from top to bottom). Although this is expected from the literature it should be noted that the high-level stimulus used to eliminate the stimulus component in the recorded signal is only 6 dB larger than the highest level employed[3] (top trace of Figure 3.4a). A further increase in the stimulus level would decrease the recorded SEOAE because the SEOAE is based on the difference of the two signals.
- A marked dip in the recorded SEOAE can be observed between 17 and 27 ms.
- The temporal extent of the dip in Figure 3.4a varies with the level of the continuous tone. Although the temporal extent of the dip can not be estimated in a reliable way in all traces, a comparison with the temporal extent of the first emission package (Figure 3.2) shows a similar decline with increasing level of the continuous tone.

Discussion of Experiment II

The result of the second experiment can be interpreted in two ways: a) The synchronized portion of the TEOAE in experiment I is traced by subtracting successive frames. As a side effect of subtracting the high-level continuous stimulus tone, a continuous SEOAE is recorded that adds to the synchronized portion of the TEOAE; b) A SEOAE is recorded in the presence of an additional tone pulse. The interpretation of the temporal dips in Figure 3.4 follows directly from this symmetry argument.

The continuous tone and the tone pulse can both be viewed as being either stimulus or suppressor. With the continuous tone as stimulus, a reduced SEOAE can be expected in the presence of a suppressing tone pulse in a similar way as a reduced TEOAE can be expected in the presence of the suppressing continuous tone.

One possible outcome of experiment II could have been an increase of the SEOAE during the temporal extent of the TEOAE. This hypothetical additional energy might have originated from that portion of the narrowband

3 The highest stimulus level is restricted by the range of the A/D converters since a fixed amplification gain is required for a satisfactory elimination of the continuous tone.

TEOAE in experiment I which is now synchronized to the continuous tone. This hypothetical result would only occur if the TEOAE and the SEOAE are independent of each other and the recorded response is a (linear) superposition from both processes. In this case, the relative phase of both types of emissions would be a crucial parameter that controls positive or negative interference.

To rule out this interference effect as an explanation of the dip in the second experiment, experiments I and II were repeated with a phase variation of the tone pulse relative to the phase of the continuous tone for two subjects. The starting phase changes in 12 steps of $\pi/6$, while the suppressor level and tone pulse level are fixed to 26 dB SPL and 46 dB SPL p.e. respectively.

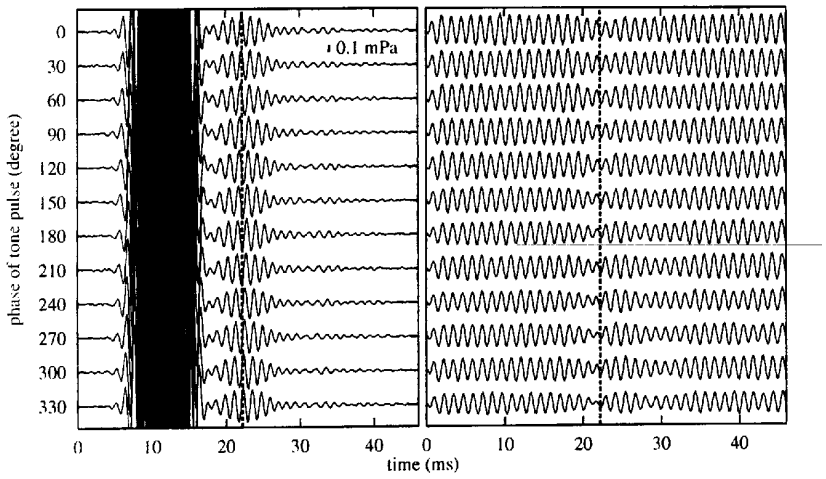

Figure 3.5: Repetition of Experiment I and II for 12 different starting phases of the tone pulse, subject JN, right ear, frequencies of tone-pulse and continuous tone: 807 Hz. The suppressor level is 26 dB SPL and the level of the tone pulse is 46 dB SPL p.e. in all traces. The results of the repetition of experiment I are shown in the left panel and the results of the repetition of experiment II are shown in the right panel. The vertical dotted line in both panels at the maximum of the first TEOAE package is drawn to demonstrate the phase shift in the left panel.

The left panel of Figure 3.5 shows the TEOAE according to experiment I. The vertical dotted line is centered at the maximum of the first TEOAE package to demonstrate the phase effects. The phase of the TEOAE strictly

follows the phase of the stimulus. The level of the TEOAE remains unchanged although the phase of the tone pulse significantly alters the envelope of the stimulus, e.g., the sum of the continuous tone and the tone pulse. The right panel shows the SEOAE according to experiment II. The small variations in the SEOAE (decreasing amplitude from top to bottom trace) originates from the limited reproducibility of the second experiment due to the subtraction of the high-level continuous tone. Small variations in one of the two signals strongly influence the amplitude of the difference signal. The temporal dip in the right panel varies slightly in shape and depth. However, the SEOAE exhibits a temporal reduction in amplitude irrespective of the phase. This result demonstrates that the dip observed in the SEOAE recordings can not be explained as a superposition of the TEOAE and SEOAE since in the case of a superposition the dip would have changed into a peak at certain phases.

The observed reduction of OAE energy in the second experiment thus provides evidence that the total energy of the otoacoustic emission is divided up into one component constituting the TEOAE and another component constituting the SEOAE. The energy of the TEOAE should be in the same order of magnitude than the energy that is missing in the SEOAE. In the experimental data, the energy of the TEOAE from experiment I should thus correlate with the reduction of SEOAE energy due to the dip.

To test the hypothesis, the RMS value of the suppressed TEOAE is calculated in a time window that encloses the first emission package. These values are correlated to the RMS of the energy that is missing in the SEOAE. The energy reduction due to the dip is estimated by subtracting the energy of the time window used for the TEOAE evaluation from the energy in an earlier reference window of the same duration.

Figure 3.6 gives a scatterplot of the resulting energy estimates for all subjects and conditions tested (crosses). The correlation coefficient of the points in Figure 3.6 is 0.61 and the slope of the linear least squares fit is 0.40. Although the energy reduction in the SEOAE is on the average larger than the "remaining" TEOAE energy and the correlation between both quantities is low, the result of Fig. 3.6 does not contradict the assumption that the total energy of both types of otoacoustic emissions (i.e., TEOAE and SEOAE) is conserved. Such a conservation of energy is consistent with a synchronization (explanation 2) rather than a "true suppression" (explanation 1). However, the evidence from experiment II is not totally convincing because the conservation of energy can not be proved directly.

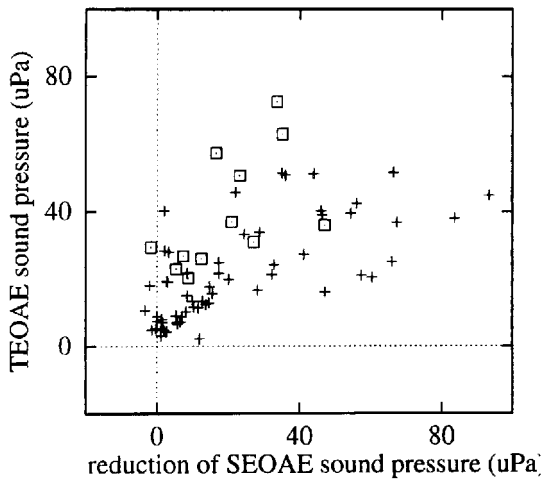

Figure 3.6: Comparison of the TEOAE energy with the estimated energy reduction due to the dip in the SEOAE for all subjects. Each cross symbol represents the results according to experiment I and II for identical levels of the tone pulse and continuous tone. The box symbols represent the results from experiment III (cf. next section).

To measure the proposed synchronization of the OAE to either the tone pulse or the continuous tone in a more direct way, a third experiment was conducted where the TEOAE and the SEOAE are recorded during the same measurement.

Experiment III

In the third experiment, the acoustical stimulation is the same as in experiments I and II: a continuous tone with alternating polarity in successive segments and a tone pulse with a fixed phase are presented. As opposed to experiments I and II, the responses from two successive segments are recorded and averaged separately. This differs from experiment I

where the sum of both segments was averaged and from experiment II where the difference was averaged. To avoid an asymmetry in the envelope of the sum stimulus between the first and the second segment, the phase of the tone pulse was set to ±90°, relative to the phase of the continuous tone. As in experiment II, a level-corrected response to a continuous tone of 50 dB SPL was subtracted from the recorded signals in order to eliminate the dominant continuous tone. Since a summation of the two segments was interpreted as a TEOAE in experiment I, any components of the signal that are identical in two subsequent segments are regarded as TEOAE. Similarly, all signal components that exhibit alternating polarity in the two segments are interpreted as SEOAE (according to experiment II).

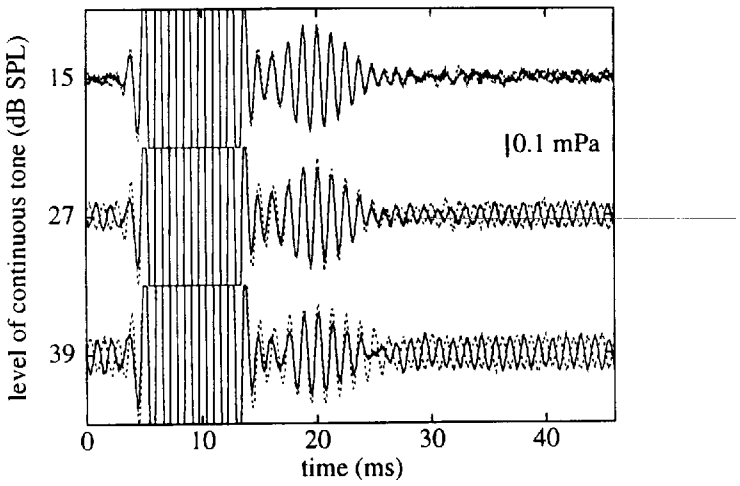

Figure 3.7: Experiment III (separation of successive segments). Recorded responses for subject JN using a continuous tone with alternating polarity and a tone pulse with fixed polarity in subsequent segments. The averaged recordings from the first segment (solid line) and from the second segment (dotted line) are plotted onto each other. Any identical components are interpreted as TEOAE (according to experiment I) and all signal components that exhibit alternating polarity are interpreted as SEOAE (according to experiment II). The level of the continuous tone varies from 15 dB SPL (top panel) to 39 dB SPL (bottom panel).

Figure 3.7 shows the resulting responses at three different levels of the continuous tone for subject JN. Each trace shows the averaged signal in the first and second segment plotted onto each other. The level of the continuous tone is 15 dB SPL in the top panel. The evoked TEOAE (identical components) is comparable to the results of the first experiment and virtually no SEOAE (components with alternating polarity) are detectable. In the middle trace and in the bottom trace (levels of the continuous tone of 27 dB SPL and 39 dB SPL, respectively), the TEOAE decreases while the SEOAE increases. The energy portion of the TEOAE and the estimated energy reduction in the SEOAE in the corresponding time segment are calculated according to the procedure in the discussion of experiment II. The results are included in Figure 3.6 as squares. The arrangement of these data points conforms with the hypotheses of the conservation of energy (cf., discussion of experiment II).

A detailed inspection of the two lines in Figure 3.7 reveals that the responses denoted by the dotted and solid lines exhibit different amplitudes. The dotted lines represent the responses to the segment in which the tone pulse exhibits a phase shift of +90° relative to the phase of the continuous tone. The TEOAE is larger for these cases, compared to the solid lines which represent the responses to the segment in which the tone pulse exhibits a phase shift of –90° relative to the phase of the continuous tone. This asymmetry can not be attributed to influences of the envelope since a phase shift of +90°/–90° raises the sum of the continuous tone and the tone pulse by the same factor of $\sqrt{2}$.

Discussion of Experiment III

The third experiment allows the simultaneous observation of the effects from experiment I and II. An off-line summation of the two signals reproduces the result of experiment I and an off-line subtraction reproduces the results of experiment II. The advantage of the third experiment is the simultaneous assessment of those parts of the emission that are synchronized to the tone pulse and those parts of the emission that are synchronized to the continuous tone. The recorded OAE signal obviously changes its behavior in the two plotted traces. Within the section where the tone pulse is dominant (17 ms to 27 ms in Figure 3.7), the emission follows the tone pulse and thus exhibits identical polarity in both lines. Outside this temporal section, the emission follows the continuous tone and thus exhibits alternating polarity in the two subsequent intervals.

The separation of the response in the two intervals reveals another effect of the interaction of the OAE with the two stimuli: The degree of interaction is determined by the relative phases of the two stimuli. This relative phase is a crucial parameter that determines the ability of a tone to entrain a TEOAE component that was previously synchronized to a continuous tone of the same frequency. This effects was predicted for the synchronization of SOAE in WILSON and SUTTON (1981): They noted that, "depending on the exact mechanism involved, there may be a greater propensity to advance the phase than to retard it, or vice versa". According to the results shown in Figure 3.7 the relative phase of the tone pulse and the continuous tone determines the synchronization. The potential of a tone pulse to advance an OAE that is previously synchronized by a tone is greater than the potential to retard it. This phase effect is not visible in the repetition of experiment I and II with different tone pulse starting phases. Thus, the phase effects seem to cancel in the summation and in the subtraction of the responses as performed in experiments I and II.

The results of the previous experiments (the dip in the SEOAE and the correlation of the partial OAE energies) did provide strong evidence that the suppression of OAE is caused by synchronization effects. The results of this section demonstrate in detail that otoacoustic emissions can be synchronized to the one or the other stimulus, according to their levels and relative phases. The separation of the response in the two successive intervals in experiment III finally exposes the cause of the suppression effect in experiment I. In the presence of a continuous tone of sufficient level, the TEOAE is partly synchronized and the TEOAE level reduction becomes just visible in the summation of the two traces. The first explanation for the suppression effect given in the introduction thus describes the cause of the suppression effect wrongly since the total emitted OAE energy is not reduced whereas explanation two seems to be correct.

3.4 Conclusions

The results of this study provide strong evidence that the suppression of narrowband-evoked TEOAE is a result of synchronization and the subsequent elimination of the synchronized energy in the cancellation technique. Hence the total energy of the OAE remains constant. In the light of these results, the shape of an "OAE suppression tuning curve" reflects that part of the emitted OAE that exhibits a forced oscillation with the frequency of the continuous suppressor. Thus, an "OAE suppression tuning curve" does not characterize the amount of emitted OAE energy. However, since the synchronization of OAE depends on the properties of the auditory filter, "OAE suppression tuning curves" may be regarded as an objective measure of frequency selectivity in the auditory system.

4 Two Tone OAE Generation

Summary

Experiments on otoacoustic emissions (OAE) in presence of a continuous tone and tone bursts and their interaction are discussed. A residual is calc u-lated from the response of the human ear to these stimuli. This nonlinear residual response method was first described by KEMP and SOUTER (1988). The principle of the measurement paradigm and the origin of the recorded residual signal is discussed in detail. The experiments show that the level of the residual strongly depends on the input levels of the stimuli. If the two tones are presented at different frequencies, several distortion products are observable. As an extension of the method described before, broadband stimuli were applied to record the response over a wide frequency range within a single measurement. The advantages and disadvantages of this approach are discussed.

4.1 Introduction

KEMP and SOUTER (1988) first described a nonlinear residual response method to record otoacoustic emissions. This method employs a "self canceling" stimulus and probe tone. A residual can be measured from normal hearing subjects as an effect of nonlinear interaction between the two stimuli and the simultaneously evoked otoacoustic emissions (SEOAE). KEMP et al. (1990a), BRASS and KEMP (1991) and BRASS and KEMP (1993) further investigated the effect of the stimulus level and the influence of equal and different frequencies of the two tones. The experiments presented by them show that the residual is delayed with respect to the onset of the tone bursts. This latency is frequency dependent and comparable to the delay of TEOAE (KEMP, 1978) and DPOAE (MAHONEY and KEMP, 1995). The level of the residual is maximal for similar frequencies of the tone-burst and the continuous stimulus.

In the case of different frequencies, SEOAE and distortion product otoacoustic emissions (DPOAE) contribute to the residual simultaneously. The level of the SEOAE-component at the frequency of the continuous tone is reduced in this case. This emission can be thought of as a zero-order distortion product (BRASS and KEMP, 1991).

The primary aim of this study is to further clarify the underlying generation mechanism for the residual described above by performing experiments on the level growth of SEOAE. Further, the level of SEOAE and DPOAE is measured as function of the spectral distance of the two stimuli. Finally, a broadband tone complex is utilized to record a broadband residual and artifacts that emerge at high stimulus levels are discussed.

4.2 Method

The experiments described in this study are based on the simultaneous presentation of a continuous tone and two tone bursts. As in KEMP and SOUTER (1988), a periodically repeated time segment is subdivided into four intervals (I_1 , I_2 , I_3 and I_4). The duration of these intervals is 46.4 ms (1024 data points at a sampling rate of 22.05 kHz) in our experiments. In contrast to

the position of the tone bursts described by Kemp and co-workers, the starting point of the tone bursts were set to the beginning of the intervals (with 4.5 ms sin2 - ramps and a duration of 31 ms, cf. Fig. 4.1). The continuous tone exhibits a phase difference of p in successive intervals. The continuity of this tone requires that the frequency follows the condition $f_n = (2n+1)\, f_r /2$ (with f_r being the interval rate and $n \in N$).

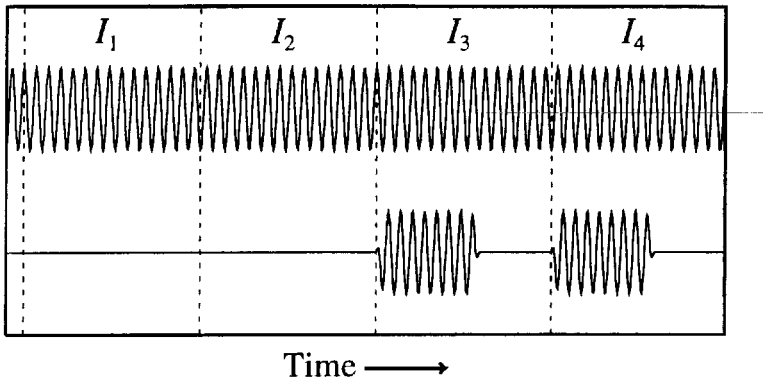

Figure 4.1: Sketch of the presented stimuli: a continuous tone with alternating polarity in successive intervals (denoted as I_1 , I_2 , I_3 and I_4) and two tone bursts with identical polarity. The vertical lines denote the beginning of the intervals.

With S_1, S_2, S_3, S_4 denoting the signals recorded in the intervals I_1 , I_2 , I_3 and I_4 resp., a residual $R = (S_1 - S_2) - (S_3 - S_4)$ is calculated from the averaged microphone signals recorded in the ear canal. The identical tone burst stimuli - and any simultaneous (linear or nonlinear) responses to the tone bursts - cancel in the second term. The continuous tone, on the other hand, adds in $S_1 - S_2$ and in $S_3 - S_4$, but cancels in the subsequent subtraction. A residual thus emerges from the difference in the signals $S_1 - S_2$ and $S_3 - S_4$ caused by a nonlinear interaction of the two stimuli. Consequently, the residual found in a cavity (artificial ear) should just contain the background noise without any periodic components (cf. Fig. 4.3, middle panel). The stimuli were presented with the ILO92 probe (Otodynamics LTD). This probe contains one microphone and two separate speakers to avoid und e-

sired nonlinear intermodulation of the stimuli. The microphone output is connected to a measurement amplifier (Brüel and Kjaer 2610) with a total gain of 50 dB. The amplified signal is sampled at a rate of 22.05 kHz using 16 bit A/D converters on a signal processing board (DSP32C, Ariel corp o-ration). All signal analysis is done digitally on the signal processing board, including signal averaging into two separate memory buffers, artifact reje c-tion, calculation of the residual and Fourier analysis.

Three experiments were performed. In the first experiment, the fr equencies of the continuous tone and the tone bursts were both set to 1001 Hz to study the level growth function of the SEOAE component. In the second experi-ment, different frequencies were used for the two stimuli to record DPOAE simultaneously. The third experiment extends the differential r ecording technique to broadband stimulation. The stimulus applied in this experi-ment is a complex of continuous tones at frequencies that are odd multiples of half the interval rate $f_r / 2 = 10.8$ Hz.

$$\text{tone complex}(t) = \sum_n \sin\left(2\pi(2n+1)\frac{f_r}{2}t + \varphi_n\right) \qquad (4.1)$$

Each individual component of the tone complex shows a phase shift of p at the beginning of successive averaging frames. In order to obtain a noise-like signal, the starting phase is randomly chosen for all components.

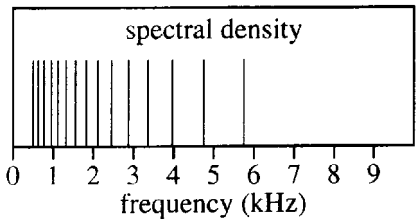

Figure 4.2: Power spectrum of a tone complex. The spacing of the harmonics is aligned to the bark scale (approximately one component per critical band). The tone complex extends from 500 Hz to 6000 Hz

Due to the logarithmic place-frequency transformation in the cochlea, this tone complex would concentrate most energy in the basal part of the basilar membrane. In order to provide a uniform excitation, an incomplete harmonic series is employed where the spacing of the harmonics is varied according to the bark scale (ZWICKER and TERHARDT, 1980). With this distribution of the harmonics, approximately the same power falls within

each critical band. The tone complexes utilized in this study exhibit a spectral range from 500 Hz to 6000 Hz and a spacing of 1 Bark (approximately one component per critical band). The power spectrum of such a tone complex is given in Fig. 4.2.

Five normal hearing subjects, one female and four male, aged from 22 to 32 years participated voluntarily in this study. One ear was tested for each subject. No subject had spontaneous otoacoustic emissions. The subjects reported no previous hearing problems and showed normal results in clinical routine audiometry. The subjects were seated in a sound-insulated chamber (IAC403A) to record the otoacoustic emissions.

4.3 Results

Figure 4.3 demonstrates the principle of the nonlinear residual response paradigm. The frequency of the continuous tone and the frequency of the tone bursts were both set to 1001 Hz for this purpose. The amplitude of the tone bursts is two times the amplitude of the continuous tone (the level of the continuous tone was 45 dB HL). The top panel of Figure 4.3 shows the averaged microphone signal in the third interval (S3), recorded in a 1.5 cm3 cavity. In this interval, both signals are simultaneously present (cf. Fig. 4.1). The center panel of Figure 4.3 shows the residual $R = (S_1 - S_2) - (S_3 - S_4)$ as recorded in the cavity with the same stimuli. This signal represents the background noise. The bottom panel of Figure 4.3 shows the residual recorded in the left ear of subject JN. A narrowband signal can be seen between 12 and 45 ms. The delay with respect to the tone burst is 8 ms. This is typical for the latency of the 1000 Hz component in transiently evoked OAEs. The signal component between 0 ms and 5 ms originates from the tail of the residual that extends beyond a single interval.

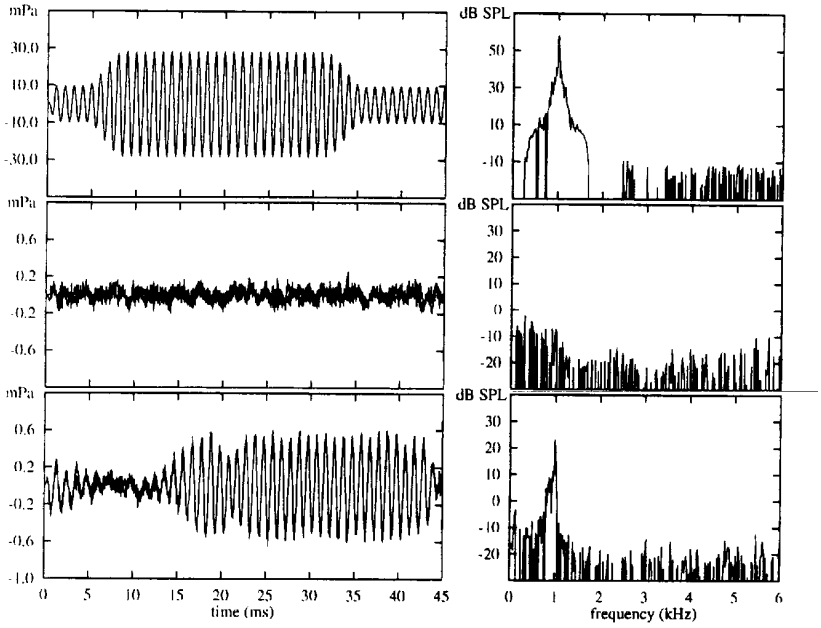

Figure 4.3: Top panel: Signal S_3 (recorded in Interval I_3). Both stimuli contribute to this signal. The power spectrum shows a peak at 55 dB SPL. Center panel: The residual $R = (S_1 – S_2) – (S_3 – S_4)$ recorded in a 1.5 cm3 cavity with the same stimuli. Note that the scale of the top panel is enlarged by a factor of 50. Bottom panel: The residual $R = (S_1 – S_2) – (S_3 – S_4)$ recorded in the left ear of subject JN with the same stimuli. The residual is delayed with respect to the tone burst (cf. the top panel) by 8 ms. The level of the residual is 23 dB SPL.

Experiment I

Figure 4.4 demonstrates that the level of the residual depends on both the strength of the otoacoustic emission and on the level and frequencies of the two stimuli. In the left panel of Figure 4.4 the level of the residual is plotted as a function of the stimulus level for two subjects. The level of the

continuous tone is given on the abscissa. The amplitude of the tone burst follows the amplitude of the continuous tone in a fixed ratio of 2:1 (the tone burst level is 6 dB above the level of the continuous tone). In both subjects, the level of the residual increases at a rate of approximately 1 dB/dB for stimulus levels below 40 dB HL and saturates for higher levels. The right panel of Figure 4.4, on the other hand, shows the level of the residual as a function of the level of the tone burst for the same two subjects. In this case, the level of the continuous tone was fixed at 45 dB HL. Negative values on the abscissa denote a lower level of the tone burst and positive values denote higher tone burst levels. The results from both subjects demonstrate that no residual is detectable for a tone burst level of 10 dB below the level of the continuous tone. Thus, the tone pulse can not influence the SEOAE at or below this level. With increasing tone burst level the level of the residual increases at a rate of approximately 2 dB/dB and saturates for a tone burst level 10 dB higher than the level of the continuous tone.

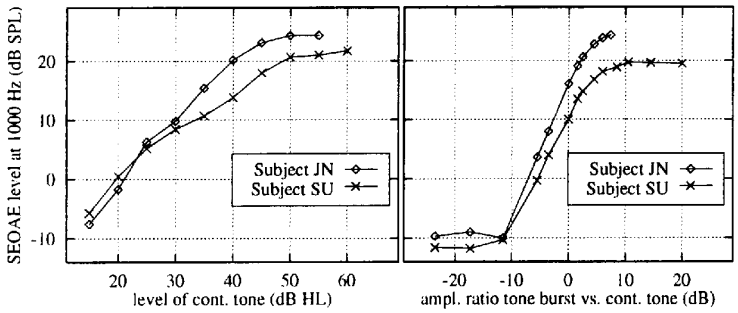

Figure 4.4: Left panel: Level of the residual as function of stimulus level. In these experiments the ratio of the amplitudes was 2:1 (tone burst vs. cont. tone). Right panel: the level of the residual as a function of the level of the tone burst at fixed level of the cont. tone of 45 dB HL for the same subjects. The values on the abscissa denote a ratio of the amplitudes of the stimuli (positive values represent higher tone burst levels).

Experiment II

The choice of different stimuli reveals another feature of the described nonlinear residual response method. Figure 4.5 gives an example from subject SU for a measurement with different frequencies for tone burst and co ntinuous tone.

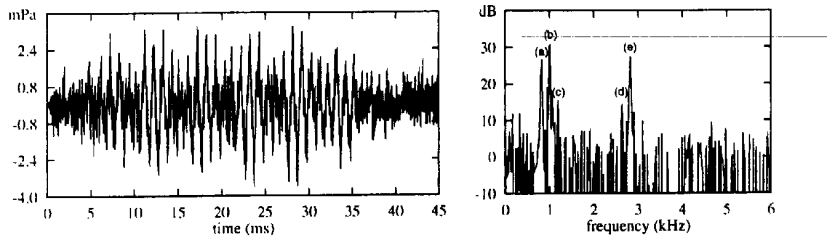

Figure 4.5: Residual from subject SU with different stimulus frequencies. Continuous tone (f2): 1001 Hz at 45 dB HL; tone burst (f1): 1819 Hz at 51 dB HL. The following components can be observed: a) f1–f2 at 818 Hz (26.7 dB SPL), b) f2 at 1001 Hz (30.6 dB SPL), c) 3f2–f1 at 1184 Hz (15.6 dB SPL), d) 2f1–f2 at 2637 Hz (27.4 dB SPL) and e) f1+f2 at 2820 Hz (14.4 dB SPL). Note that no component is visible at f1 (1819 Hz).

The right panel of Figure 4.5 shows the spectrum of the residual. The SEOAE can be seen as component (b). The other prominent lines indicated as (a), (c), (d) and (e) are distortion product emissions. The levels of the most frequently observed distortion products are summarized for four su bjects in Table 4.1 for a frequency of the continuous tone of 1001 Hz.

Table 4.1 demonstrates that only the "SEOAE" component at f2 is o bservable in any of the tested conditions. The detection of the component at 2f1–f2 is increasingly difficult if the frequency of the tone burst approaches the frequency of the continuous tone since the level of the DPOAE decreases and the limited duration of the residual implies spectral smearing in the data analysis. The data in Table 4.1 also shows that the level of the comp onent at f1 depends on the frequency of the tone burst.

		Subject SU				Subject SL		
f_1	$L(f_2)$	$L(f_2-f_1)$	$L(2f_1-f_2)$	$L(f_1+f_2)$	$L(f_2)$	$L(f_2-f_1)$	$L(2f_1-f_2)$	$L(f_1+f_2)$
506	21.1	23.5	---	24.9	5.0	6.8	---	-1.3
807	25.2	21.9	23.2	23.9	20.7	---	22.1	---
915	30.2	---	20.0	25.7	25.1	---	17.7	2.2
958	30.7	---	24.7	24.4	23.4	---	10.8	4.7
1001	34.9	---	---	22.9	27.4	---	---	-1.8
1065	31.5	---	---	18.7	24.6	---	8.9	2.3
1108	30.7	---	---	19.7	24.4	---	8.4	4.0
1216	28.4	22.6	19.2	25.2	25.5	---	9.1	0.4
1410	28.7	25.4	---	20.3	23.4	---	---	---
1819	30.6	26.7	14.4	27.4	13.3	---	---	---
2400	29.4	24.4	12.7	24.1	13.4	---	--	---
	$L(f_2)$	Subject MG				Subject MM		
f_1		$L(f_2-f_1)$	$L(2f_1-f_2)$	$L(f_1+f_2)$	$L(f_2)$	$L(f_2-f_1)$	$L(2f_1-f_2)$	$L(f_1+f_2)$
506	8.6	2.3	---	---	-1.4	---	---	---
613	16.8	---	---	---	2.6	---	---	---
721	24.3	---	10.9	---	4.0	3.9	7.8	---
807	28.6	---	13.5	---	9.6	---	---	---
893	31.0	---	13.0	---	11.4	---	9.0	---
915	31.9	---	11.1	11.3	14.4	---	10.1	---
936	32.9	---	---	13.5	16.5	---	8.2	---
958	31.8	---	---	12.4	17.3	---	---	---
979	32.6	---	---	12.8	18.3	---	---	---
1001	33.9	---	---	13.3	21.8	---	---	---
1044	24.0	---	---	---	19.6	---	---	---
1065	25.8	---	---	---	20.2	---	---	---
1130	25.7	---	---	---	20.2	---	---	---
1216	26.5	---	---	---	20.4	---	10.1	---
1302	26.2	---	-2.0	---	19.5	---	---	---
1475	25.8	---	---	---	16.2	---	2.1	---
1668	21.0	---	---	---	13.8	---	---	---
1819	16.7	---	---	---	3.4	---	---	---

Table 4.1: Levels of the most prominent components in the spectrum of the residual from measurements with different frequencies of the cont. tone and the tone bursts (experiment II). The frequency of the continuous tone (f_2) is fixed at 1001 Hz at 45 dB HL and the frequency of the tone burst at 51 dB HL varies.

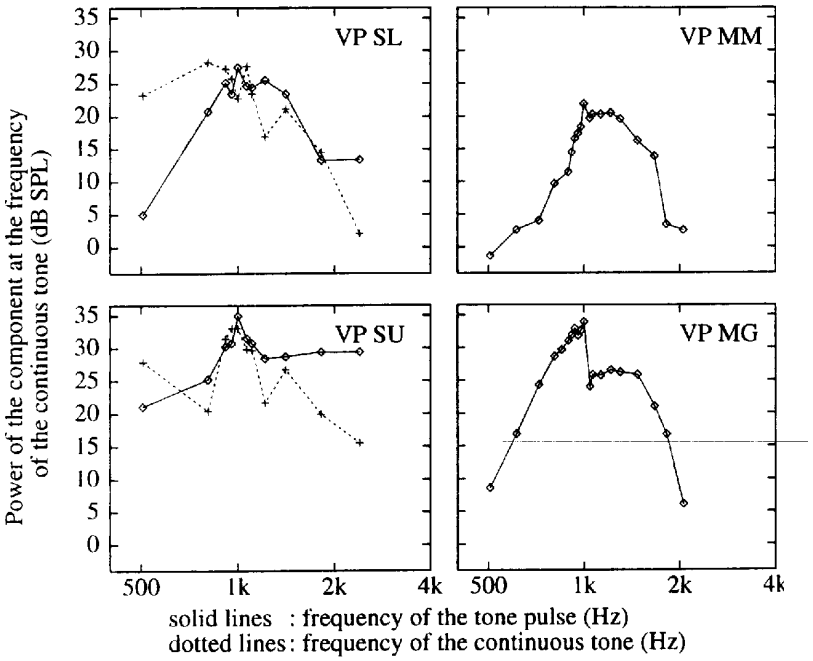

Figure 4.6: Solid lines: Level of the 1001 Hz component in the residual for four subjects as function of tone burst frequency. Dotted lines: level of the continuous tone in experiments, where the frequency of the tone burst was fixed to 1001 Hz and the frequency of the continuous tone is varied. The abscissa gives the frequency of the continuous tone for this data.

The solid lines in Figure 4.6 show the level of the SEOAE component as function of the frequency of the tone burst for the same subjects as listed in Table 4.1. The level of the residual is maximal in all panels if the frequencies of the tone burst and of the continuous tone are identical. The OAE level decreases with increasing difference between the frequencies of the two stimuli. The dotted lines in the two left panels (subjects SL and SU) represent the results of an experiment in which the frequency of the tone burst was fixed to 1001 Hz and the frequency of the continuous tone is var-

ied. The level of the continuous tone is plotted over the frequency of the continuous tone in this case. The shape of the resulting (dotted) lines does not show the same structure as the results from the previous experiment at a fixed frequency of the continuous tone. This variability might originate from variations in the SEOAE level across frequency, because data from different frequencies of the continuous tone is compared in this case.

Experiment III

Figure 4.7 shows the results from a measurement with broadband stimulation (subject JN, left ear). The level of the applied continuous tone complex was set to 35 dB HL. As in the previous experiment, the amplitude of the tone complex burst in the third and fourth interval is two times the amplitude of the continuous signal. A broadband residual can be observed. A detailed inspection of the time signal reveals that the delay of the low frequency components in the residual is comparable to the delay of the 1001-Hz-SEOAE from the same subject (cf. lower panel of Fig. 4.3). A comparison with the spectrum of the tone complex (cf. Fig. 4.2) shows that the spectrum from the broadband recording contains most components of the tone complex (except for 1325 Hz, 4750 Hz and 5740 Hz). This result is in agreement with the TEOAE spectrum from subject JN which does not contain any components at these frequencies.

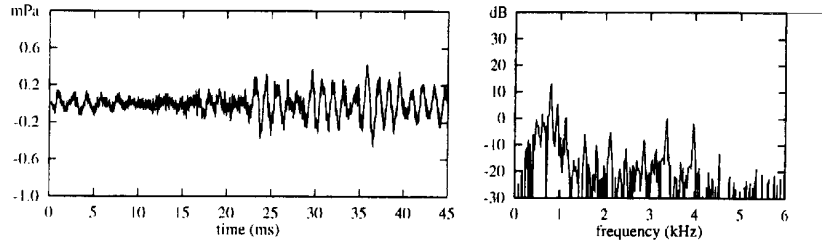

Figure 4.7: Residual from broadband stimulation with a tone complex ranging from 500 Hz to 6000 Hz (cf. Fig. 4.2)

Effects at high stimulus levels in Experiment II and III

Figure 4.8 shows the result from a measurement at a higher stimulus level from subject JN using two tonal stimuli. The level of the continuous tone was 65 dB HL (at 1001 Hz) and the level of the tone burst was set to 71 dB SPL (at 1453 Hz). The frequency of the tone burst is clearly visible in the spectrum of the residual as line (c). In addition, the latency of the residual is only about 3 ms with respect to the tone burst (cf. upper panel of Fig. 4.3).

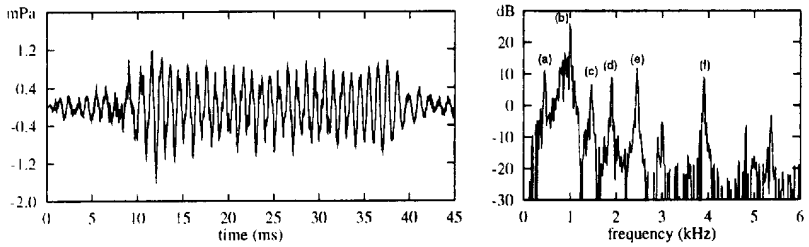

Figure 4.8: Residual from subject JN at high stimulus level: Continuous tone (f2): 1001 Hz at 45 dB HL; tone burst (f1): 1453 Hz at 51 dB HL. The following lines can be resolved: (a) f1–f2 at 452 Hz, (b) f2 at 1001 Hz, (c) f1 at 1453 Hz, (d) 2f1–f2 at 1905 Hz, (e) f1+f2 at 2454 Hz and (f) 2f1+f2 at 3907 Hz.

This result contradicts the explanation of the origin of the residual, since the tone burst and any - linear or nonlinear - responses should completely cancel in the calculation of the residual. Similar results were obtained for all other tested subjects at stimulus levels above 70 dB HL, irrespective of the spectral properties of the stimuli (broadband and narrowband). It should be noted that the experimental setup condition was thoroughly tested in the test cavity. A detailed investigation of this effect inspired the experiments described in NEUMANN et al. (1996) on the acoustic reflex. The influence of the stapedius muscle on the recorded residual signal shall be shortly illustrated: If the level of the stimuli is high enough to elicit the acoustic reflex,

the acoustic compliance of the middle ear changes. Since the interstimulus interval between the two tone bursts is 15 ms respectively 117 ms, the contraction of the stapedius muscle can only, or primarily, influence the acoustical compliance during the second stimulus. This causes a difference in the level of the recorded signals which may be interpreted, wrongly, as "residual". For a detailed description of this effect, cf. NEUMANN et al., 1996. It should be noted at this point that the effect of the acoustic reflex has to be taken into account if a residual is recorded at high stimulus levels. In order to eliminate this undesired effect, the experimental paradigm can be altered into a 6-interval setup. The continuous tone is again presented with a phase difference of p in successive intervals. Two tone bursts with identical polarity are presented in the first and fourth interval. The altered residual can be defined as $R = (S_1 - S_2) - (S_3 - S_4)$. This paradigm differs from the paradigm described by KEMP and SOUTER (1988) in the regular rhythm. The residuals recorded with the altered 6-interval paradigm are identical to the residuals recorded with the 4-interval paradigm. At high stimulus levels, however, the 6-interval paradigm does not show the effect of the acoustic reflex as described above due to the symmetry in the stimulation pattern.

4.4 Discussion

The nonlinear residual response method described in this study is not the only technique to record SEOAE or DPOAE. The problem with recording SEOAE is that the evoked OAE is present at the same time and frequency as the stimulus. The separation of these two signals has to make use of the nonlinear properties of otoacoustic emissions. One alternative paradigm for the recording of SEOAE (first reported by KEMP and CHUM, 1980a) is based on the nonlinearity of the level growth function of SEOAE. The response of the ear is recorded at low stimulus level in a first measurement and the stimulus is eliminated by subtracting the re-scaled result from a second measurement that is performed at high stimulus level. The remaining signal is dominated by the SEOAE since the contribution of the SEOAE to the second measurement is very small (ZWICKER and SCHLOTH, 1984; DALLMAYR, 1987; JURZITZA and HEMMERT, 1992). However, if the amplitude of the linear portion varies slightly in one of the measurements, the difference signal would be interpreted, wrongly, as SEOAE. The

differential recording technique presented KEMP and SOUTER (1988) has the advantage to record SEOAE in a single measurement. This approach is thus very robust against variances due to probe fitting and other temporal changes. The results presented in this study demonstrate that the nonlinear residual response method is an efficient technique to record SEOAE and DPOAE simultaneously.

Discussion of the origin of the residual

The explanation of the residual given by Kemp and co-workers (KEMP and SOUTER, 1988; BRASS and KEMP, 1991; KEMP et al., 1990a; BRASS and KEMP, 1993) is based on suppression effects. From this point of view, the continuous tone serves as stimulus and the tone burst serves as suppressor. In their contribution, KEMP and SOUTER, (1988, page 118) remarked that "The residual signal can arise from two causes, a) direct interference by the disturbing agent with the stimulus response production, which can only occur whilst the interfering agent persists at the stimulus response site, i.e. simple nonlinear suppression, and b) indirect interference, which requires that the interfering agent temporally changes the primary response mechanism's characteristics in some way". Two pages later, they state "We are sure that the phenomenon discussed below is a genuine stimulus response suppression and not a desynchronisation/resynchronisation phenomenon".

In the scope of this paper, the terms suppression and suppressor were avoided because synchronization effects of OAE can explain the observed experimental data in a similar manner. In this conjecture, both stimuli (the continuous tone and the tone bursts) have an equal potential to stimulate the OAE generator. It seems reasonable that these stimuli interact nonlinearly on the same OAE generator. The emitted OAE might thus follow the phase of the tone bursts which would result in an identical polarity of the OAE in successive intervals. In this case, the OAE cancels in the difference signals $S_1 - S_2$ and $S_3 - S_4$. Alternatively, the OAE might follow the phase of the continuous tone which would result in an OAE with alternating polarity in successive intervals. In the this case, the emission contributes to the signals in $S_1 - S_2$ and $S_3 - S_4$. If both stimuli are presented simultaneously (as in the third and fourth interval), the otoacoustic emission is partly synchronized to one stimulus and partly synchronized to the other stimulus. Thus, the residual $R = (S_1 - S_2) - (S_3 - S_4)$ represents the portion of the SEOAE

that was previously evoked by the continuous tone and is subsequently "desynchronized" to the tone bursts.

The two explanations given above present a different perspective on the level reduction of the OAE in I3 and I4. The experiments presented in this study can not distinguish between these two explanations, since a desynchronized SEOAE and a suppressed SEOAE both result in the same residual. For a detailed analysis on the suppression and synchronization of narrowband evoked OAE cf. NEUMANN et al., 1997a.

Discussion of experiment I

The left panel of Figure 4.4 demonstrates the compressive nonlinearities level growth function of SEOAE. The dependency of the OAE level on the level on the stimulus is an important attribute of OAE. Similar compressive nonlinearities in level growth functions can be found in TEOAE and DPOAE (HARRIS and PROBST, 1990).

The steep level increase in the right panel of Figure 4.4 demonstrates the strong nonlinearity of the interaction between the SEOAE and the tone burst. A growth of the SEOAE level at a rate of 2 dB/dB was also reported by BRASS and KEMP (1993) in their Fig. 6. This data resembles the growth of the level reduction of OAE by a low-frequency external tone (ZUREK, 1981). This level reduction could be caused by suppression or synchronization (NEUMANN et al., 1997a)

Discussion of experiment II

Figure 4.5 and Table 4.1 show that several combination tones are observable when the frequency of the tone pulse (f1) differs from the frequency of the continuous tone (f2). The most frequently observed distortion products are f2, f2–f1, f2+f1, –f2+f1, –f2+2f1 and 3f2-f1. Figure 4.6 shows that the spectral distance of the stimuli seem to determine the grade of interaction in the inner ear. One might ask why no OAE component at f1 and no distortion products such as 2f2–f1 can be observed in any of the recordings. All observed components originate from odd multiples of f2. The reason is, that - due to the phase settings of the continuous tone - even multiples of f2 exhibit identical polarity in successive intervals. Thus, the SEOAE does not

contribute to the signal from $S_1 - S_2$ or to the signal from $S_3 - S_4$ in this case.

The shape of these curves might be related to the bandwidth of the auditory filters, since the data represent the ability of the tone pulse to influence an OAE that is generated at the frequency of the continuous tone. However, the data displayed in Fig. 4.6 shows rather large inter-individual fluctuation. These fluctuations might partly originate from the simultaneous generation of SEOAE and DPOAE. If these "types of OAE" are generated by the same mechanism, the emitted OAE energy might be shifted from the SEOAE towards the DPOAE and vice versa. Other experiments, including the synchronization of narrowband TEOAE, provide a better correlate to subjective measures of the bandwidth of the auditory filters (cf. NEUMANN et al., 1997b).

Discussion of experiment III

The results from the third experiment shows that the SEOAE can be evoked at multiple frequencies simultaneously. One consideration of this approach is the (desired or undesired) interaction of multiple SEOAE in the cochlea. The applied tone complex is a compromise between a wide spacing of the harmonics in order to reduce this interaction to a minimum and a narrow spacing in order to test the functionality of the complete basilar membrane in a single measurement. One could expect that the level of the residual increases with multiple stimuli. The drawback of this approach is that the energy of the stimulus is spread over the stimulated frequency range. Consequently, the excitation of local OAE generators is reduced. Further research is necessary to develop an optimal broadband stimulus. This broadband approach is highly desirable since the restriction to sinusoidal stimuli clearly limits the applicability of SEOAE in a clinical environment.

Measurement at high stimulus levels

The experimental data shown in Figure 4.8 show that results obtained at high stimulus levels should be interpreted with caution. The unexpected component at the frequency of the tone burst might be related to the influence of the acoustic reflex. The influence of the stapedius reflex on OAE measurements is usually not considered in the evaluation of OAE data,

since the acoustic reflex threshold is reported to range between 80 dB HL and 100 dB HL for pure-tone stimulation in normal-hearing subjects (e.g., GELFAND, 1984). This value is derived from the detection of the change in the acoustic compliance of the middle ear. On the other hand, it should be considered that the experimental setup developed for the recording of OAE might be far more sensitive than the setup used for the detection of changes in the compliance of the middle ear. OAE recordings extensively utilize averaging techniques to improve the signal-to-noise ratio of the measurement. The computation of the difference of two acoustic signals (e.g., the nonlinear residual) is more sensitive to minor changes in these signals than merely detecting a difference in the level of two signals (as utilized for the detection of the acoustic reflex).

4.5 Prospects

The approach described in this study might combine the advantages of TEOAE and DPOAE recordings in a single measurement. However, further research on the interrelation of TEOAE and DPOAE with the residual is required prior to a possible clinical application for the prediction of the threshold of hearing.

5 Detection of the Acoustic Reflex below 80 dB HL*

Summary

A new method for detecting the acoustic reflex is introduced and discussed that utilizes standard otoacoustic emissions (OAE) recording techniques. Two successive identical tone bursts of 100 ms duration and 10 ms interstimulus interval are presented in the occluded ear canal at a repetition rate of one per second. If the acoustic reflex is elicited, the contraction of the stapedius muscle is delayed with respect to the onset of the first stimulus. Hence, the acoustic compliance in the ear canal decreases primarily during the second stimulus. The difference of the microphone signals produced by the two stimuli is computed and averaged across a certain number of repetitions of the sequence. The presentation level is increased until this difference is larger than -40 dB (with respect to the stimulus level) and if its signal-to-noise ratio exceeds 20 dB. For normal hearing subjects the acoustic reflex threshold measured with this method is on average 8 dB lower in comparison to the results obtained with a standard clinical setup. In five out of the ten tested hearing impaired subjects the new method could detect an acoustic reflex at one or more frequencies where no reflex was detected with the clinical setup.

---

* published in: Neumann, J., Uppenkamp, S., Kollmeier, B. (1996). *"Detection of the acoustic reflex below 80 dB HL",* Audiology and Neurootology 1, 359-369.
filed as patent: *"Verfahren und Vorrichtung zur Erkennung eines Reflexes des menschlichen Stapedius-Muskels",* Patentamt München, #196289785

5.1 Introduction

The recording and interpretation of the acoustic reflex is a powerful diagnostic technique in clinical audiology which is mostly included in standard audiometric testing. The absence of an acoustic reflex can result from conductive or sensorineural hearing loss, from disorders in the auditory nerve (cranial nerve VIII), or from disorders in the motor neurons in the facial nerve (cranial nerve VII). The most important parameter of the acoustic reflex is the acoustic reflex threshold (ART). This is the lowest stimulus intensity at which a contraction of the stapedius muscle can reliably be detected. Many researchers have documented that the ART ranges between 80 dB hearing level (HL) and 100 dB HL for pure-tone stimulation in normal hearing subjects (METZ, 1952; MØLLER, 1962; JEPSEN, 1963; JERGER, 1970; MARGOLIS and POPELKA, 1975; WILSON and MCBRIDE, 1978; SILMAN et. al., 1978; GELFAND, 1984). The median ART for an ipsilateral stapedius reflex is approximately 85 dB HL for pure-tone signals and 65 dB HL for a broadband noise (FRIA et. al., 1975). The individual ART provides useful information during the audiological examination of a hearing impaired patient. The acoustic reflex test has a high sensitivity for the detection of middle ear pathology. Although the ART is not directly related to the hearing threshold, the test can also help to assess a sensorineural hearing impairment and to assist the fitting of hearing aids in young children. The hearing aid user's most comfortable loudness level (MCL) setting can be related to the acoustic reflex threshold (RAPPAPORT and TAIT, 1976).

The principles of the measurement of the acoustic reflex have not changed since the investigations of METZ in 1952. The acoustic reflex is detected as a change of the middle ear compliance. Two stimuli are presented to the subject: a low frequency tone of typically 226 Hz is used to measure the compliance of the middle ear, and an additional high level tone of limited duration is used to elicit the acoustic reflex (cf. Fig. 5.1, upper panel). Various stimuli can be utilized for this purpose, such as (e.g.) broadband or filtered noise, tone pulses or sequences of tone pulses. If the level of the additional sound is high enough to elicit the acoustic reflex, the acoustic compliance decreases and the level of the measurement tone increases. The increase of the measurement tone level can be detected with a microphone

placed in the ear canal. In most commercially available sy stems, the voltage at the microphone output is maintained at a constant level by means of an electroacoustic impedance bridge. An overview of the physiology, physics and history of the acoustic reflex detection measurement can be found in GELFAND, 1990 and NORTHERN and GABBARD, 1994.

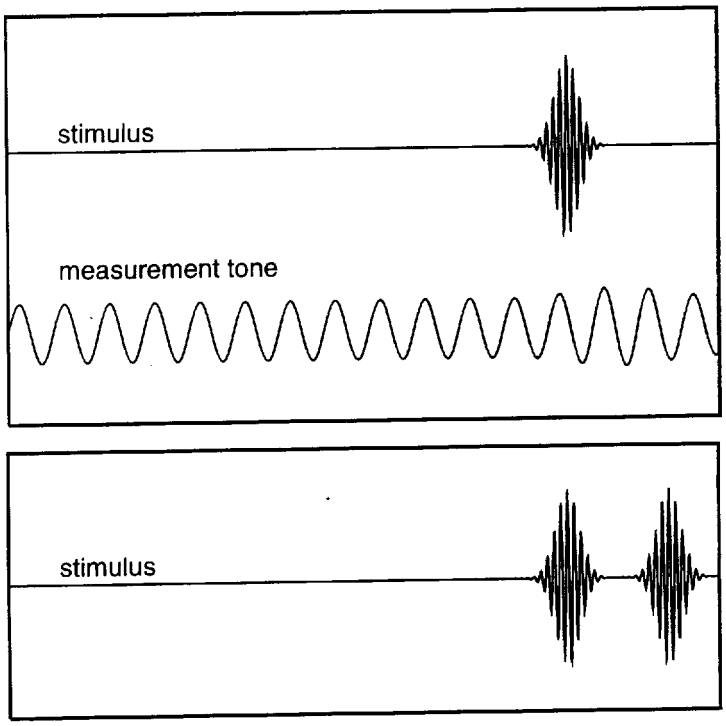

Figure 5.1: Sketch of the acoustic stimulation in experiment I (standard audiometry, upper panel) and in experiment II (new paradigm, bottom panel). In experiment I, the decrease of the acoustic compliance is detected as increase in the level of the measurement tone. In the second experiment, the decrease of the compliance is detected as difference between the responses from the two (identical) stimuli.

This study presents a new method to detect the acoustic reflex which is based on the techniques usually employed for recording of otoacoustic emissions. As opposed to the method described above, no additional measurement tone is needed. Instead, two identical short stimuli are presented in a short succession (cf. Fig. 5.1, lower panel), and the sequence is repeated at a comparatively long period. The method utilizes the fact that the acoustic reflex does not occur immediately after the onset of a stimulus. Instead, the impedance changes with a latency of 80 to 120 ms (for a quantification of the parameters of the acoustic reflex cf. SELLARI-FRANCESCHINI et. al., 1986).

5.2 Method

5.2.1 Stimuli and Experimental Setup

For all subjects employed in this study two experiments were performed. In the first experiment, a standard audiometrical examination of the acoustic reflex threshold (ART) was performed with a clinical routine impedance meter (Grason-Stadler middle ear analyzer GSI 33). This device uses ten successive tone pulses with carrier frequencies of 500 Hz, 1000 Hz, 2000 Hz and 4000 Hz to elicit the reflex (stimulus duration of 50 ms, rise time 1.5 ms, decay time 2 ms, interval between successive pulses 60 ms) and a continuous tone of 226 Hz to measure the acoustic compliance in the ear canal. A probe is used to present the stimuli and to record the measurement tone which seals the ear canal with a soft rubber olive. Each stimulus is presented at least three times at the same level. The stimulus level is increased from 70 dB HL in steps of 5 dB until an acoustic reflex is detected, the maximum output level of the setup is exceeded, or the discomfort level of the subject is reached. The acoustic reflex threshold is defined as the lowest stimulus level for which a change of the compliance is detectable in at least two traces of the three repetitions. An experienced clinician evaluated the results from the first experiment and determined the ART according to the rules used in standard audiometry.

In the second experiment, the measurement of the ART utilizes a standard setup for the recording of OAE. Two identical tone pulses are employed with the same carrier frequencies as in the first experiment and a duration of 100 ms (rise time 5 ms, decay time 5 ms; interval between successive

pulses 10 ms). Since the duration of the tone pulses matches the typical latency of the acoustic reflex, its effect primarily influences the acoustical compliance during the second stimulus. The stimulus pairs are separated by a pause of one second duration to allow for a complete recovery from the stapedius reflex. The difference between the recorded acoustic responses elicited by the two respective stimuli is calculated by the recording system employed in this experiment. For this purpose, the response signals recorded during the respective first and second stimulus have to be aligned exactly. The level of the difference signal computed from the aligned responses is the basis for the new method to determine the ART (see below).

If the stimulus level is high enough to elicit the acoustic reflex, the acoustic compliance decreases thereby increasing the amplitude of the microphone signal recorded during the second stimulus. In addition, any phase changes between the acoustic stimulus and the recorded microphone signal caused by the contraction of the stapedius muscle will increase the amplitude of the difference signal. Such a phase change cannot be detected with the conventional measurement technique which only monitors the level in the sealed ear canal.

The acoustic reflex threshold is set to the lowest stimulus level for which a difference signal is observable that meets the following criteria:

Criterion 1:	The spectrum of the difference signal shows a peak at the carrier frequency of the stimuli at least 20 dB above the background noise level calculated across an octave band centered at the carrier frequency.
Criterion 2:	The amplitude of the difference signal exceeds 1% of the amplitude of the stimuli, i.e., the level of the difference signal has to be larger than -40 dB with respect to the stimulus level.

The first criterion helps to detect the influence of the acoustic reflex since the spectral power density in nearby frequencies serves as an estimate of background noise at the test frequency. The second criterion excludes artifacts introduced by the experimental setup that occur above a stimulus level of 90 dB HL. This is necessary because at very high stimulus levels devia-

tions of the recording setup from a linear time-invariant system yield the effect that the first condition is already matched in a 1.5 cm^3 cavity.

Both experiments were performed in an IAC403A sound-insulated chamber. An ILO92 probe from Otodynamics Ltd. was utilized for the second experiment which was originally constructed to record otoacoustic emissions. It was selected because it allows presentation of high level signals without distortion. The microphone signal is passed through a low-noise amplifier including butterworth high-pass filter at 300 Hz and low-pass filter at 10 kHz to reduce noise (Stanford Research 560). The signal is digitized using a 16-bit A/D converter on a DSP-32C signal-processing board (Ariel corporation). Each tone pulse pair is presented 15 times. Then the difference of the response signals is averaged. The digital signal processor calculates the difference signal in real time and performs an automatic artifact rejection based on the power of the difference signal. Segments with high RMS values are rejected while segments with low RMS values contribute to the averaged difference signal. Throughout the recording session this signal and its power spectrum is monitored on a host PC. A peak in the spectrum indicates the component of the difference signal that is caused by the acoustic reflex.

Calibration

In order to be able to compare the results, both experiments have to be performed with exactly the same stimulus level. Therefore, a cross-calibration of the probes used in both experiments was performed. The output level of the GSI 33 middle ear analyzer was set to 70 dB HL. The ILO92 probe was then calibrated to match this level. For this purpose, the GSI probe was inserted into one end of a 2 cm^3 tube cavity. At the other end, the sound pressure level was measured with an ER-10C microphone (Etymotic Research). In a next step, the GSI probe was replaced by the ILO92 probe and the stimulus level was adjusted to yield the same level at frequencies 500 Hz, 1000 Hz, 2000 Hz and 4000 Hz. This measurement was used for calibrating the respective output levels of both probes.

To validate this calibration, the sound pressure was measured in the ear canal of one subject with a Rastronics PM12 in-situ microphone. The recorded levels of the GSI middle ear analyzer and the ILO92 probe showed only minor deviations of -1.9 dB at 500 Hz, -1.0 dB at 1000 Hz, -

0.4 dB at 2000 Hz and -4.0 dB at 4000 Hz. The calibration of the output level of the ILO92 probe thus yields a good match to the output level of the GSI 33 middle ear analyzer. The stimulus levels thus obtained were also verified subjectively by a normal hearing subject with a flat audiogram (± 5 dB). A loudness matching of the two probes performed by the subject did not yield any significant deviations from the calibration procedures described above.

Two control conditions were frequently tested in order to exclude measurement artifacts. Firstly, for both experiments, the measurements were repeated in a 1.5 cm^3 cavity to exclude any influence of the recording system (such as phase shifts or amplitude variability). If experiment I was performed with the 1.5cm^3 cavity, the compliance of the test cavity did not change in the presence of external stimuli. If experiment II was performed with the cavity employing stimulus levels above 90 dB HL, a peak was visible in the spectrum of the difference signal that is due to deviations from time-invariant system behavior in the recording system. However, the second criterion given above (i.e., minimal level of 40 dB below the stimulus level) was not reached in any case.

An additional control condition was performed for experiment II where the interstimulus interval of the two signals was increased to 500 ms and the interval between successive repetitions of the stimulus pairs was reduced to 500 ms. Hence, a symmetrical temporal pattern was achieved and the influence of the first stimulus on the recording during the presence of the second stimulus is identical to the influence of the second stimulus on the recording during the presence of the first stimulus. Each subject was tested with this control condition. Single, unaveraged difference signals can show small amplitudes in this condition since the effect of the stapedius muscle contraction is not perfectly reproducible. The fluctuations in this contraction effect is reflected in a clearly visible peak in the spectral analysis of the averaged signal. However, the averaged signal did not exceed both ART criteria in any case.

Subjects

Fourteen subjects, aged from 19 to 65 years, participated voluntarily in this study. They underwent a clinical standard examination prior to partic ipating in the experiment. Four subjects had a normal pure-tone hearing threshold on both sides, i.e. a deviation of less or equal 10 dB from the ref erence

headphone threshold between 0.25 and 6 kHz. The remaining sub jects had a cochlear hearing loss of different etiology on at least one side. Thirteen of the tested ears from these ten subjects showed a high-frequency hearing loss, two ears showed low-frequency hearing loss, two had a notch, and two ears exhibited a profound hearing loss A tympanogram was r ecorded prior to the acoustic reflex measurements to exclude static pressure differences and other middle ear dysfunctions. The shape, symmetry, and height of the tympanogram pressure curve was within the normal range for all subjects employed. The hearing loss of the tested subjects is listed in Table 5.1.

5.3 Results

Experiment I

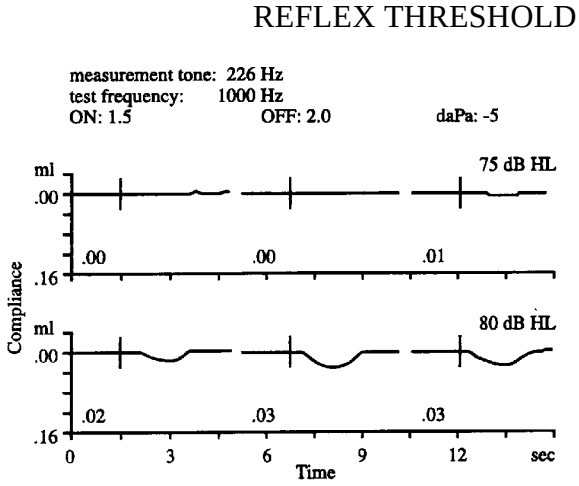

Figure 5.2: Result from experiment I for normal hearing subject JN (right ear) for a 1000 Hz probe tone with a duration of 50 ms. The figure is arranged according to the printout of the clinical impedance audiometer (GSI 33). The traces show the compliance of the middle ear as function of time in three repetitions. The vertical line indicates the onset of the stimulus. The stimulus level is given at the top right of each trace. A decrease of the compliance is detectable for a stimulus level above 80 dB HL. The numbers below the traces give the decrease in ml detected by the apparatus for each respective recording.

Figure 5.2 shows a typical example of the result from the first experiment. The figure shows the influence of the middle ear reflex on the compliance for a normal hearing subject (JN, right ear) at a stimulus frequency of 1000 Hz. The upper trace shows that no decrease of the acoustical compliance is detectable at 75 dB HL. In the lower three traces a change of the compliance is detectable at 80 dB HL. In Table 5.1 the ARTs from the first experiment are listed for all subjects. Note that the step size in presentation level is 5 dB which results in a measurement error of the ART of at least 2.5 dB. It also may cause a bias towards higher levels of up to 2 dB since the experienced clinician did not extrapolate the ART between stimulus levels if the criterion was exceeded at a given stimulus level but was not reached at a 5 dB lower level.

For subjects without hearing impairment, the stapedius reflex can be detected at most frequencies if the clinical setup is used (four center columns of Table 5.1). In several subjects, however, the acoustic reflex is not detectable at 4000 Hz. For normal hearing subjects the median ART is 87 dB HL at 500 Hz, 87 dB HL at 1 kHz, 89 dB HL at 2 kHz, and 94 dB HL at 4 kHz. These values are consistent with values reported in the literature on the acoustic reflex (e.g. [9]). As expected, the ART increases for hearing impaired subjects. In most cases, the increase of the ART is smaller than the hearing threshold [1]. This effect has been denoted as “Metz recruitment”.

Experiment II

Figure 5.3 shows the result from the second experiment for the same subject as in Figure 5.2. The difference of the microphone signals from the two stimuli is plotted for various stimulus levels. Below 70 dB HL, no signal is detectable whereas above 70 dB HL, the level of the difference signal increases rapidly. Figure 5.4 gives the level of the difference signals as a function of the stimulus level. For stimulus levels below 65 dB HL, the level of the difference signal depicted in Figure 5.4 is determined by the background noise of the recording system. Above this level, the signal increases with a slope of about 2.8 dB/dB. This abrupt and steep level increase demonstrates the strong nonlinearity of the acoustic reflex.

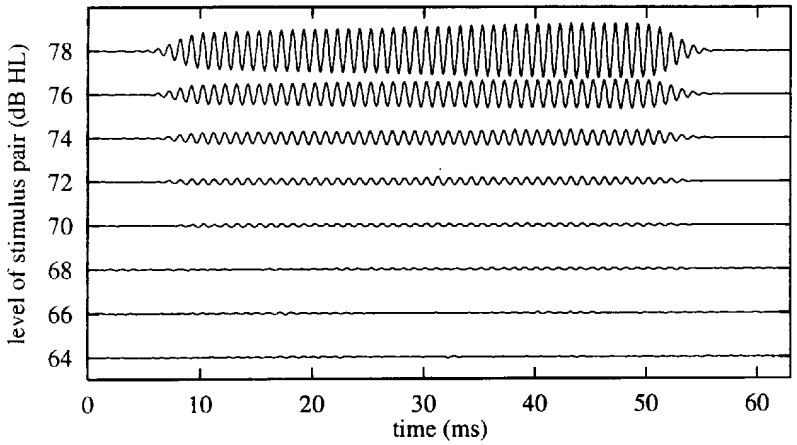

Figure 5.3: Difference of the microphone signal from the two stimuli for subject JN, right ear. The stimulus frequency was 1000 Hz. The level of the stimuli varies from 64 dB HL to 78 dB HL in steps of 2 dB.

The ART is determined in the second experiment according to the cr iteria described in the previous section. For the recorded difference signals displayed in Figures 5.3 and 5.4, the ART is 76 dB HL (cf. Table 5.1). This threshold is markedly higher than the lowest stimulus level for which an effect is visible in the Figures 5.3 and 5.4. This is due to the conservative threshold criteria employed in order to yield a high reliability of the test. Hence, these criteria produce a bias towards higher levels which amounts to approximately 10 dB for the example given in Figure 5.4 and is larger than the bias of approximately 2 dB in experiment I. One advantage of these criteria is that the ART can be based on data from only a few stimulus levels without the necessity to sample the complete level growth function. Thus, a step size in stimulus level of 5 dB might be employed that equals the size used in experiment I. Note however, that the actual step size of the increase in stimulus level employed here was 2 dB. This results in a measurement error of at least 1 dB.

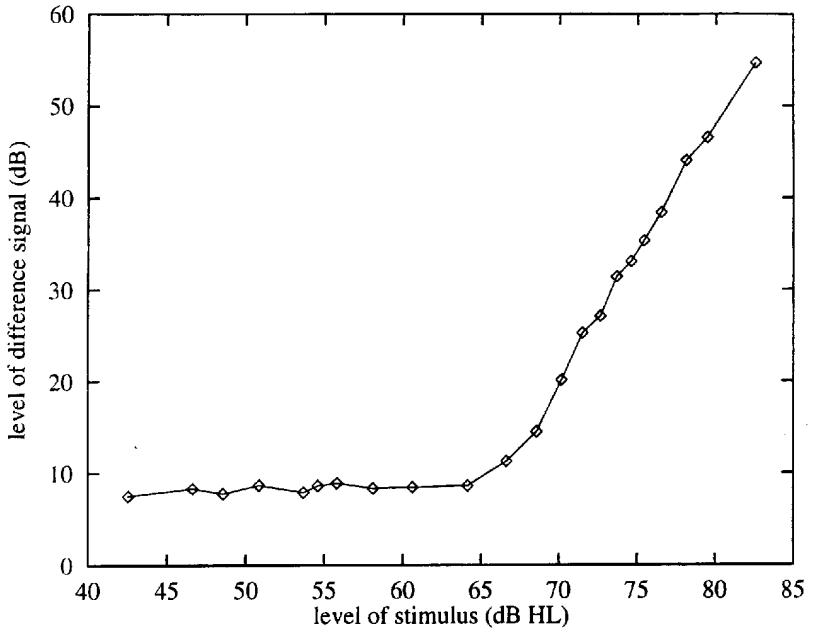

Figure 5.4: Level of the signal difference as function of stimulus level for subject JN at 1000 Hz.

The ART values from the second experiment are listed for all subjects in the four rightmost columns of the Table 5.1. For normal hearing subjects the median ART is 81 dB at 500 Hz, 78 dB at 1 kHz, 82 dB at 2 kHz and 84 dB at 4 kHz. As in the first experiment, the ART is higher for hearing impaired subjects. However, in five out of ten tested hearing impaired subjects a reflex could be detected at one or more frequencies where no reflex is detectable in the first experiment. Figure 5.5 summarizes the results for all subjects.

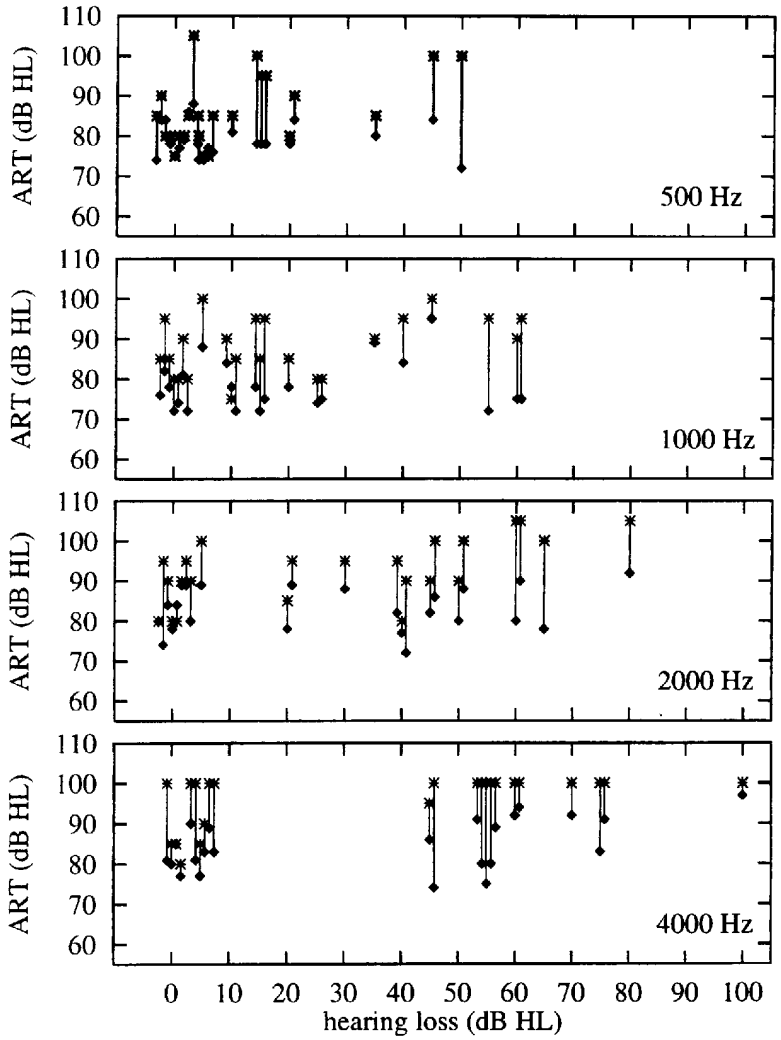

Figure 5.5: Difference between acoustic reflex threshold from experiment I (*) and from experiment II ( ). In each panel the data are ordered as function of hearing loss. In most cases the ART from experiment II is lower than the ART from experiment I.

		Hearing Loss[dB HL]				ART (Exp. I) [dB HL]				ART (Exp. II) [dB HL]			
Subj.	Side	0.5	1	2	4	0.5	1	2	4	0.5	1	2	4
JN	left	0	0	0	5	85	85	90	>100	79	74	84	81
JN	right	0	0	0	0	80	80	80	>100	78	76	78	81
SU	left	0	0	0	0	85	80	80	80	78	72	80	77
SU	right	0	0	0	5	85	85	90	>100	74	76	80	83
TD	left	0	0	0	5	85	90	95	90	86	81	89	83
TD	right	0	0	0	0	80	85	90	85	84	78	89	85
HR	left	0	5	0	5	>105	>100	>95	>100	89	88	74	89
HR	right	0	0	0	5	90	95	90	100	84	82	84	90
BM	left	0	10	5	70	75	90	100	>100	75	84	89	>92
BM	right	5	10	20	60	75	75	95	100	77	78	89	>92
EW	left	15	15	30	60	100	95	95	>100	78	78	88	>94
EW	right	15	10	20	45	95	85	85	95	78	72	78	86
MR	left	35	40	45	0	85	95	100	85	80	84	86	77
MR	right	20	35	45	0	80	90	90	85	78	89	82	80
KS	left	5	25	40	55	80	80	80	>100	74	74	77	80
KS	right	0	20	40	55	80	85	95	>100	77	78	82	80
FN	left	5	15	40	55	85	85	90	>100	76	72	72	68
FN	right	10	25	50	45	85	80	90	>100	81	75	80	68
HB	left	20	60	60	55	90	90	>105	>100	84	75	80	89
HB	right	15	60	60	55	95	95	>105	>100	78	75	>90	>91
IW	right	5	15	80	100	75	95	>105	>100	74	75	>92	>97
JK	left	50	55	65	75	100	95	100	>100	72	72	78	>83
JK	right	45	45	50	75	100	100	100	>100	84	95	88	>90
KS	right	75	70	>100	75	---	---	---	---	>92	>92	>85	>88
IL	right	80	>100	>100	>100	---	---	---	---	>94	>89	>88	>91

Table 5.1: Acoustic reflex threshold (ART) from the first and second experiment for all subjects. The subjects are arranged according to their average hearing loss.

Comparison of the results from both experiments

The panels in Figure 5.5 show the results from both experiments for the four tested frequencies respectively. The results from the subjects are arranged according to their respective hearing loss at that particular frequency. With rare exceptions, the ART from experiment II (rhombi) is lower than the ART from experiment I (crosses). The median difference between the ART from the standard setup and the new method is 6 dB for 500 Hz, 9 dB for 1000 Hz, 10 dB for 2000 Hz and 10 dB for 4000 Hz. Note, however, that this difference would be larger if a less conservative threshold criterion would have been used in experiment II. At 4000 Hz, a valid ART could not be detected for most hearing-impaired subjects in experiment I whereas a valid ART estimate below 100 dB HL could be obtained in experiment II. This demonstrates the poor sensitivity of the first experiment at 4000 Hz.

5.4 Discussion

The results of this study can be summarized as follows:

1. The difference signal of the acoustic responses to two successive identical stimuli can be used to detect the acoustic reflex.
2. The average acoustic reflex threshold obtained with the difference method (second experiment) is 8 dB lower than in the one obtained with the standard procedure.
3. At 4000 Hz, a valid ART estimate can be obtained for many subjects with the new method although no ART was obtained with the clinical standard method employed in the first experiment.

It should be noted that the second experiment was inspired by experiments in the recording of simultaneously evoked otoacoustic emissions (NEUMANN, 1996, unpublished data). It is known that the onset of otoacoustic emissions exhibits a frequency dependent time delay (latency) in comparison to the onset of the acoustical stimulation. One might thus argue that otoacoustic emissions influence (or cause) the results of these experiments. However, the difference signal in the second experiment can not be explained as an effect of otoacoustic emissions because of several reasons. Firstly, no difference signal is observable below a tone-pulse level

of 60 dB HL in the second experiment, whereas otoacoustic emissions can be observed at much lower stimulus levels. Furthermore, two of the subjects in this study showed a strong difference signal in the second experiment although no otoacoustic emissions were recordable in these subjects. They were tested for spontaneous otoacoustic emissions, transitory evoked otoacoustic emissions and simultaneously evoked otoacoustic emissions. Finally, some subjects reported that they could sense the contraction of the stapedius muscle for stimulus levels above the measured acoustic reflex threshold.

Similar arguments hold to verify that the effect reported for experiment II is not due to artifacts or nonlinearities of the apparatus at high stimulus levels. To exclude such effects, several control conditions were measured (c.f. "Methods" section). Also, the absence of an acoustic reflex in profoundly hearing-impaired ears (subjects KS and IL, cf. Table 5.1) can be considered as additional evidence that the difference signal observed in experiment II is not caused by artifacts of the setup.

With respect to the second result (lower ART for the second experiment) it should be noted that the sensitivity in detecting the ART is higher for the new method because of several reasons: Firstly, the new method utilizes artifact rejection and signal averaging to increase the signal-to-noise ratio of the "target" frequency component produced by the acoustic reflex. In the standard setup, on the other hand, the stimulation is only repeated three times and the interpretation of the result is based on three unaveraged traces (cf. Fig. 5.2). The evaluation of the ART from this technique necessitates the interpretation of the data by an experienced clinician who can visually detect and exclude traces with artifacts. This procedure might result in an increase in sensitivity and reliability that is comparable to the averaging and artifact rejection utilized in the new method at least in some cases. On the average, however, the more formal noise reduction employed in the new method might explain a part of the quantitative difference in the ART for the two methods.

The second reason for the higher sensitivity of the new method is that - in contrast to the first experiment - no low frequency measurement tone is required. In the first experiment, low-frequency noise from the recording system or from the subject (due to breathing, movements or blood circulation) produces some variability in the level of the low-frequency tone which may limit the accuracy of the results from the first experiment. With the

new method, however, the influence of low-frequency noise is eliminated both by high-pass filtering of the recorded microphone signal and by separating the "target" spectral component from the background noise in the frequency domain.

The third reason for the higher sensitivity of the new method is that the difference of two acoustic signals is computed. This difference is more sensitive to minor changes both in the phase and time-dependent level of the signals than merely detecting a change of the total level (as utilized in the standard setup). The contraction of the stapedius muscle changes both the magnitude and the phase of the acoustic signal recorded in the sealed ear canal. Even small changes in the phase of the acoustic signal recorded during the second stimulus can notably increase the amplitude of the difference signal. Since these phase changes do not influence the level of the measurement tone they can thus not be detected in the first experiment. Hence, these phase effects obviously contribute to the higher sensitivity of detecting the acoustic reflex with the new method.

The method employed in experiment II appears to be advantageous for audiological routine examinations for the following reasons:

The stimulus levels typically presented in a standard ART test can - if not carefully selected - exceed the uncomfortable level (UCL) in some subjects. This might even cause some damage to the inner ear and hence limits the applicability of ART tests for infants and patients with a sudden or noise-induced hearing loss. A more sensitive ART test that yields reliable results at lower stimulus levels might therefore still be applicable with these patients.

The fact that the test yields a reliable ART estimate even at high frequencies where standard ART methods fail makes this method applicable for objectively assessing hearing in neonates and infants. It should be noted, however, that no absolute threshold estimation can be performed with this method. Instead, ART measurements are often used to objectively estimate the MCL (or the UCL). Therefore, this new method might also be helpful for the prescription and adjustment of hearing aids for infants.

The time required for the new method is proportional to the number of averages. In this study, 15 averages were used for each stimulus level spaced with a step size of 2 dB. For a clinical application of this test, a

reduced number of averages and an increased step size might be sufficient. Thus, the duration of the measurement is comparable to the standard clinical setup. The interpretation of the experimental data, on the other hand, is eased by the artifact rejection and signal averaging.

The apparatus required for administering the new technique is the same as used for the recording of evoked OAE. Since this apparatus has become widely available, the new method described here should easily be added to the routine hearing screening program that employs OAEs at various audiological centers.

5.5 Conclusions

The differential recording method presented in this study is capable of detecting a contraction of the stapedius muscle at stimulus levels well below the levels reported in the literature on the acoustic reflex. This test might help to improve the diagnostic potential of the acoustic reflex.

6 Relations between notched-noise suppressed TEOAE and the psychoacoustical critical bandwidth*

Summary

Narrowband transitory evoked otoacoustic emissions (TEOAE) were recorded for nine normal hearing subjects in the presence of a broadband tone complex suppressor. Introducing a spectral notch at the frequency of the narrowband stimulus causes the suppression effect to decrease, the more so the wider the notch. This decrease in suppression permits an estimate of the size of one critical band. One advantage of this approach is that no active participation of the subjects is required. The estimated critical bandwidth is then compared with independent estimates based on a simultaneous masking experiment, using the same stimuli. The two measures of the critical bandwidth coincide well for those six subjects with spontaneous otoacoustic emissions. However, the bandwidth estimate based on the OAE measurements is too large for the other three subjects without spontaneous emissions. Simulations of the suppression effect with a driven van der Pol oscillator with moderate undamping produce critical bandwidth estimates consistent with those observed in the psychoacoustical experiments. This allows an estimate of the "effective" amount of undamping on the basilar membrane that is required to produce the critical bandwidth observable in psychoacoustic experiments.

---

* published in: Neumann, J., Uppenkamp, S., and Kollmeier, B. (1997a). *"Interaction of otoacoustic emissions with additional tones: Suppression or synchronization?"* J. Acoust. Soc. Am., in press.

6.1 Introduction

The recording of otoacoustic emissions allows one to obtain data on the peripheral hearing system without any active participation of the subject. Clinical interest in otoacoustic emissions is typically focused on the determination of hearing thresholds. The spectrum of transitory evoked otoacoustic emissions (TEOAE) or the distortion product otoacoustic emissions (DPOAE, "DPgram") usually serve as an estimate of the audiogram. However, otoacoustic emissions are mostly measured with stimuli well above the threshold of hearing so that they might relate better to suprathreshold phenomena than to the audiogram. Therefore, otoacoustic emissions might help in determining functional parameters of the inner ear that relate to parameters derived from suprathreshold psychoacoustical tests.

One of the most important parameters of this kind is the critical bandwidth (CBW). It describes the width of the frequency band within which spectral energy of a masker is integrated (FLETCHER, 1940; GREENWOOD, 1961; ZWICKER and FELDTKELLER, 1967). The size of one critical band also has great importance for experiments that study the interaction of tones within the auditory system. For example, the level of a perceived cubic difference tone decreases for a ratio of the primaries f_2 and f_1 larger than 1.2 (GOLDSTEIN, 1967; HALL, 1972; SMOORENBURG, 1972; WEBER and MELLERT, 1975). Similarly, the level of combination tones measured as distortion product otoacoustic emissions (DPOAE) in the ear canal vary with the spectral distance of the primaries f_2 and f_1 (HARRIS et al., 1989; GASKILL and BROWN, 1990).

BROWN et al. (1993) quantitatively compared this "characteristic of the DPOAE-filters" with the psychoacoustical critical bandwidth expressed as equivalent rectangular bandwidth (ERB) for each of a set of subjects. The CBW was determined in a forward masking experiment using noise maskers with differing spectral notchwidth according to PATTERSON (1976). BROWN et al. concluded that the DPOAE-tuning curve may serve as an estimate for the size of one critical band. One problem with these OAE-experiments is that the stimuli and procedures to estimate the critical bandwidth differ considerably from those utilized in the psychoacoustical experiment. Since experimental paradigms as well as the assumed shape of

the auditory filter significantly influence the estimates of the CBW (KOLLMEIER and HOLUBE, 1992), a quantitative comparison between the CBW based on DPOAE and the CBW based on masking experiments seems to be difficult for the experiments described so far.

The experiments presented here therefore use the same stimuli for measurements of the suppression of narrowband TEOAE and for psychoacoustical CBW measurements. The OAE experiments are based on the observation that TEOAE can be synchronized by additional tones (KEMP, 1979, KEMP and CHUM, 1980a; WILSON, 1980; WIT et al., 1981, ZWICKER and SCHLOTH, 1984; LONG et al., 1988). In the case of TEOAE or synchronized spontaneous otoacoustic emissions (SOAE), the effect of an additional sinusoid decreases with increasing spectral distance to the suppressed emission component. The variation of this distance allows the recording of characteristic "tuning curves" based on the level of the suppressed TEOAE (UPPENKAMP and KOLLMEIER, 1994). This tuning curve exhibits a bandwidth that approximates one critical band, with Q_3 varying between 3 and 8 for subjects with SOAE and Q_3 varying between 1 and 3 for subjects without SOAE. However, the relation between this effect and the critical bandwidth measured with psychoacoustical methods is not yet completely understood.

In contrast to the experiments described by UPPENKAMP and KOLLMEIER (1994), a broadband tone complex with a variable spectral notch is used in this study. This tone complex serves as suppressor in the TEOAE recordings and as masker in the notched-noise masking experiments. In both experiments, the width of the notch in the tone complex is varied. In addition, the same tone pulse is used in both experiments. In the TEOAE-experiments the tone is used to evoke the otoacoustic emission, whereas in the psychoacoustical masking experiment it serves as the signal that the subject is requested to detect.

6.2 Methods

Experimental setup for OAE measurements

Otoacoustic emissions are recorded in an IAC403-A sound-insulated chamber. The acoustic stimulation of the ear is carried out with an insert ear

phone (Etymotic Research ER-2), which has a flat frequency response up to 10 kHz. The acoustic signal is recorded in the sealed ear canal with a miniature electret microphone (Knowles EA 1843). The microphone sensitivity, including a pre-amplifier with a gain of 46 dB, is 1.55 V per Pa at 1000 Hz. The output of the pre-amplifier is connected to a custom-designed amplifier with a gain of 20 dB. The signal is then passed through a butterworth high-pass filter with a cut-off frequency of 200 Hz to reduce low-frequency noise. The signal is digitized using a 16-bit A/D converter on a signal-processing board (Ariel corporation DSP-32C) and recorded in two separate memory buffers.

The digital signal processor is used to calculate the root-mean-square of the signal in real time. Noise reduction is carried out by an averaging technique that uses the inverse of the RMS value of the response to the signal as a weighting factor. These segments have a duration of 46 ms, yielding a stimulus rate of 21.6 Hz. Segments with high RMS values are rejected and segments with little noise receive a high weight. Furthermore, the cross-Fourier-transform of the two buffers is calculated concurrently. The real part of this cross-spectrum is summed for all frequencies to serve as an estimate of the level of the otoacoustic emission. The noise level is estimated by the RMS of the difference of the two buffers. The time signals and TEOAE spectra are displayed on the host PC throughout the recording session.

Subjects

Nine normal hearing subjects, aged from 23 to 34 years, 5 male and 4 female, participated voluntarily in this study. They all exhibit normal hearing, as indicated by ear inspection and routine audiometry. Six subjects show spontaneous otoacoustic emissions (SOAE). For three subjects the level of the SOAE is more than 14 dB above the noise floor which exhibits a spectral power density of approximately $14\,\mathrm{mPa}/\sqrt{\mathrm{Hz}}$ (i.e. -3 dB SPL / Hz)

OAE experiments

The experimental procedure can be subdivided into four steps:

Step 1:	Broadband stimulation of TEOAE to select a prominent spectral component.
Step 2:	Recording of narrowband-evoked TEOAE at a low stimulus level at the frequency of a prominent spectral component.
Step 3:	Suppression of the narrowband TEOAE with suppressors of variable notchwidths.
Step 4:	Evaluation of the CBW from changes in the suppression effect.

These four steps are described in detail in the following sections and illustrated by exemplary measurements for a normal hearing subject (BG). This subject has a spontaneous otoacoustic emission (SOAE) at 1058 Hz (cf. Fig. 6.1).

Broadband stimulation of TEOAE

In the first step, a broadband TEOAE is recorded in nonlinear averaging mode according to BRAY and KEMP (1987) at a stimulus level of 40 dB SPL peak equivalent. The stimulation utilizes a short chirplet signal with spectral power in the range of 500 Hz to 6000 Hz (cf. NEUMANN et al., 1994). In contrast to click stimuli, chirplet signals allow an optimal stimulation of any frequency range, narrowband as well as broadband. In addition, chirplet signals contain more energy than a click stimulus with the same maximum amplitude. Figure 6.2 shows the chirplet-evoked TEOAE from subject BG and a sketch of the broadband chirplet stimulus as an insert at the left panel.

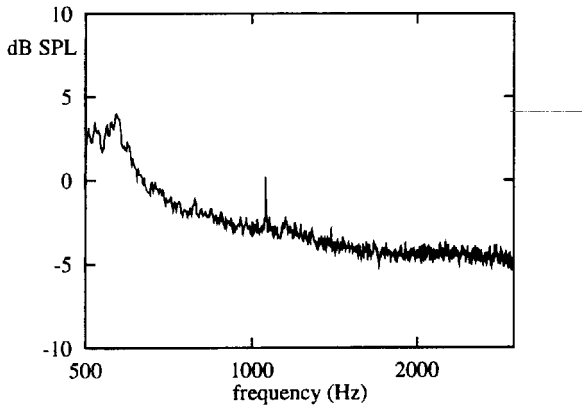

Figure 6.1: Spontaneous otoacoustic emission (SOAE) from the left ear of normal hearing subject BG. The ordinate gives the spectral power density in dB SPL. The component at 1058 Hz is 3.2 dB above the noise floor.

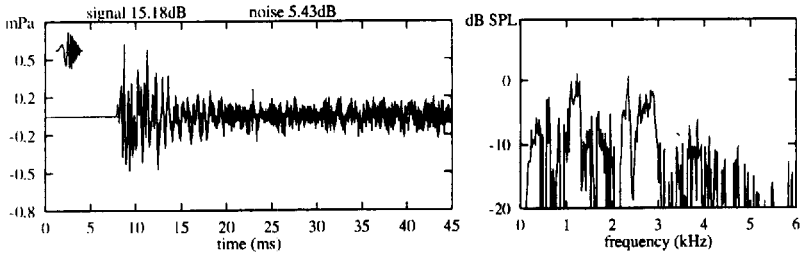

Figure 6.2: Otoacoustic emissions from normal hearing subject BG. Left: time signal of chirplet-evoked TEOAE, right: spectrum of the TEOAE. The insert at the left panel shows the broadband chirplet stimulus employed. The TEOAE spectrum of this subject shows a typically peaked structure with major components between 500 Hz and 3000 Hz. The component at 1058 Hz is selected for narrowband stimulation.

Narrowband stimulation of TEOAE

In the second step, a prominent component is selected from the spectrum of the recorded broadband emission. In some cases this component is a synchronized spontaneous otoacoustic emission. For example, the SOAE at 1058 Hz of subject BG is visible as one major peak in the TEOAE spectrum. This component is selected for the subsequent narrowband stimulation.

The stimulation with a tone pulse is always a compromise between the limited maximal duration of the stimulus and the concentration of the spectral power. An optimal tone pulse with a Gaussian envelope and a constant relative bandwidth of $Df_{3dB} = 0.17$ is employed. These tone pulses are theoretically described by STRUBE (1989) and were utilized for OAE recordings by UPPENKAMP and KOLLMEIER (1994). The time signal of such a tone pulse is given by

$$s(t) = e^{-0.005(\omega t)^2} \cos(\omega t) \qquad (6.1)$$

The duration of this tone pulse varies with the center frequency. For example, a 1000 Hz tone pulse has an amplitude above 1% of the maximum for a duration of 9.7 ms. The recording of the TEOAE is performed in linear averaging mode. The stimulus level is successively reduced until the emission disappears in the background noise. The output level of the acoustic transducer is then set 10 dB above this level. As an example, Figure 6.3 shows the narrowband-evoked emission for subject BG where a stimulus frequency of 1058 Hz and a stimulus level of 18 dB SPL peak equivalent was used.

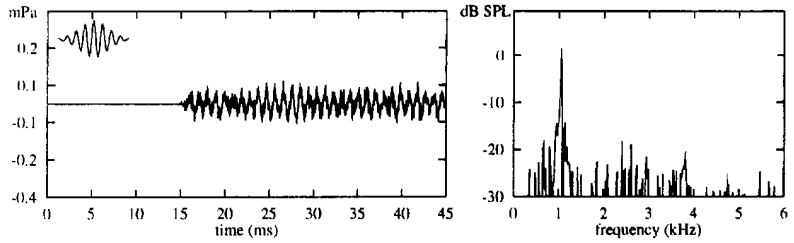

Figure 6.3: Narrowband-evoked TEOAE from subject BG at low stimulus level (same data representation as in Fig. 6.2). The insert at the left panel shows the tone pulse stimulus employed. The carrier frequency of the tone pulse is 1058 Hz. The SOAE clearly contributes to the transitory evoked otoacoustic emission in this case.

Suppression of the narrowband TEOAE

In the third step, the TEOAE is suppressed with a broadband tone complex. This suppressor is designed to cancel out during the averaging procedure in order not to interfere with the recording procedure of the TEOAE. Therefore, a complex of continuous tones is generated at frequencies that are odd harmonics of half the stimulus rate $f_r / 2 = 10.8$ Hz:

$$\text{tone complex}(t) = \sum_n \sin\left(2\pi(2n+1)\frac{f_r}{2}t + \varphi_n\right) \qquad (6.2)$$

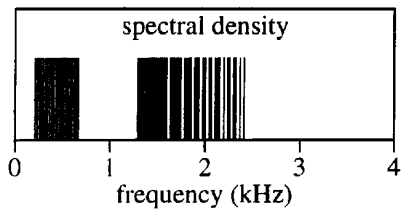

Figure 6.4: Power spectrum of a tone complex with an incomplete harmonic series (10 components per critical band in two octaves) that is used as suppressor signal. A spectral notch of 300 Hz is placed at 1000 Hz. The omitted frequency components are added at the spectral boundaries. The harmonics of the resulting tone complex extend from 380 Hz to 2180 Hz.

Each individual component of the tone complex shows a phase shift of p at the beginning of successive averaging frames. In order to obtain a signal with a noise-like waveform within each period, the starting phase j_n is randomly chosen for all frequency components. If the averaging procedure is based on pairs of successive frames, the suppressor is canceled out in the resulting signal. The weighted averaging for noise reduction is also based on the RMS value of pairs of successive frames. Thus, the suppressor has no influence on the weighted averaging and the noise reduction thus achieved. Due to the logarithmic place-frequency transformation in the cochlea the tone complex described so far would concentrate most energy in the basal part of the basilar membrane. In order to provide a uniform excitation by the suppressor, only an incomplete harmonic series is employed where the spacing of the harmonics is varied according to the bark scale (ZWICKER and TERHARDT, 1980). With this distribution of the harmonics, approximately the same power falls within each critical band. The tone complexes utilized in the experiments exhibit a spacing of 0.1 Bark (10 components per critical band). The complexes extend across a minimum spectral range of two octaves centered around the probe tone frequency. A spectral notch with variable bandwidth is placed at the frequency of the tone pulse. In order to keep the total power of the suppressor constant for different values of the notch, the spectral extent of the suppressor is varied. The same number of frequency components that is omitted in the region of the notch is added symmetrically both at the upper and lower spectral boundary of the original tone complex to keep the signal power constant. The width of the spectral notch was varied in the experiments from 0 Hz to 400 Hz in 10 steps of increasing size. An example of the power spectrum of such a notched tone complex is given in

Fig. 6.4. To obtain a strong suppression effect, the level of the suppressor is set higher than the level of the tone pulse. Figure 6.5 shows the narrowband TEOAE in the presence of a suppressor without notch for subject BG. As in Figure 6.3, the stimulus frequency is 1058 Hz and the stimulus level is 18 dB SPL peak equivalent. The level of the suppressor was set to 44 dB SPL in this case.

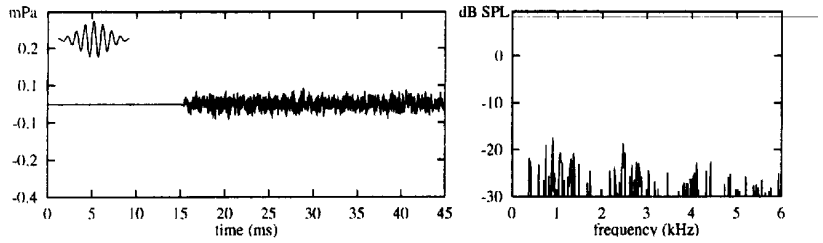

Figure 6.5: Narrowband-evoked TEOAE from subject BG in the presence of a suppressor tone complex with a spectral range of two octaves without spectral notch (same data representation as in Figs. 6.2 and 6.3). Note that the suppressor itself is not visible in the averaged time signal. In comparison with Fig. 6.3 the level of the emission is reduced.

Bandwidth determination from otoacoustic emissions (CBW$_{OAE}$)

In the fourth and last step, the influence of the notchwidth on the suppressed TEOAE is used to evaluate the critical bandwidth (CBW $_{OAE}$). The parameter observed is the energy of the TEOAE which is calculated within an octave band centered at the tone pulse frequency. The TEOAE level decreases in the presence of a suppressor without a spectral notch, but recovers with increasing notchwidth. The CBW $_{OAE}$ is estimated from this data in a manner similar to that well-known from psychoacoustics. For this purpose the suppression effect is calculated as the difference between the level of the unsuppressed TEOAE and the level of the TEOAE in the respective suppressed condition. Figure 6.6 shows the decrease of the suppression effect with growing notchwidth for subject BG (rhombi). The filter

describing the influence of the notched suppressor on the narrowband evoked TEOAE is assumed to be a symmetrical rounded exponential filter roex(f,f_m,a) centered at the frequency f_m (cf. GLASBERG and MOORE, 1990). The prediction of the suppression effect is based on the assumption that the suppression effect SE is proportional to the energy of the suppressor in the auditory filter:

$$SE \sim \int_{-\infty}^{\infty} \text{roex}(f, f_m, a) \cdot S_{\text{sup}}(f)\, \mathrm{d}f. \tag{6.3}$$

$S_{\text{sup}}(f)$ is the spectrum of the employed tone complex suppressor and the roex-filter is defined as

$$\text{roex}(f, f_m, a) = \begin{cases} \frac{1}{2a}\left(1 - \frac{f - f_m}{a}\right)\exp\left(\frac{f - f_m}{a}\right) & \text{for } f < f_m \\ \frac{1}{2a}\left(1 - \frac{f_m - f}{a}\right)\exp\left(\frac{f_m - f}{a}\right) & \text{for } f \geq f_m \end{cases} \tag{6.4}$$

The roex-filter can be described by a single parameter a. This parameter a can be determined by fitting the roex-filter-based suppression prediction to the experimental data. For this purpose, a modified least-squares fit using a Lorentz error distribution is used which is more tolerant towards extremely deviating values than the standard least-squares fit. In the following, the CBW_{OAE} is characterized by the value of $4a$. This is the bandwidth of a rectangular filter with the same total power (ERB). For the concept of the equivalent rectangular bandwidth cf. MOORE (1993) and KOLLMEIER and HOLUBE (1992). The solid line in Figure 6.6 shows the roex-filter-based suppression prediction for subject BG. An optimal fit is achieved for a = 62.5, which corresponds to a CBW_{OAE} of $4a$ = 250 Hz.

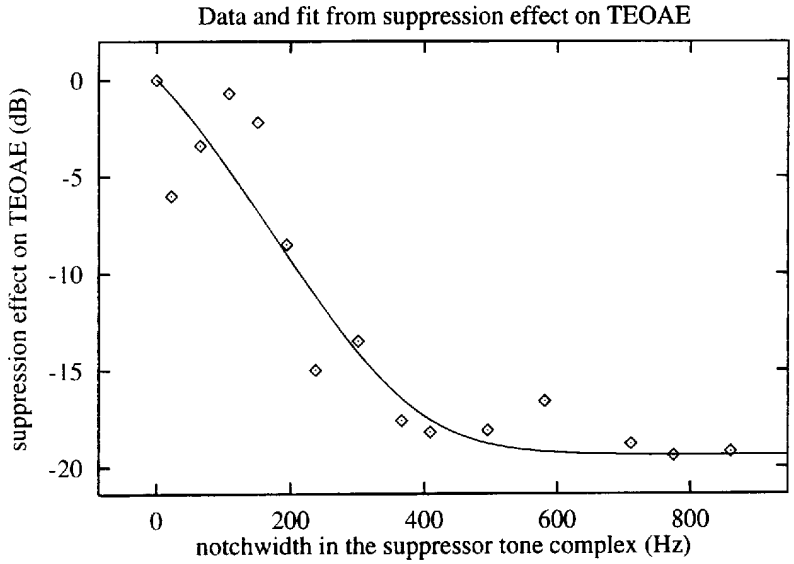

Figure 6.6: Suppression effect of different tone complexes on the narrow-band TEOAE for subject BG. The suppression effect is expressed as the decrease of the OAE level due to the suppressor within an octave band centered around the stimulus frequency. Abscissa: width of the spectral notch in the tone complex. Ordinate: magnitude of the suppression effect in relation to the maximal observed suppression, normalized to 0 dB. The suppression effect decreases with increasing notchwidth. The solid line shows the prediction of the suppression effect based on a roex-filter with parameter a = 62.5. This value of a corresponds to a CBW_{OAE} of 4a = 250 Hz.

Psychoacoustical experiments

In order to quantitatively compare the individual CBW_{OAE} with the psychoacoustical critical bandwidth (CBW_{PSY}), simultaneous masking experiments were performed that resemble the "classical" notched-noise experiments (PATTERSON, 1976). The acoustic stimuli are the same as those used in the TEOAE experiments. The stimuli are transformed to analog

signals by a 16-bit D/A converter at a sampling rate of 22050 Hz. They were lowpass-filtered, adjusted in level and monaurally presented to the subjects via a headphone (Sennheiser HDA200) in a soundproof booth. The timing, stimulus presentation and the recording of the responses was computer-controlled by a Sun workstation. The subject's task is to detect the probe tone in one out of three intervals in each trial (3-IFC paradigm). Subject responses were given via a computer keyboard.

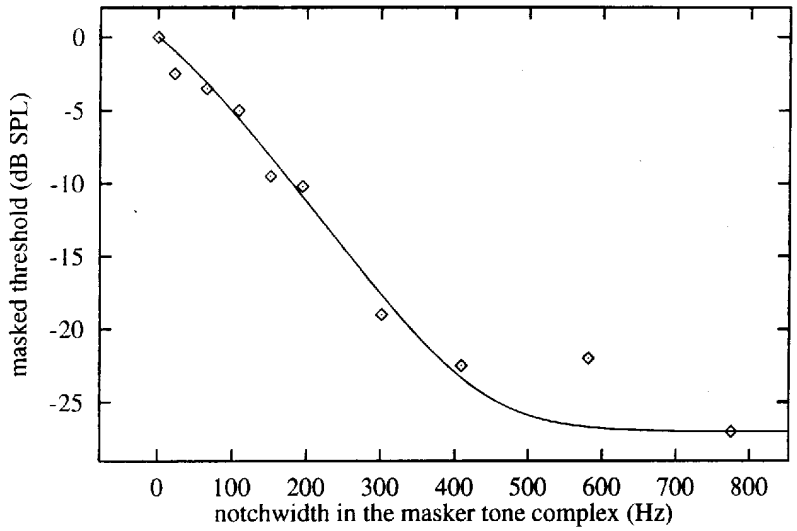

Figure 6.7: Decrease in masked threshold of a 1058-Hz-tone pulse presented 60 ms after the onset of a notched tone complex with varying notchwidth, subject BG, right ear. The masking effect is normalized to the condition with the maximum effect (= 0 dB), i.e. suppressor without spectral notch. The masking effect decreases with increasing notchwidth. The solid line represents the roex-filter-based fit of the data which is optimal for a = 54.5, corresponding to a CBW_{PSY} of 4a = 218 Hz.

The same harmonic tone complex that was used as suppressor in the OAE experiments serves as masker, and the same tone pulse stimulus serves as probe tone in these experiments. The masker is set to a level of 30 dB

above subjective threshold (This threshold was determined in a pilot experiment by three normal hearing subjects using the method of adjustment). As in the OAE experiments, the spectral notch is centered at the frequency of the tone pulse. In contrast to the OAE experiments, the tone pulse is placed 60 ms after the start of the masker to avoid an overshoot effect (ZWICKER, 1965). The level of the probe tone is changed in an one-up-two-down paradigm. The initial step size of 8 dB was reduced by a factor of 2 after each upper reversal during the initial phase of the track, with a minimal step size of 1 dB. The average level for the last six reversals in each adaptive track was used as threshold estimate. The threshold estimation is made three times for each of ten different notchwidths.

Bandwidth determination from psychoacoustical experiments (CBW_{PSY})

Figure 6.7 shows the masking effect of the tone complex on the dete ction of the test tone for subject BG. The masked threshold plotted on the ordinate is normalized to the condition with the highest masking e ffect (= 0 dB). As expected, the masked threshold strongly depends on the width of the notch in the suppressor. The determination of the CBW_{PSY} is based on this dependence. The data from Fig. 6.7 is used as input data to a roex-filter-based masking prediction. As described in the previous section, the prediction of the CBW_{PSY} is based on a Lorentz-fit to the experimental data. The parameter of the roex filter (a = 54.5) corresponds to a CBW_{PSY} of $4a$ = 218 Hz in Fig. 6.7. The quality of the roex-filter based fit is a useful value for determining how appropriate the model assumptions are in predic ting the measured data. For this purpose, the nonlinear deviation measure B_{nl} was employed (SCHACH and SCHÄFER, 1978; PRESS et al., 1992). It is defined for N measured data points y_i with mean $\bar{y}$ and the respective predicted values yi:

$$B_{nl} = 1 - \frac{\sum_{i=1}^{N} (y_i - \hat{y}_i)^2}{\sum_{i=1}^{N} (y_i - \bar{y})^2} \qquad (6.5)$$

In the case of a perfect fit B_{nl} = 1. B_{nl} is zero if the mean $\bar{y}$ is used as prediction $\hat{y}_i$ for all data points. If the prediction of the measured data is worse, B_{nl} can be negative. The prediction of the masking effects displayed in Fig. 6.7 exhibits a value of B_{nl} = 0.997. Thus, the model assumptions based on the roex-filter seems to provide a good description of the data.

6.3 Results

Figure 6.8 gives the results of both experiments for all subjects. In contrast to Figures 6.6 and 6.7, the "raw" data are shown in this figure to allow an estimate of the interindividual differences. The three left panels show the levels of the TEOAE in presence of the different tone complexes as a function of the width of the spectral notch in the suppressor tone complex. The three right panels show the corresponding psychoacoustic results, that is, the masked threshold of the test tone relative p.e. to the masker fixed at a sensation level of 30 dB. The subjects are divided into three groups: subjects without SOAE (upper panels), subjects with moderate SOAE (middle panels) and subjects with strong SOAE (one or more SOAE components more than 14 dB above the noise floor, lower panel).

In the three left panels, the suppression effect decreases with increasing notchwidth for all subjects. The effect is stronger for subjects with strong or moderate SOAE than for subjects without SOAE (upper left panel). Furthermore, the decrease of the suppression effect is not monotonic. Some subjects show a local minimum of the suppression effect below 200 Hz. The three panels on the right show the individual masking effects in the psychoacoustical experiment. As expected from the literature on notched-noise masking experiments, all subjects exhibit a decrease of the masked threshold with increasing notchwidth. For eight out of the nine subjects, the interquartile ranges are smaller than 3 dB in most conditions. One subject with strong SOAE had large interquartile ranges (Subject TB, lower right panel). This subject reported difficulties in detecting the probe tone in a reliable way. The level of the SOAE at 1553 Hz is 13.6 dB SPL for this subject. This is in the range of the masked threshold, because the masker level employed in the psychoacoustical experiments is 30 dB SL. The difficulties in detecting the probe tone might thus originate from an interaction of the SOAE with the perceived probe tone.

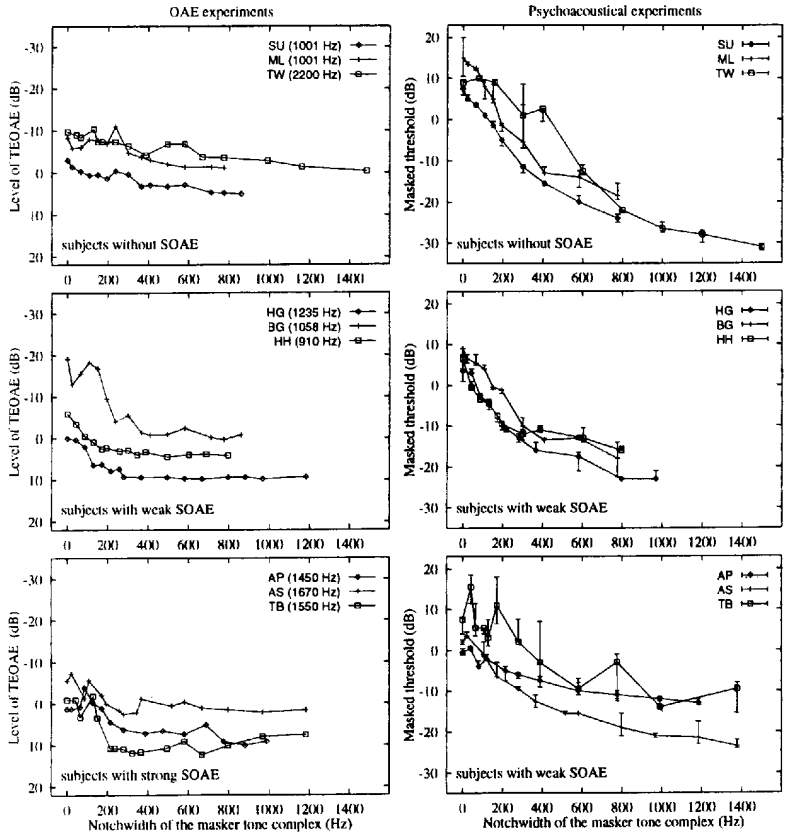

Figure 6.8: Results from both experiments for three sets of subjects: subjects without SOAE (upper panel), subjects with weak SOAE (middle panel) and subjects with strong SOAE (more than 14 dB above the noise floor, bottom panel). Left: sound pressure level of the narrowband TEOAE in dependence on the width of the notch in the suppressor. Please note the reversed ordinate in the left column, that is, higher levels are plotted pointing downwards. Right: results of notched-noise masking experiments. Threshold is given here relative p.e. to the masker set to a sensation level of 30 dB.

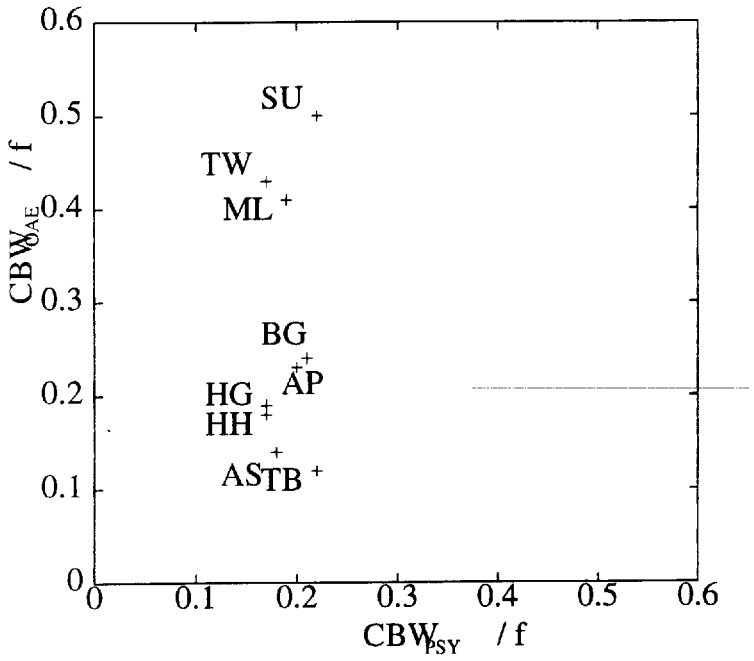

Figure 6.9: Comparison of CBW_{OAE} and CBW_{PSY}. Subjects with SOAE (BG, HG, TB, AP, HH, AS) exhibit similar values of CBW_{PSY}/f and CBW_{OAE}/f, whereas subjects without SOAE (SU, ML, TW) exhibit a CBW_{OAE}/f that is twice as high as the CBW_{PSY}/f.

As described in the previous section, estimates of the CBW_{OAE} and CBW_{PSY} are derived from the data displayed in Figure 6.8. Table 6.1 lists these values for all subjects. The prediction of the suppression and masking effects displayed in Figure 6.8 exhibits values of B_{nl} in the range between 0.96 and 1. Thus, the theoretical curves based on a roex-filter shape yield an accurate description of both sets of data.

Table 6.1 also lists the relative critical bandwidth (CBW_{PSY}/f or CBW_{OAE}/f.) These values are plotted as a scatter diagram in Figure 6.9. For all subjects the CBW_{PSY}/f corresponds well with the value of 0.2 that

is reported in the literature (cf. GLASBERG and MOORE, 1990). However, the CBW_{OAE}/f varies substantially across subjects: While six subjects with SOAE (BG, AP, HG, HH, AS and TB) also show a CBW_{OAE}/f value close to 0.2, the three subjects without SOAE (SU, TW and ML) exhibit a substantially larger CBW_{OAE}/f of 0.4 to 0.5.

Subj	**side**	**SOAE (dB)**	**Freq.**	**L_{puls} (dB)**	**L_{sup} (dB)**	**L_{OAE}**	**CBW_{OAE}**	**CBW_{OAE}/f**	**B_{nl}**	**CBW_{PSY}**	**CBW_{PSY}/f**	**B_{nl}**
ML	right	none	1000	26	47	9.9	408	0.41	0.963	192	0.19	1.000
SU	right	none	1000	30	51	8.1	502	0.50	0.961	219	0.22	0.998
TW	left	none	2200	20	45	9.9	938	0.43	0.975	368	0.17	0.999
BG	left	3.2	1058	18	44	18.7	250	0.24	0.993	218	0.21	0.997
HH	left	5.1	910	25	47	10.4	160	0.18	0.997	150	0.17	0.984
HG	right	11.1	1235	30	52	9.8	232	0.19	0.994	212	0.17	0.999
AS	left	14.1	1666	30	51	9.8	234	0.14	0.966	292	0.18	0.994
AP	left	15.1	1459	25	48	13.9	334	0.23	0.971	298	0.20	0.998
TB	left	18.0	1553	28	50	14.1	182	0.12	0.989	334	0.22	0.992

Table 6.1: Values of the critical bandwidth in Hz determined from OAE-measurements (CBW_{OAE}) and from psychoacoustic experiments (CBW_{PSY}) for all subjects. For comparison, the relative bandwidth is also given (CBW_{PSY}/f and CBW_{OAE}/f). The goodness of fit is expressed by the nonlinear correlation coefficient B_{nl} that ranges between -1 and 1 (for perfect fit). The fifth and sixth column give the sound pressure levels of the stimuli applied in the OAE experiment (L_{Puls}: level of evoking tone pulse, L_{Sup}: level of suppressor tone complex). The seventh column (ΔL_{OAE}) gives the maximum suppression effect in dB. The masker in the psychoacoustical task was set to a sensation level of 30 dB for all subjects.

6.4 Simulations with a driven van der Pol Oscillator

The generation of otoacoustic emissions can be modeled with simulations of basilar membrane mechanics including active mechanisms (DAVIS, 1983; KOSHIGOE and TUBIS, 1983; DUIFHUIS et al., 1986; ZWICKER, 1986; TALMADGE et al., 1990; VAN DEN RAADT and DUIFHUIS, 1990; NEELY and STOVER, 1993; KANIS and de BOER, 1993). These models, however, have many free parameters and predict the detailed generation of OAE by a variety of different mechanisms. Under the simplifying assumption that the generation of otoacoustic emissions is a local oscillation process on the basilar membrane, including some "negative damping", a single van der Pol oscillator may be used to model the main physical principle of OAE generation.

The van der Pol oscillator as a model for OAE

The van der Pol oscillator equation is the simplest example of a nonlinear self-sustained oscillator. If $x(t)$ denotes the time-dependent elongation of the oscillator which is driven by an external force $E(t)$, the van der Pol equation can be written as:

$$\ddot{x} + (-d_1 + d_2 x^2)\dot{x} + \omega_0^2 x = E(t) \qquad d_1, d_2 \geq 0 \qquad (6.6)$$

In equation (6.6), the parameter d_1 denotes a constant undamping term and represents the "active" properties of the oscillator. The parameter d_2 determines the nonlinear damping which becomes dominant for large elongations. The parameter ω_0 is the characteristic circular frequency of the oscillator without damping. Depending on the choice of the parameters d_1, d_2 and the force $E(t)$, the oscillator may produce a stationary sinusoidal oscillation, or even behave like a chaotic strange attractor (PARLITZ and LAUTERBORN, 1987).

The single van der Pol oscillator has been shown to be a suitable model for some properties of spontaneous otoacoustic emissions, including suppression tuning curves and entrainment to external tones (e.g. van DIJK and

WIT, 1990a; LONG et al., 1988; LONG at al., 1991), and several time constants determining the relaxation dynamics (TALMADGE et al., 1990; MURPHY et al., 1995). A detailed analysis of amplitude and frequency fluctuations of spontaneous emissions illustrates that a linear stiffness oscillator, as given in equation (6), can not account completely for the experimental findings (VAN DIJK and WIT, 1990b). Nevertheless, with the van der Pol damping profile added as stabilizing nonlinearity into a one-dimensional full cochlear model with instability modes (TALMADGE and TUBIS, 1993), even more complex properties resembling the interaction of emissions along the cochlea, such as the observed 0.4 Bark periodicity in frequency spectra and the connection to evoked emissions, can be explained.

As shown before (UPPENKAMP and KOLLMEIER, 1994), the single van der Pol oscillator can be utilized to model some experimental findings in the interaction of narrowband transitory evoked otoacoustic emissions with additional continuous tones as well. In those simulations, the external force $E(t)$ consisted of the evoking stimulus tone pulse and one continuous sinusoid that served as suppressor and canceled out in successive averaging frames. The power of the simulated emission showed a decline if the frequency of the additional tone was near the circular frequency of the oscillator ω_0. Hence, the synchronization of the emission with the original stimulus is reduced and the "response" of the system to the original stimulus is attenuated.

In analogy to the experiments in section II, simulations of narrowband evoked otoacoustic emissions in presence of tone complexes have now been performed using the simple model of a single driven van der Pol oscillator.

Numerical results

Since the single van der Pol oscillator does not include the function of the middle ear and the wave propagation along the cochlear partition, the time function $x(t)$ of the driven oscillator has to be interpreted in terms of movement of the basilar membrane at a certain place, characterized by its best frequency. This signal is segmented into sections of 46 ms (the stimulus repetition rate). The signal following each tone pulse stimulus is interpreted as evoked otoacoustic emission.

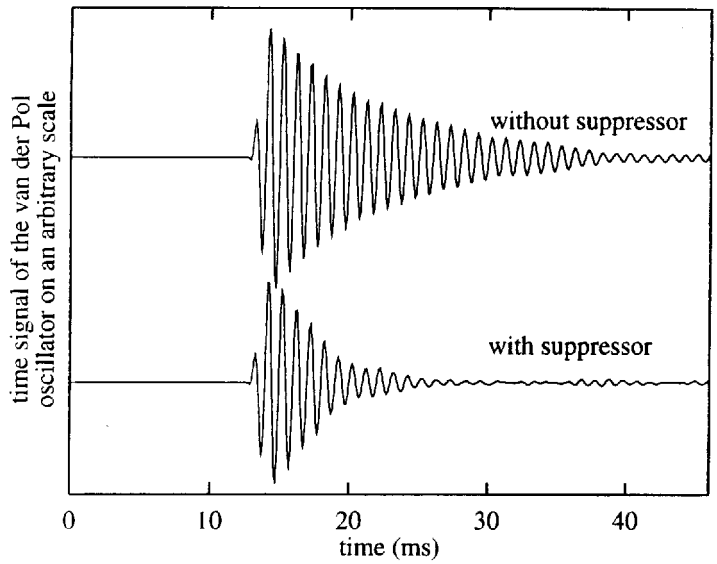

Figure 6.10: Averaged output of a van der Pol oscillator with $\omega_0/2\pi$ = 1000 Hz*, evoked by a* 1000 Hz *tone pulse. The value of the damping term* d_2 *was set to* 10000 *and the undamping term* d_1 *was set to* 100*. The external force includes a tone pulse with an amplitude of* $6.33\ w_0^2$ *and a noise term with an amplitude of* $0.32\ w_0^2$*. Upper curve: simulated "emission" on an arbitrary scale. Lower curve: simulated suppressed "emission". The time signal is set to zero during the evoking tone pulse.*

Thus, the time delay between the generation of the OAE and the signal at the recording microphone is neglected. The temporal development of the system was computed using a numerical integration procedure (fourth order Runge-Kutta, cf. PRESS et al., 1992). Figure 6.10 gives an example of a simulated narrowband TEOAE with and without the suppressor tone complex. During the temporal extent of the stimulus the time signal is set to zero. The simulated otoacoustic emission is calculated for 17 different values of the undamping parameter d1 ranging from -800 to 800 and for 31 different notchwidths of the suppressor tone complex. As shown in Fig.

6.11, the reduction of the level of the simulated emission depends on the width of the spectral notch in the suppressor tone complex and on the value of d_1. The dynamic range of the suppression effect is least for large negative values of the undamping parameter d_1. For positive values of d_1, a minimum of the "emission level" can be observed for notchwidths in the suppressor tone complex ranging between 50 Hz and 150 Hz. This might correspond to the local minima found in the OAE-data for subjects with a strong SOAE (cf. lower left panel of Fig. 6.8).

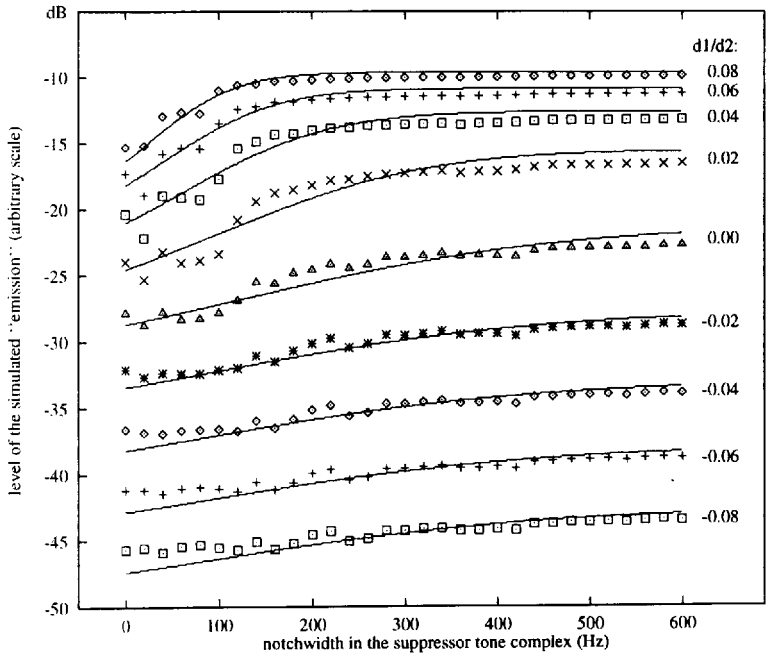

Figure 6.11: Level of the simulated "emissions" in the presence of suppressor tone complexes with varying notchwidth (symbols) and the appropriate roex-filter-based fit (solid lines). The parameter d_1 *varies from a ratio of* $d_1/d_2 = 0.08$ *to* $d_1/d_2 = -0.08$. *For positive undamping (upper curves) a local minimum of the suppression effect can be observed below* 100 Hz. *The dynamic range of the suppression effect as well as the level of the "emission" is reduced in the case of undamping (lower curves).*

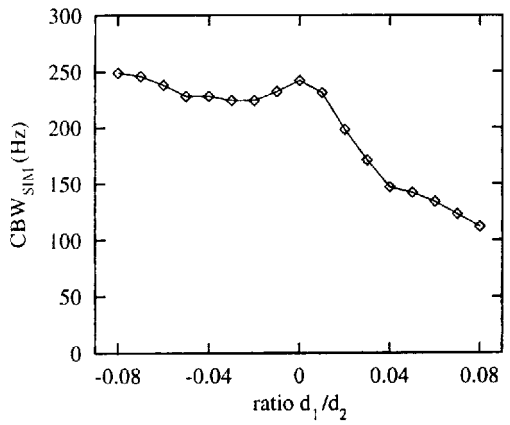

Figure 6.12: Values of CBW_{SIM} for different ratios d_1/d_2. The grade of undamping is changed while the parameter d_2 is kept at a constant value of 10000.

Similar to the method desribed in section II, the level of the suppressed emisions can serve as input for a roex-filter-based prediction. The estimates of the simulated critical bandwidth (CBW_{SIM}) is based on the predictions shown as solid lines in Figure 6.11. Figure 6.12 gives the resulting values of CBW_{SIM} as a function of d_1/d_2, i.e., the ratio of the undamping parameter d1 and the nonlinear damping parameter d_2. Apparently, CBW_{SIM} decreases for positive values of d_1 (undamping), whereas the CBW_{SIM} is larger for negative values (damping). In this aspect, the van der Pol oscillator behaves as expected from a linear resonator. The local maxima of the CBW_{SIM} near a value of $d_1 = 0$ is due to the local minimum of the emission level for small notchwidth (see above). This causes a reduced slope of the roex-filter based fit (solid lines in Figure 6.11) for values of d_1/d_2 between 0 and 0.04 and thus results in a larger value of CBW_{SIM}.

6.5 Discussion

The major results of this study can be summarized as follows:

1. The level of narrowband TEOAE is reduced in the presence of a suppressor tone complex.
2. The decline of this suppression effect with increasing notchwidth in the suppressor allows one to estimate the width of one critical band. A

similar bandwidth can be obtained from simulations of the suppression effect using a single driven van der Pol oscillator.

3. The values of CBW_{PSY} and CBW_{OAE} differ significantly for subjects without SOAE.

With respect to the first point it should be noted that the reduction of the TEOAE level in the presence of a suppressor can be explained as a synchronization effect (NEUMANN et al., 1997a). The suppressor tone complex exhibits a phase difference of p in successive segments and the time segments are averaged in pairs of two. Thus, the suppressor and the synchronized portion of the otoacoustic emission completely cancels in the averaged signal. The strength of this synchronization effect strongly depends on the spectral distance between the suppressed components of the emission and the components of the suppressor. In most cases, the maximum suppression effect is achieved for a tone complex without spectral notch (left panels in Fig. 6.8). In some cases, however, an additional local minimum of the suppression effect occurs for a notchwidth between 40 Hz and 300 Hz (e.g., subjects ML, AS, TB and BG). Subjects with SOAE exhibit a strong suppression effect of 14 to 23 dB. The suppression effect levels off for notchwidths greater than about 300 Hz. Subjects without spontaneous otoacoustic emissions, on the other hand, exhibit only a small reduction of the emission level of 8 to 10 dB. Although the upper bandwidth limit for the suppression effect is less pronounced for these subjects, the general dependence of the suppression effect on the notchwidth of the suppressor is comparable.

With respect to the second point it should be noted that the decline of the suppression effect with increasing notchwidth shows the same general shape as the decline of the masked threshold in the psychoacoustical experiments. Both experiments use the same acoustical stimuli and depend on the interaction of energy in a localized region on the basilar membrane. Both experiments are compatible with the concept of auditory filters. It can be assumed that the spectral range within which an additional tone can suppress an otoacoustic emission is related to the range within which masking energy is integrated across frequency. The lower cluster in Figure 6.9 shows that values of CBW_{OAE} and CBW_{PSY} coincide well for subjects with SOAE. Both estimates of the critical bandwidth also agree with the value of $CBW_{PSY}/f \approx 0.2$ given in the literature (GLASBERG and MOORE, 1990; ZWICKER, 1982). However, within this cluster, the variations of CBW_{OAE}

and CBW_{PSY} seem to be independent. In addition, the lack of a coincidence for subjects without SOAE also shows that no strict relation can be found between CBW_{OAE} and CBW_{PSY} (see below).

The simulation of the suppression effect with a driven van der Pol oscillator can repeat most findings of the OAE experiments. With an appropriate choice of the amount of undamping, the results of the suppression experiments can be simulated for subjects with and without SOAE. This finding is not surprising in view of the previous work by LONG et al., 1988, 1991, and UPPENKAMP and KOLLMEIER, 1994, who showed that the van der Pol equation with an appropriate undamping yields a frequency-dependent suppression effect which resembles the well-known critical bandwidth effect. However, these authors did not derive critical bandwidth estimates in the same way as performed here (that is motivated by psychoacoustical bandwidth estimation procedures). The suppression effect simulated here has the same order of magnitude as that in the OAE experiments and depends on the size of the spectral notch in the suppressor tone complex (cf. Fig. 6.11). This figure also shows that the total range of the suppression effect is large for positive values of the undamping parameter d_1, and limited for large negative values of d_1. This corresponds with the observation that the suppression effect is greater for subjects with SOAE whereas subjects without SOAE exhibit shallow slopes (left panels of Fig. 6.8). A local minimum similar to the minimum of the suppression effect in subjects without SOAE can be observed in the simulations for positive undamping (cf., upper traces of Fig. 6.11). The size of the critical bands in the simulations (cf. Fig. 6.12) is in the same range as found in the actual OAE experiments. The rate of undamping is the most important parameter for the value of CBW_{SIM}. The bandwidth estimate is large for positive damping ($d_1 < 0$) and decreases in the case of positive undamping ($d_1 > 0$). The value that corresponds to the critical bandwidth of a normal hearing subject ($CBW_{SIM}/f \approx 0.2$) can be observed for $d_1/d_2 \approx 0.02$. Thus, the results from the simulations of a cochlear amplifier with moderate undamping (i.e., amplification gain just above one) are in good agreement with the data from normal hearing subjects. It may even be argued that this agreement at small positive values provides an estimate of the "effective" mechanical undamping at the basilar membrane level that is required for a normal function of the auditory system.

With respect to the third point it should be noted that the CBW_{OAE} is larger for subjects without SOAE than for subjects with SOAE (cf. Fig. 6.9). This

result is visible in the shallow slopes of the suppression effect in the upper left panel of Fig. 6.8. The CBW_{OAE} does not coincide with the CBW_{PSY}, since the CBW_{PSY} is approximately the same for all subjects. For those subjects that do not exhibit a SOAE close to the test frequency, the obtained CBW_{OAE} value overestimates the actual CBW_{PSY} value. There are several possible explanations of the divergence of CBW_{OAE} and CBW_{PSY} values. In the first place, the level of narrowband TEOAE is comparably low in the absence of SOAE. As a consequence, the maximal achievable suppression effect is limited and the spread of the data might be too large to derive a valid estimate of the critical bandwidth. Nevertheless, this can not explain the observed systematic divergence between CBW_{OAE} and CBW_{PSY}.

The observation of greater interindividual variability in the OAE data (left panels of Figure 6.8) that can not be found in the masked threshold data (right panels of Figure 6.8) supports the conjecture that both methods test a different subset of the properties of the auditory system. The psychoacoustical detection task might involve effects like "off-frequency listening" or central processes that do not primarily reflect cochlear mechanisms and can not be tested with otoacoustic emissions. These effects might cause a psychoacoustical critical bandwidth that is smaller than expected from OAE experiments. On the other hand, the recording of otoacoustic emissions involves properties of the auditory system that do not directly contribute to sound perception. For example, the propagation of the emission from the place of its origin to the apex, in the middle ear, and into the recording system might suppress and substantially alter the signal. Thus, the OAE as they are generated in the inner ear might not be entirely represented by the signal recorded in the ear canal. These processes might also influence the apparent arbitrariness of the occurrence of SOAE. Apart from involving a different subset of the properties of the auditory system, the frequency range that contributes to either CBW_{OAE} or CBW_{PSY} might differ in principle. The psychoacoustical task is based on the global excitation pattern on the cochlea whereas the analysis of the suppression effect evaluates the level of a single frequency component and does not account for level changes at other frequencies. Possibly, this difference is less pronounced in the presence of a spontaneous otoacoustic emission. It is known that a "leading" SOAE oscillation is able to synchronize nearby oscillators (VAN HENGEL and MAAT, 1993). As a consequence, the SOAE oscillation might concentrate most OAE energy at a single frequency

whereas multiple oscillators are involved in the generation of TEOAE. This might explain why the values of CBW_{OAE} and CBW_{PSY} are in agreement for subjects with SOAE only.

6.6 Conclusion

The present OAE experiments as well as the masked threshold experiments depend on the interaction of energy in a localized region on the basilar membrane. The prediction of the size of a critical band from an OAE experiment succeeds for those subjects with spontaneous otoacoustic emissions (six out of the nine tested). For the remaining subjects without spontaneous emissions, the critical bandwidths from the OAE experiment were larger than in the psychoacoustical experiment. The OAE experiment could be modeled with a single driven van der Pol oscillator that produced critical bandwidth estimates consistent with those observed in the psychoacoustical experiment if a moderate undamping was chosen. Therefore, the "effective" amount of undamping at the basilar membrane level can be estimated which is required to provide the critical bandwidth observed in psychoacoustic experiments.

References

Allen, J.B., Fahey, P.F. (1992). "Using acoustic distortion products to measure the cochlear amplifier gain on the basilar membrane," J. Acoust. Soc. Am. 92, 178-188.

Arthur, R.M., Pfeiffer, R.R., Suga, H. (1971). "Properties of 'two tone inhibition' in primary auditory neurons," J. Physiol. 212, 593-609.

Avan, P., Bonfils, P., Loth, D., Narcy, P. and Trotoux, J. (1991). "Quan titative assessment of human cochlear function by evoked otoacoustic emissions, Hear. Res. 52, 99-112.

Bonfils, P., Piron, J. P., Uziel, A. and Pujol, R. (1988). "A correlative study of evoked otoacoustic emissions from adults and infants: Clinical applications," Acta Otolaryngol. (Stockh) 105, 445-449.

Brass, D., Kemp, D.T. (1991). "Time-domain observations of otoacoustic emissions during constant tone stimulation," J. Acoust. Soc. Am. 90, 2415-2427.

Brass, D., Kemp, D.T. (1993). "Suppression of stimulus frequency otoacoustic emissions," J. Acoust. Soc. Am. 93, 920-939.

Bray, P., Kemp, D.T. (1987). "An advanced cochlear echo technique suitable for infant screening," Brit. J. Audiol. 11, 191-204.

Brown, A.M., Gaskill, S.A., Carylon, R.P., Williams, D.M. (1993). "Acoustic distortion as a measure of frequency selectivity: relation to psy chophysical equivalent rectangular bandwidth," J. Acoust. Soc. Am. 93, 3291-3297.

Brownell, W.E., Bader, C.R., Bertrand, D., Ribaupierre, Y. (1985). "Evoked mechanical responses of isolated cochlear outer hair cells," Science 227, 194-196.

Burgess, J.C. (1991). "Chirp design for acoustical system identification," J. Acoust. Soc. Am. 91, 1525-1530.

Collet, L., Veuillet, E., Chanal, J.M., Morgon, A. (1991). "Evoked otoacoustic emissions: correlates between spectrum analysis and audiogram," Audiology 30, 164-172.

Dallmayr, C, "Stationary and dynamic properties of simultaneous evoked otoacoustic emissions," Acustica, vol. 63, pp. 243-255, 1987.

Davis, H. (1983). "An active process in cochlear mechanics," Hear. Res. 9, 79-91.

van Dijk, P., Wit, H.P. (1990a). "Synchronization of spontaneous otoacoustic emissions to a 2f1-f2 distortion product," J. Acoust. Soc. Am. 88, 850-856.

van Dijk, P., Wit, H.P. (1990b). "Amplitude and frequency fluctuations of spontaneous otoacoustic emissions," J. Acoust. Soc. Am. 88, 1779-1793.

Duifhuis, H., Hoogstraten, H.W., van Netten, H.W., Diependaal, R.J., Bialek, W. (1986). "Modelling the cochlear partition with coupled van der Pol-Oscillators", in: *Peripherial Auditory Mechanisms*, edited by J.B. Allen, J.L. Hall, A.E. Hubbard, S.T. Neely, A. Tubis (Springer, Berlin), Lecture Notes in Biomathematics 64, pp. 290-297.

Fletcher, H. (1940). "Auditory patterns," Review of Mod. Physics 12, 47-65.

Fria, T., LeBlanc, J., Kristensen, R., Alberti, P.W. (1975). "Ipsilateral acoustic reflex stimulation in normal and sensori neural impaired ears: a preliminary report," Canad. J. Otol., 4, 695-703.

Gaskill, S.A., Brown, A.M. (1990). "The behaviour of the acoustic distortion product, 2f1-f2, from the human ear and its relation to auditory sensitivity," J. Acoust. Soc. Am. 88, 821-839.

Gelfand, S.A. (1984). "The contralateral acoustic-reflex threshold," in: S. Silman (Ed.), *The Acoustic reflex: Basic Principles and Clinical Applications*, Academic Press, New York, 137-186.

Gelfand, S.A. (1990). *Hearing - An Introduction to Psychological and Physiological Acoustics*, M. Dekker, New York.

Glasberg, B.R., Moore, B.C.J. (1990). "Derivation of auditory filter shapes from notched-noise data," Hear. Res. 47, 103-138.

Goldstein, J.L. (1967). "Auditory nonlinearity," J. Acoust. Soc. Am. 41, 676-689.

Grandori, F. (1985). "Nonlinear phenomena in click- and toneburst evoked otoacoustic emissions from human ears," Audiology 24, 71-80.

Greenwood, D.D. (1961). "Critical bandwidth and the frequency coordinates of the basilar membrane," J. Acoust. Soc. Am. 33, 1344-1356.

Hall, J.L. (1972). "Auditory distortion products f2-f1 and 2f1-f2," J. Acoust. Soc. Am. 51, 1863-1871.

Harris, F.P., Lonsbury-Martin, B.L., Stagner, B.B., Coats, A.C., Mar tin, G.K. (1989). "Acoustic distortion products in humans: systematic changes in amplitude as a function of f2/f1 ratio," J. Acoust. Soc. Am. 85, 220-229.

Harris, F.P., Probst, R. (1990). "Growth functions of tone burst evoked and distortion-product otoacoustic emissions in humans," in: P Dallos, CD Geisler, JW Matthews, MA Ruggero, CR Steele (Eds.), *The mechanics and biophysics of hearing*, Lecture Notes in Biomathematics 87, Springer, Berlin, 178-186.

Harris, F.P., Probst, R., Xu, L. (1992). "Suppression of the 2f1-f2 otoacoustic emission in humans," Hear. Res. 64, 133-141.

van Hengel, P., Maat, A. (1993). "Periodicity in frequency spectra of click evoked and spontaneous OAE, theory meets experiment," in: *Biophysics of hair cell sensory systems*, edited by H. Duifhuis, J.W. Horst, P. van Dijk, S.M. van Netten (World Scientific, Singapore), pp. 47-53.

Hind, J.E., Anderson, D.J., Brugge, J.F., Rose, J.E. (1967). "Coding of information pertaining of paired low-frequency tones in single auditory nerve fibers of the squirrel monkey," J. Neurophysiol., 30, 794-816.

Horst, J.W., Wit, H.P., Ritsma, R.J. (1983). "Psychophysical aspects of cochlear acoustic emissions ('Kemp-tones')," in: R. Klinke, R. Hartmann (Eds.), *Hearing - Physiological Bases and Psychophysics*, Springer, Berlin, 89-96.

Jepsen, O. (1963). "The middle ear muscle reflexes in man," in: J. Jerger (Ed.) *Modern Developments in Audiology*, Academic Press, New York, 194-239.

Jerger, J. (1970). "Clinical experience with impedance audiometry," Arch. Otol. 92, 311-321.

Jurzitza, D., Hemmert, W. (1992). "Quantitative measurements of simultaneous evoked otoacoustic emissions," Acustica 77, 93-99.

Kanis, L.J., de Boer, E. (1993). "The emperor's new clothes: DP emissions in a locally-active nonlinear model of the cochlea," in: *Biophysics of hair cell sensory systems*, edited by H. Duifhuis, J.W. Horst, P. van Dijk, S.M. van Netten (World Scientific, Singapore), pp. 304-314.

Kemp, D.T. (1978). "Stimulated acoustic emissions from within the human auditory system," J. Acoust. Soc. Am. 64, 1386-1391.

Kemp, D.T. (1979). "Evidence of mechanical non-linearity and frequency selective wave amplification in the cochlea," Arch. Otorhino l. 224, 37-45.

Kemp, D.T., Brass, D.N., Souter, M. (1990a). "Observation on simultaneous SFOAE and DPOAE generation and suppression," in: P. Dallos, C.D. Geisler, J.W. Matthews, M.A. Ruggero, C.R. Steele (Eds.), The mechanics and biophysics of hearing, Lecture Notes in Biomathematics 87, Springer, Berlin, 202-209.

Kemp, D.T., Ryan, S., Bray, P. (1990b). "Otoacoustic emission analysis and interpretation for clinical purposes," in: F. Grandori, G. Cianfrone, D.T. Kemp (Eds.), *Cochlear mechanisms and otoacoustic emissions*, Karger, Basel, 77-89.

Kemp, D.T. Chum R. (1980a) "Observations on the generator mechanism of stimulus frequency acoustic emissions - Two tone suppression," in: G. van den Brink, F.A. Bilsen (Eds.), *Psychophysical, physiological and behavioral studies in hearing*, Delft Univ Press, 34-42.

Kemp, D.T., Chum, R. (1980b). "Properties of the generator of stimulated acoustic emissions," Hear. Res. 2, 213-232.

Kemp, D.T., Souter, M. (1988). "The dynamics of cochlear perturbations following brief acoustic and efferent stimulation otoacoustic and CM data," in: H. Duifhuis, J.W. Horst, H.P. Wit (Eds.), Basic Issues in Hearing, Academic Press, London, 116-123.

Klauder, J.R., Price, A.C., Darlington, S., Albersheim, W.J. (1960). "The theory and design of chirp radar," Bell System Techn. J. 39, 745-808.

Kollmeier, B., Holube, I. (1992). "Auditory filter bandwidths in binaur al and monaural listening conditions," J. Acoust. Soc. Am. 92, 1889-1901.

Koshigoe, S., Tubis, A. (1983). "A nonlinear feedback model for outer hair-cell stereocilia and its implications for the response of the auditory periphery," in: *Mechanics of Hearing*, edited by E. de Boer, M.A. Viergever (Delft Univ. Press), pp. 153-160.

Kummer, P., Janssen, T., Arnold, W. (1995). "Suppression tuning characteristics of the 2f1-f2 distortion-product otoacoustic emission in humans," J. Acoust. Soc. Am. 98, 197-210.

Legouix, P.J., Remond, M.C., Greenbaum, H.B. (1973). "Interference and two-tone inhibition," J. Acoust. Soc. Am., 53, 409-419.

Long, G. R., Tubis, A. (1988). "Modification of spontaneous and evoked otoacoustic emissions and associated psychoacoustic microstructure by aspirin consumption," J. Acoust. Soc. Am. 84, 1343-1353.

Long, G.R., Tubis, A., Jones, K.L. (1991). "Modeling synchronization and suppression of spontaneous otoacoustic emissions using Van der Pol oscillators: effects of aspirin administration," J. Acoust. Soc. Am. 89, 1201-1212.

Long, G.R., Tubis, A., Jones, K.L., Sivaramakrishnan, S. (1988). "Modification of the external-tone synchronization and statistical properties of spontaneous otoacoustic emissions by aspirin consumption," in: *Basic Issues in Hearing*, edited by H. Duifhuis, J.W. Horst, H.P. Wit (Academic Press, London), pp. 93-100.

Mahoney, C.F.O. Kemp, D.T. (1995). "Distortion product otoacoustic emission delay measurement in human ears," J. Acoust. Soc. Am. 97, 3721-3735.

Margolis, R., Popelka, G. (1975). "Loudness and the acoustical reflex," J. Acoust. Soc. Am. 58, 1330-1332.

Metz, O. (1952). "Threshold of reflex contractions of muscles of middle ear and recruitment of loudness," Arch Otol., 55, 536-543.

Møller, A. (1962). "The sensitivity of contraction of tympanic muscle in man," Ann. Otol. 71, 86-95.

Moore, B.C.J. (1993). "Frequency analysis and pitch perception," in: *Human Psychophysics*, edited by W.A. Yost, A.N. Popper, R.R. Fay (Springer, Berlin), pp. 56-115.

Murphy, W.J., Talmadge, C.R., Tubis, A., Long, G.R. (1995). "Relaxation dynamics of spontaneous otoacoustic emissions perturbed by external tones: I. Response to pulsed single-tone suppressors," J. Acoust. Soc. Am. 97, 3702-3710.

Neely, S.T., Stover, L.J. (1993). "Otoacoustic emissions from a nonlinear, active model of cochlear mechanics," in: *Biophysics of hair cell sensory systems*, edited by H. Duifhuis, J.W. Horst, P. van Dijk, S.M. van Netten (World Scientific, Singapore), pp. 64-71.

Neumann, J., Uppenkamp, S., Kollmeier, B. (1993). "Frequenzspezifische Stimulation von TEAOE bei Schwerhörigkeit," in: *Fortschritte der Akustik* - DAGA '93. DPG GmbH, Bad Honnef, 720-723.

Neumann, J., Uppenkamp, S., Kollmeier, B. (1994). "Chirp evoked oto a-coustic emissions," Hear. Res. 79, 17-25.

Neumann, J., Uppenkamp, S., Kollmeier, B. (1995). "Aufzeichnung von simultan evozierten otoakustischen Emissionen mit Tonkomplexen," in *Fortschritte der Akustik - DAGA 95*, Deutsche Gesellschaft für Akustik e.V., Oldenburg, 235-238.

Neumann, J., Uppenkamp, S., Kollmeier, B. (1996). "Detection of the acoustic reflex below 80 dB HL," Audiology and Neurootology 1, 359-369.

Neumann, J., Uppenkamp, S., and Kollmeier, B. (1997a). "Interaction of otoacoustic emissions with additional tones: Suppression or synchroni-zation?" Hear. Res., in press.

Neumann, J., Uppenkamp, S., Kollmeier, B. (1997b). "Relation between notched-noise suppressed TEOAE and the psychoacoustical critical bandwidth," J. Acoust. Soc. Am., in press.

Northern, J.L., Gabbard, S.A. (1994). "The acoustic reflex," in: Katz, J. (Ed.), *Handbook of Clinical Audiology*, 4th edition, Wiliams and Wilk-ins, Baltimore, 300-316.

Norton, S.J. (1992). "Basic and applied applications of otoacoustic emis-sions," XXIth Internat. Congr. Audiol., R2-1.

Norton, S.J., Neely, S.T. (1987). "Tone-burst evoked otoacoustic emissions from normal-hearing subjects," J. Acoust. Soc. Am. 81, 1860-1872.

Parlitz, U., Lauterborn, W. (1987). "Period-doubling cascades and devil`s staircases of the Driven van der Pol oscillator," Physical Review A 36, 1428-1434.

Patterson, R.D. (1976). "Auditory filter shapes derived with noise stimu la-tion", J. Acoust. Soc. Am. 59, 640-654.

Patuzzi, R., Robertson, D. (1988). "Tuning in the mammalian cochlea," Physiol. Rev. 68, 1009-1082.

Press, W.H., Teukolsky, S.A., Vetterling, W.T., Flannery, B.P. (1992). *Numerical Recipies in C* (Cambridge University Press, Cambridge).

Probst, R., Coats, A.C., Martin, G.K., Lonsbury-Martin, B.L. (1986). "Spontaneous, click- and toneburst evoked otoacoustic emissions from normal ears," Hear. Res. 21, 261-275.

Probst, R., Lonsbury-Martin, B.L. and Martin, G.K. (1991). "A review of otoacoustic emissions," J. Acoust. Soc. Am. 89, 2027-2067.

van den Raadt, M.P.M.G., Duifhuis, H. (1990). "A generalized Van der Pol-oscillator cochlea model," in: *The mechanics and biophysics of hearing*, edited by P. Dallos, C.D. Geisler, J.W. Matthews, M.A. Rug gero, C.R. Steele (Springer, Berlin), Lecture Notes in Biomathematics 87, pp. 227-234.

Rappaport, B, Tait, C. (1976). "Acoustic reflex threshold measurement in hearing aid selection," Arch Otol. 102, 129-134.

Rhode, W.S., Robles, L. (1974). "Evidence from Mössbauer experiments for nonlinear vibrations in the cochlea," J. Acoust. Soc. Am. 55, 588-596.

Ruggero, M.A., Rich, N.C., Freyman, R. (1983). "Spontaneous and impu l-sively evoked otoacoustic emissions: indicators of cochlear pathology?," Hear. Res. 10, 283-300.

Ruggero, M.A., Rich, N.C. (1991). "Application of a commercially-manu-factured Doppler-shift laser velocimeter to the measurement of basilar-membrane vibration," Hear. Res 51, 215-230.

Schach, S., Schäfer, T. (1978) *Regressions- und Varianzanalyse: Eine Ein-führung* (Springer, Berlin).

Schloth, E. (1983). "Relation between spectral composition of spontaneous otoacoustic emissions and fine-structure of hearing threshold in quiet," Acustica 53, 250-256.

Schroeder, M.R. (1970). "Synthesis of low peak-factor signals and binary sequences with low autocorrelation," IEEE Trans. Information Theory 13, 85-89.

Sellari-Franceschini, S., Bruschini, P., Pardini, L., Berrettini, S. (1986). "Quantification of the parameters of the acoustic reflex in normal ears," Audiology 25, 165-175.

Silman, S., Popelka, G., Gelfand, S.A. (1978). "Effect of sensorineural hearing loss on acoustic stapedius reflex growth functions," J. Acoust. Soc. Amer. 64, 1406-1411.

Smoorenburg, G.F. (1972). "Audibility region of combination tones," J. Acoust. Soc. Am. 52, 603-614.

Strube, H.W. (1989). "Evoked otoacoustic emissions as cochlear Bragg reflections," Hear. Res. 38, 35-45.

Sutton, G.J. (1985). "Suppression effects in the spectrum of evoked otoacoustic emissions," Acustica, 58, 57-63.

Talmadge, C.L., Long, G.R., Murphy, W.J., Tubis, A. (1990) "Quantitative evaluation of limit-cycle oscillator models of spontaneous otoacoustic emissions," in: *The mechanics and biophysics of hearing*, edited by P. Dallos, C.D. Geisler, J.W. Matthews, M.A. Ruggero, C.R. Steele (Springer, Berlin), Lecture Notes in Biomathematics 87, pp. 235-242.

Talmadge, C.L., Tubis, A. (1993). "On modeling the connection between spontaneous and evoked otoacoustic emissions," in: *Biophysics of hair cell sensory systems*, edited by H. Duifhuis, J.W. Horst, P. van Dijk, S.M. van Netten, S.M. (World Scientific, Singapore), pp. 25-32.

Uppenkamp, S. (1992). *Grundlagen und Anwendung der otoakustischen Emissionen zur objektiven Hörprüfung*. Dissertation, Universität Göttingen.

Uppenkamp, S., Kollmeier, B. (1994). "Narrowband stimulation and synchronization of otoacoustic emissions," Hear. Res. 78, 210-220.

Uppenkamp, S., Neumann, J. (1996). "Otoacoustic emissions from normal hearing subjects: some experimental results in connection to psychoacoustics," in: B. Kollmeier (Ed.), *Psychoacoustics, Speech and Hearing Aids*, World Scientific, Singapore, 19-24

Uppenkamp, S., Neumann, J., Aurbach, G., Kollmeier, B. (1992). "Evozierte otoakustische Emissionen bei Erwachsenen: Auswertekriterien für den klinischen Einsatz," HNO 40, 422-428.

Weber, R., Mellert, V. (1975). "On the nonmonotonic behavior of cubic distortion products in the human ear," J. Acoust. Soc. Am. 57, 207-214.

White, K.R., Vohr, B.R., Behrens, T.R. (1993). "Universal newborn hearing screening using transient evoked otoacoustic emissions: results of the Rhode Island hearing assessment project," Seminars in hearing 14, 18-29.

Wilson, J.P. (1980). "Evidence for a cochlear origin for acoustic re-emissions threshold fine-structure and tonal tinnitus," Hear. Res. 2, 233-252.

Wilson, J.P., Sutton, G.J. (1981). "Acoustic correlates of tonal tinnitus," in: D. Evered, G. Lawrenson (Eds.), *Tinnitus*, CIBA Found Symp 85, Pitman, London, 8 2-100.

Wilson, R.H., McBride, L.M. (1978). "Threshold and growth of the acoustic reflex," J. Acoust. Soc. Amer. 63, 147-154.

Wit, H.P., Langevoort, J.C., Ritsma, R.J. (1981). "Frequency spectra of cochlear acoustic emissions ('Kemp-Echoes')," J. Acoust. Soc. Am. 70, 437-445.

Wit, H.P., Ritsma, R.J. (1979). "Stimulated acoustic emissions from the human ear," J. Acoust. Soc. Am., 66, 911-913.

Wit, H.P., Ritsma, R.J. (1980). "Evoked acoustical responses from the human ear: some experimental results," Hear. Res., 2, 253-261.

Zenner, H.P. (1986). "Motile responses in outer hair cells," Hear. Res. 22, 83-90.

Zurek, P.M. (1981). "Spontaneous narrowband acoustic signals emitted by human ears," J. Acoust. Soc. Am. 69, 514-523.

Zwicker, E. (1965). "Temporal effects in simultaneous masking by white-noise bursts," J. Acoust. Soc. Am. 37, 653-663.

Zwicker, E. (1982). *Psychoakustik*, Springer, Berlin.

Zwicker, E. (1983). "Delayed evoked otoacoustic emissions and their suppression by Gaussian shaped pressure impulses," Hear. Res. 11, 359-371.

Zwicker, E. (1986). "'Otoacoustic emissions' in a nonlinear cochlear hardware model with feedback," J. Acoust. Soc. Am. 80, 154-162.

Zwicker, E. (1990). "On the frequency separation of simultaneously evoked otoacoustic emissions' consecutive extrema and its relation to cochlear traveling waves," J. Acoust. Soc. Am. 88, 1639-1641.

Zwicker, E., Feldtkeller, R. (1967). *Das Ohr als Nachrichtenempfänger* (Hirzel, Stuttgart).

Zwicker, E., Schloth, E. (1984). "Interrelation of different oto acoustic emissions," J. Acoust. Soc. Am. 75, 1148-1154.

Zwicker, E., Terhardt, E. (1980). "Analytical expression for critical-band rate and critical bandwidth as a function of frequency," J. Acoust. Soc. Am. 68, 1523-1525.